Assessment of structural attributes of even-aged *Eucalyptus grandis* forest plantations using small-footprint discrete return lidar data

Solomon G. Tesfamichael

March 2009

Assessment of structural attributes of even-aged *Eucalyptus grandis* forest plantations using small-footprint discrete return lidar data

Solomon G. Tesfamichael

Dissertation submitted to the Faculty of Science and Agriculture, at the University of KwaZulu-Natal in fulfilment of the requirements for the degree of

Doctor of Philosophy

in

Environmental Sciences

March 2009

Pietermaritzburg, South Africa

Abstract

Assessment of forest structural attributes has major implications in the management of forestry by providing information of ecological and economic importance. The traditional methods of assessment involve collecting data in the field and are regarded as labour-intensive and expensive. In plantation forestry, field campaigns are generally time consuming and costly, and may compromise profit maximisation. The introduction of lidar (light detection and ranging) remote sensing in forestry has shown promise to add value to the traditional field inventories mainly through large spatial coverages in a timely and cost-effective manner. Lidar remote sensing is an advanced system capable of acquiring information in both the vertical and horizontal dimensions at relatively high resolutions. Numerous studies have established that these qualities of lidar data are suited to estimating forest structural attributes at acceptably high accuracies. The generic approach in most studies is to use lidar data in combination with field data. Such an approach still warrants a high cost of inventory. It is therefore useful to explore alternative methods that rely primarily on lidar data by reducing the necessity for field-derived information.

The aim of this study was to derive structural attributes of even-aged *Eucalyptus grandis* forest plantations using lidar data. The attributes are of significance to timber resource assessments and include plot-level tree height attributes, stems per hectare (SPHA), and volume. The surveyed field data included tree counting and measurement of tree height and diameter at breast height for sample plots. Volume was then calculated using standard allometric models. Small-footprint lidar data of the plantations were also acquired coincident with the field inventories. Mean tree height and dominant height were estimated at a range of simulated lidar point densities between 0.25 points/m^2–6 points/m^2. Various plot-level distributional metrics were extracted from height values of lidar non-ground points and related with field mean and dominant height values using stepwise regression analysis. The results showed that both attributes could be estimated at high accuracies with no significant differences arising from variations in lidar point density.

Estimation of SPHA relied on the exploration of semi-variogram range as a mean window size for applying local maxima filtering to the lidar canopy height surface. A comparative approach of window size determination used pre-determined within-row tree spacing, based on planting information. Two secondary objectives were addressed: comparing spatial resolutions of canopy height surfaces interpolated from non-ground height values and comparison of lidar point densities simulated at three levels. Comparison of spatial resolutions of canopy height surfaces were performed at 0.2 m, 0.5 m, and 1 m using a lidar point density of 5 points/m^2. The results indicated that 0.2 m is the most appropriate resolution for locating trees and consequently deriving SPHA. Canopy height surfaces of 0.2 m resolution were created at simulated densities of 1 point/m^2, 3 points/m^2, and 5 points/m^2. While all estimates were negatively biased relative to field-observed SPHA, lidar densities of 3 points/m^2 and 5 points/m^2 returned similar accuracies, which were both superior to 1 point/m^2. It was concluded that 3 points/m^2 was sufficient to achieve the accuracy level obtained from higher lidar point densities.

Plot-level mean height, dominant height, and volume of trees were estimated for trees located using local maxima filtering approaches at the three lidar point densities. Mean height and dominant height were both estimated at high accuracies for all local maxima filtering techniques and lidar point densities. The results were also comparable to the approach that employed regression analysis that related lidar-derived distributional metrics and field measurements. Estimated dominant height and SPHA, as well as age of trees, were used as independent variables in a function to estimate plot-level basal area. The basal area was then used to compute diameter of the tree with mean basal area, referred to as quadratic mean diameter at breast height (QDBH). Mean tree height and QDBH were used as independent variables in a standard equation to calculate mean tree volume, which was then scaled up to the plot-level. All estimates for the local maxima filtering approaches and lidar point densities returned negatively biased volume, when compared to field observations. This was due to the underestimation of SPHA, which was used as a conversion factor in scaling up from tree-level to plot-level. Volume estimates across lidar point densities exhibited similarities. This suggests that low lidar point densities (e.g., 1 point/m^2) have potential for accurate volume estimation.

It was concluded that multiple forest structural attributes can be assessed using lidar data only. The accuracy of height derivation meets the standards set by field inventories. The underestimation of SPHA may be comparable to other studies that applied different methods. However, improved estimation accuracy is needed in order to apply the approaches to commercial forestry scenarios. The significance of improving SPHA estimation extends to improved volume estimation. In addition, the potential improvement should also take into consideration the density of lidar points, as this will impact on the cost of acquisition. This research has taken a significant step towards determining if lidar data can be used as a stand-alone remote sensing data source for assessment of structural plantation parameters. Not only does such an approach seem viable, but the lower required point densities will help to reduce acquisition costs significantly.

Preface

This research was undertaken at the Forestry and Forest Products Research Centre (FFP) in Durban, KwaZulu-Natal, South Africa during August 2005 through March 2009. FFP is a centre established by Natural Resources and the Environment division of the Council for Scientific and Environmental Research (CSIR) and the University of KwaZulu-Natal (UKZN).

The supervisors of the research were:

Prof. Fethi Ahmed, School of Environmental Sciences, University of KwaZulu-Natal, South Africa.

Dr. Jan van Aardt, Rochester Institute of Technology, Centre for Imaging Science - Laboratory for Imaging Algorithms and Systems, Rochester, NY, 14623, USA.

I would like to declare that the work reported in this thesis has never been submitted in any form to any other university. It therefore represents my original work except where due acknowledgments are made.

Solomon G. Tesfamichael _____ March 2009

As the candidate's supervisors, we certify the above statement and have approved this thesis for submission.

1. Prof. Fethi Ahmed Signed: _____ Date: _____

2. Dr. Jan van Aardt Signed: _____ Date: _____

Declaration 1 - Plagiarism

I, Solomon G. Tesfamichael, declare that:

1. The research reported in this thesis, except where otherwise indicated, is my original research.

2. This thesis has not been submitted for any degree or examination at any other university.

3. This thesis does not contain other persons' data, pictures, graphs or other information, unless specifically acknowledged as being sourced from other persons.

4. This thesis does not contain other persons' writing, unless specifically acknowledged as being sourced from other researchers. Where other written sources have been quoted, then:
   a. Their words have been re-written but the general information attributed to them has been referenced
   b. Where their exact words have been used, then their writing has been placed in italics and inside quotation marks, and referenced.

5. This thesis does not contain text, graphics or tables copied and pasted from the Internet, unless specifically acknowledged, and the source being detailed in the thesis and in the References sections.

Signed _____

Declaration 2 - Publications

1. Roberts, J. W., Tesfamichael, S., Gebreslasie, M., van Aardt, J., and Ahmed, F. B. 2007. Forest structural assessment using remote sensing technologies: an overview of the current state of the art. *Southern Hemisphere Forestry Journal*. 69, 183 – 203.

2. Tesfamichael, S. G., Ahmed, F. B., and van Aardt, J. A. N. Accepted. Investigating the impact of discrete return lidar point density on estimations of mean and dominant plot-level tree height in *Eucalyptus grandis* plantations. *International Journal of Remote Sensing*.

3. Tesfamichael, S. G., Ahmed, F. B., van Aardt, J. A. N., and Blakeway, F. In Press. A semi-variogram approach for estimating stems per hectare in *Eucalyptus grandis* plantations using discrete return lidar height data. *Forest Ecology and Management*.

4. Tesfamichael, S. G., van Aardt, J. A. N., and Ahmed, F. B. In Review. Estimating plot-level tree height and volume of *Eucalyptus grandis* plantations using small-footprint, discrete return lidar as singular data source. *ISPRS Journal of Photogrammetry and Remote Sensing*.

Paper 1 was written by Roberts, Tesfamichael, and Gebreslasie. The last two co-authors edited the paper in their capacity as supervisors. Tesfamichael was responsible for the part related to the application of active remote sensing in forest structural assessment.

Tesfamichael was responsible for the conceptual development, analysis, and writing papers 2, 3, and 4. The contribution of the co-authors was providing comments during the analysis stage, as well as editing of the manuscripts.

Signed _____

Dedication

To my family who is always encouraging me with words of God.

Success

“Unless the Lord builds the house,
its builders will have toiled in vain.
Unless the Lord keeps watch over a city,
in vain the watchman stands on guard.
In vain you rise up early and go late to rest,
toiling for the bread you eat;
he supplies the need of those he loves.”
Psalms 127:1-2

Acknowledgments

The financial support for the study and my living allowance was provided by a cooperative, MONDI South Africa Division (MONDI SA) – Council for Scientific and Industrial Research (CSIR) Remote Sensing Cooperative, which was initiated at the CSIR's Forestry and Forest Products Research Centre (FFP). This study has really given me the opportunity to upgrade my skills in conducting research. It has also significantly improved my knowledge of forestry and the importance of remotely-sensed data in forestry.

I am in debt to many people who contributed for the realisation of the work, the results of which are presented in this thesis. I would like to thank Prof. Fethi Ahmed for all his support during the course of the study as a supervisor. He gave me the opportunity to undertake this study, following his supervision of my M.Sc. work. As usual, he was always available whenever needed. His continuous monitoring and unwavering encouragement was an important impetus in my work. Thank you very much for believing in my dedication to research.

My thanks also go to Dr. Jan van Aardt. His coming on board as a supervisor was immense particularly due to his own recent Ph.D. study involving lidar applications in forestry. The wealth of knowledge he had from such an involvement meant that I would never deviate from the realities of what lidar can or cannot achieve. His critical comments helped me improve on my knowledge in different ways, including lidar-forest subject matter and writing skills. It really was a privilege to share all my ideas in the study with him as I always received more feedback than I bargained for.

The field data collection was conducted by myself, Wesley Roberts, Michael Gebreslasie, Wesley Naidoo, and Thamsanqa Mzinyane. The data were used by the first three on the list, all of whom were undertaking concurrent studies. I especially would like to extend my sincere gratitude to Wesley Naidoo and Thamsanqa Mzinyane for making the usually difficult task of forest inventory an enjoyable experience. They showed me how such a task could be met with fun.

Wesley Roberts (GIS/Remote Sensing Researcher: Earth Observation, CSIR) was always there, happy and ready, to help me with all the manuscripts. His comments were constructive and focused. I would like to extend my sincere appreciation for all your help in shaping the papers up considerably. I am also indebted to Dr. Mark Norris-Rogers (GIS/Remote Sensing Specialist: MONDI SA Forest Operations) for his critical comments that came with all his experience in both remote sensing and plantation forestry.

I would also like to thank Felicity Blakeway (Competence Area Manager: Forestry, CSIR) for all her support. Apart from laying the platform for the study, she was also involved in offering critical comments on the outputs of the respective studies, as well as proof reading the thesis.

My special thanks also goes to Dr. Tammy Bush (Research Group Leader: FFP, CSIR) for facilitating all aspects of administrative matters in a very timely manner. Her personal advice and encouragements on capacity building and career development will never be forgotten.

I am grateful to Sue Price (UKZN) for helping me in outsourcing the literature. Her dedication was to the extent that she became familiar with my specific needs and knew what is relevant or not to my study. Sue, you also showed me what I was missing for a very long time – going to Church. The words of God are truly energising and bring hope to my life.

Table of contents

List of figures

List of tables

Abbreviations

ALS	Airborne Laser Solutions
ANN	Artificial Neural Network
ANOVA	Analysis of Variance
(A)SAR	(Advanced) Synthetic Aperture Radar
ASTER	Advanced Spaceborne Thermal Emission and Reflection Radiometer
BA	Basal Area
CASI	Compact Airborne Spectrographic Imager
CCA	Canonical Correlation Analysis
CHM	Canopy Height Model
CSIR	Council for Scientific and Industrial Research
CV	Coefficient of Variation
DEM	Digital Elevation Model
DTM	Digital Terrain Model
DWAF	Department of Water Affairs and Forestry
ESRI	Environmental Systems Research Institute
E(TM)	(Enhanced) Thematic Mapper
FFP	Forestry and Forest Products Research Centre
FAO	Food and Agriculture Organisation of the United Nations
GDP	Gross Domestic Product
GIS	Geographic Information System
GLCM	Grey-level Co-occurrence Matrix
(D)GPS	(Differential) Global Positioning System
HH / VH / HV / VV	Horizontal-Horizontal / Vertical-Horizontal / Horizontal-Vertical / Vertical-Vertical
IMU	Inertial Management Unit
INS	Inertial Navigation System
JERS	Japanese Earth Resources Satellite
k-NN	k-Nearest Neighbours
LAI	Leaf Area Index
Lidar	Light Detection And Ranging

LM	Local Maxima
MAE	Mean Absolute Error
MEIS	Multi-detector Electro-optical Imaging Sensor
MLC	Maximum Likelihood Classification
MONDI SA	Mondi South Africa
NASA/JPL	National Aeronautics and Space Administration/Jet Propulsion Laboratory
NDVI	Normalise Difference Vegetation Index
PRESS	Prediction Residual Sum of Squares
(Q)DBH	(Quadratic mean) Diameter at Breast Height
RMSE	Root Mean Square Error
Radar	Radio Detection And Ranging
SAS	Statistical Analysis Software
SD	Standard Deviation
SFRA	Stream Flow Reduction Activity
SLICER	Scanning Lidar Imager of Canopies By Echo Recovery
SPHA	Stems Per Hectare
SPOT	Systeme Probatoire d'Observation de la Terra
SR	Simple Ratio
TIDA	Tree Identification and Delineation Algorithm
UKZN	University of KwaZulu-Natal
WGS	World Geodetic System

Units of measurement

°	degrees of arc
%	percent
^{o}C	degree Celsius
mm	millimetre
cm	centimetre
m	metre
km	kilometre
mrad	milliradians
dB	decibel

ha	hectare
t/ha	tonnes per hectare
kHz	kilohertz
nm	nanometre

CHAPTER ONE

GENERAL INTRODUCTION

1.1 Forest structural assessment and remote sensing

Forest structural attributes refer to the size, shape, and distribution of forest components in both the horizontal and vertical dimensions (Parker, 1995; Spies, 1998). In timber resource management, the most important structural characteristics include areal coverage of a stand, canopy height, canopy cover, tree diameter, and volume. Measurement of these attributes is a crucial part of forest management and can be accomplished using different methods. Avery and Burkhart (2001) summarised three types of measurements: direct, sampling, and predictive. Direct measurements involve the quantification of attributes through close observation of the object of interest. This method, however, has limited application due to the difficulty of measuring individual trees within a population. As a result, conducting measurements on a specified number of trees selected through a sampling strategy is a common choice of measurement. Measurement by prediction is concerned mainly with attributes that are derived from relatively easily and directly measurable attributes such as diameter at breast height (DBH) and tree height. Typical examples of predicted forest attributes are volume and biomass. All three methods of measuring forest structural attributes involve field visits that are labour-intensive and expensive (von Gadow and Bredenkamp, 1992; Schreuder *et al*., 1993; Avery and Burkhart, 2001). However, the application of remote sensing technologies in forestry has shown relative success in addressing these constraints. Furthermore, such technologies provide a synoptic view of often extensive areas with continuous spatial coverage, including places that are difficult to access during field visits.

Optical imagery is the earliest remote sensing technology employed in forestry (Boyd and Danson, 2005). Advances of the technology over the years have resulted in significant improvements in spatial and spectral resolutions that are suitable for detailed information extraction (Wulder, 1998; Boyd and Danson, 2005). This, in combination with development in sophisticated machine computing capabilities, has

enabled the characterisation of forest attributes at even the tree-level (e.g., Gougeon, 1995; Dralle and Rudemo, 1996; Brandtberg and Walter, 1998; Wulder *et al*., 2000; Pouliot *et al*., 2002; Pollock, 1998; Wang *et al*., 2004, Chubey *et al*., 2006). Spectral, spatial, and textural information are important features of imagery in structural characterisations (Wulder, 1998). Structural attributes derived from these features are mostly related to the horizontal dimension of forests. Specific examples of such attributes include forest area holding (Wynne *et al*., 2000; Chubey *et al*., 2006), crown cover (Wu and Strahler, 1994; Ozdemir, 2008; Song and Dickinson, 2008), leaf area index (LAI) (McAllister and Valeo, 2007; Song and Dickinson, 2008), and stand density (Wu and Strahler, 1994; Franco-Lopez *et al*., 2001). Attributes that require inputs from the vertical dimension such as height, volume, and biomass, are often inferred empirically from attributes with horizontal features (e.g., Mäkelä and Pekkarinen, 2001; Hall *et al*., 2006; Chubey *et al*., 2006; Ozdemir, 2008). Another common shortcoming relates to the saturation of information embedded in optical imagery at high levels of biomass or leaf area index (Sader *et al*., 1989; Nemani *et al*., 1993; Foody and Curran, 1994; Chen and Cihlar, 1996; Steininger, 1996; Turner *et al*., 1999; Lu, 2006).

1.2 Forest structural assessment and lidar data

Research has shown that lidar (light detection and ranging) remote sensing overcomes many of the constraints of optical data. As such, lidar remote sensing is designed to capture information both in the horizontal and vertical dimensions, as well as discerning structural variations at high biomass levels (Lefsky *et al*., 2002). As an active system, a lidar sensor emits high frequency laser pulses of short wavelength electromagnetic energy and records the total travel time of the reflected pulses. Travel time is converted to distance using the speed of light and provides a measurement of distance between the sensor and the reflecting object (Baltsavias, 1999; Wehr and Lohr, 1999). A GPS unit integrated into the sensor records the geographical position of each pulse. Lidar systems are generally divided into two categories based on the mode of recording reflected pulses: waveform and discrete return systems (Wehr and Lohr, 1999). Waveform lidar captures reflectance in near-continuous time intervals, while discrete return systems record a specified number of

returns from each reflected pulse. A further parameter distinguishing the two lidar systems is the typically larger footprint size of pulses of the waveform system compared to discrete return systems (Dubayah and Drake, 2000). Recent developments, however, have introduced waveform recording at small-footprint sizes (Wagner *et al*., 2008; Reitberger *et al*., In Press). Such systems are not discussed here, given the infant stage they are currently in.

Waveform lidar systems offer the opportunity of capturing information over the entire range of the vertical dimension of forest components (Lefsky *et al*., 1999a; Lim *et al*., 2003). Thus, canopy components ranging from the top to the ground underneath are sampled accurately (Mallet and Bretar, 2009). The degree of accuracy at which various forest structural attributes are estimated using these systems has been proven adequate (Blair *et al*., 1999; Lefsky *et al*., 1999a, b; Means *et al*., 1999; Harding *et al*., 2001; Drake *et al*., 2002; Hyde *et al*., 2005). However, there are a number of factors limiting the application of waveform recording systems. First, the large footprint size of the pulses implies that multiple trees are aggregated and thus trees are not characterised individually (Lim *et al*., 2003), with the exception of latest systems (Wagner *et al*., 2008; Reitberger *et al*., In Press). Second, a large volume of data is captured due to the continuously digitised reflectance and this would require considerable storage space and processing resources (Mallet and Bretar, 2009). Third, only a few operational systems exist currently and these are accessible mainly to the research community. This particular aspect arguably is the main reason for the failure of introducing these systems to operational forestry management scenarios in many parts of the world.

Discrete return, small-footprint lidar data are widely used by foresters and researchers alike, given the ever-increasing commercial firms involved in the provision of such data. Derivation of forest structural attributes using small-footprint lidar data can generally be categorised into two approaches depending on the scale and accuracy needed and the density of lidar pulses employed (Reutebuch *et al*., 2005; Hyyppä *et al*., 2008). These are canopy height distribution methods that quantify aggregate features of trees in a given area and may not require a high density of pulses. Such a distributional approach derives statistical metrics, e.g.,

canopy height and canopy density, at various percentiles/quantiles and relates them to forest inventory data using regression analysis (Lefsky *et al*., 2001; Næsset, 2002; Holmgren, 2004; Næsset, 2004; Hall *et al*., 2005; Thomas *et al*., 2006; van Aardt *et al*., 2006; Næsset, 2007; Jensen *et al*., 2008). It is evident that regression functions must be robust if they are to be used for prediction purposes. Moreover, models may not be transferable across forest types, therefore the development and/or modification of a model representing each forest type or geographical region is necessary.

Assessment of structural attributes at the tree-level requires locating individual trees. Various methods of tree identification exist with most of them originally developed for optical imagery (Hyyppä *et al*., 2004). Height information and spatial relation among neighbouring samples are the main features of lidar data employed in the identification process. The most common tree identification method is local maxima filtering which searches for 'tree top' using a moving window over an interpolated lidar canopy height model surface (Popescu *et al*., 2002; McCombs *et al*., 2003; Hyyppä *et al*., 2004; Maltamo *et al*., 2004; Kwak *et al*., 2007). Popescu *et al*. (2003) used a variable window size to segment crowns of individual trees and eventually estimate plot-level tree volume and biomass. Morsdorf *et al*. (2004) applied clustering of lidar pulses around points chosen using local maxima filtering. Kwak *et al*. (2007) adopted watershed segmentation to delineate individual trees and consequently estimate tree height. A similar segmentation approach was followed by Heurich (2008) to derive tree height and crown diameter which are then used to estimate volume. Accuracy of detecting individual trees compared to field mapped trees is rather low in most of the aforementioned studies. This is one of the primary reasons for the slow integration of lidar data into operational management of forestry and in particular in the commercial sector which requires high-accuracy measurements. In addition, the cost of lidar data acquisition is higher for individual tree-based assessment than for area-based assessment, since greater laser pulse density is often required in the former case (Reutebuch *et al*., 2005; Hyyppä *et al*., 2008; Næsset, 2009). Finally, the geographical and species context of forestry-specific lidar studies also deserves mention.

The majority of the lidar studies targeted forest types, such as pine trees, that are characterised by conical geometrical shapes of tree crowns. Forest types such as *Eucalyptus* species, which are generally characterised by elliptical/rounded crown shapes, have attracted little attention with only a few documented studies (e.g., Goodwin *et al*., 2006; Tickle *et al.*, 2006). Nelson (1997) demonstrated that canopy shape affects laser return characteristics, as reflected by eventual height estimation accuracies. More research is therefore needed to investigate the utility of lidar data in characterising the structural attributes of *Eucalyptus* plantations.

1.3 Objectives of the study

The main aim of this study was to derive forest structural attributes for even-aged *Eucalyptus grandis* plantations in KwaZulu-Natal, South Africa, using small-footprint, discrete return lidar data. The age per stand of the plantations at the time of the survey ranged four to nine years old. The selection of these plantations for this is justified by a number of reasons. Firstly, there is a strong desire within the forestry community to investigate the utility of lidar remote sensing for estimation of structural attributes at suitable accuracy. Secondly, most studies in the field of lidar-forestry have focussed on boreal forests of the northern hemisphere and thus little is done on Eucalyptus species. Thirdly, the methods that were applied in this study especially to estimate timber volume have been developed exclusively for plantation environments.

The specific objectives of the study are given within each chapter whereas the following are the general objectives of the study:

1. To estimate plot-level mean and dominant tree height,
2. To derive stems per hectare from canopy height models using local maxima filtering, and
3. To estimate plot-level volume from lidar-derived height and stems per hectare.

1.4 Significance of the study

Forest ecosystems in South Africa have a relatively low spatial coverage due mainly to limited rainfall in most parts of the country (DWAF, 2008). Natural forests cover approximately 0.5 million ha, while commercial plantation forests make up about 1.4 million ha out of a total land area of 122.1 million ha (DWAF, 2008). Despite the small areal coverage, the forestry sector plays a significant role in the country's economy. The commercial sector alone contributes up to 2% of the GDP. Forestry also contributes up to 9% of the country's agricultural output and 4% of total export (DWAF, undated). According to the Department of Water Affairs and Forestry (DWAF) figures compiled in 2007, hardwood species cover 47% of the forested areas. Of these, *Eucalyptus grandis* is the dominant single species with a coverage of 46%. Evidence from the past few years indicates that there is an increase in the proportion of this particular species or its clones (DWAF, 2008). More than 80% of *Eucalyptus* species are younger than nine years (DWAF, 2008), which is indicative of the quick harvest cycle of the species. It is therefore clear that there is an ever-increasing demand for the species, which necessitates more focused management efforts to optimise its usage. In this regard, the use of lidar data to extract the main forest structural attributes associated with *E. grandis* timber characteristics has great promise. If the results of this study are deemed satisfactory in context of the ultimate goals, the advantages of lidar will prove to be immense in minimising overall cost of forest inventories, since the need for field inventory will be minimised. This is accomplished due to the fact that field inventory data are only required at the initial, model development and validation stages. A comparison of lidar point densities will furthermore determine the optimal density level required for deriving or estimating an attribute. A suitable accuracy for attribute estimation at a relatively low density level will translate into an economically affordable lidar data acquisition.

1.5 Description of study area

The study area is located within Sisonke municipality in the KwaZulu-Natal province of South Africa (Figure 1.1). It is approximately 50 km south of Pietermaritzburg, near the town of Richmond. The topography of the Richmond area is flat with undulating hills and is classified by Schulze (1997) as being low mountains. Altitude ranges from 300 m to over 2100 m above mean sea level with an average of approximately 874 meters. The soils in the area are characterised by fine sandy clay, humic topsoils, underlain by yellow or red apedal subsoils. Inanda and Magwa soil forms dominate the area (both approximately similar to Humic Ferralsol – FAO), with Hutton (Ferrasols – FAO) being the subdominant soil form (Soil Classification Working Group, 1991). Clay content varies between 34% and 45% in topsoil horizons, while deeper soils contain up to 60% clay. Mean annual rainfall in the area ranges from 746 mm to 1100 mm, with most of the rain falling during summer (Schulze, 1997). Rainfall is associated with either frontal weather systems originating from the south or thunderstorms generated from convection activity. Winters are cold and dry, while summers are characterised by warm and wet climate. Temperatures in general range from the high 20's to below 10 ^{o}C.

The primary land use in the Richmond area is agriculture, including plantation forestry, sugar cane, and dairy farming. Local subsistence farming also takes place in and around rural villages. Richmond forests fall within Zone 7 (KwaZulu-Natal Midlands) of the Forestry Economic Zones of the country that were demarcated based on political, physical, silvicultural, economic, and historic considerations (DWAF, 2008). This zone is one of the three predominant zones in terms of spatial coverage of the forests (Smith *et al*., 2005). Plantation forests in the area comprise both hardwood and softwood species that are grown primarily for pulp and paper production, while smaller industries in the area use timber for furniture and construction purposes. Softwood species include pine species with *Pinus patula, P. taeda,* and *P. elliottii* being predominant, while hardwood species are either from the *Eucalyptus* (gum) or *Acacia* (wattle) genera. The *Eucalyptus* species can be categorised into two groups based on their wood density. Soft gums, with a relatively low wood density, are grown in the warm areas and hard gums, characterised by

high wood density, are typically grown in colder climates than soft gums. Soft gum species include *Eucalyptus saligna* and *E. grandis*, while hard gums include the *E. dunnii, E. nitens*, and *E. smithii* variants. The forestry industry recently has introduced clonal hybrids such as *E. grandis* x *E. nitens* (Norris-Rogers, 2006). This study will focus on *E. grandis*. The sites of the study are all managed by the Midlands District of MONDI SA.

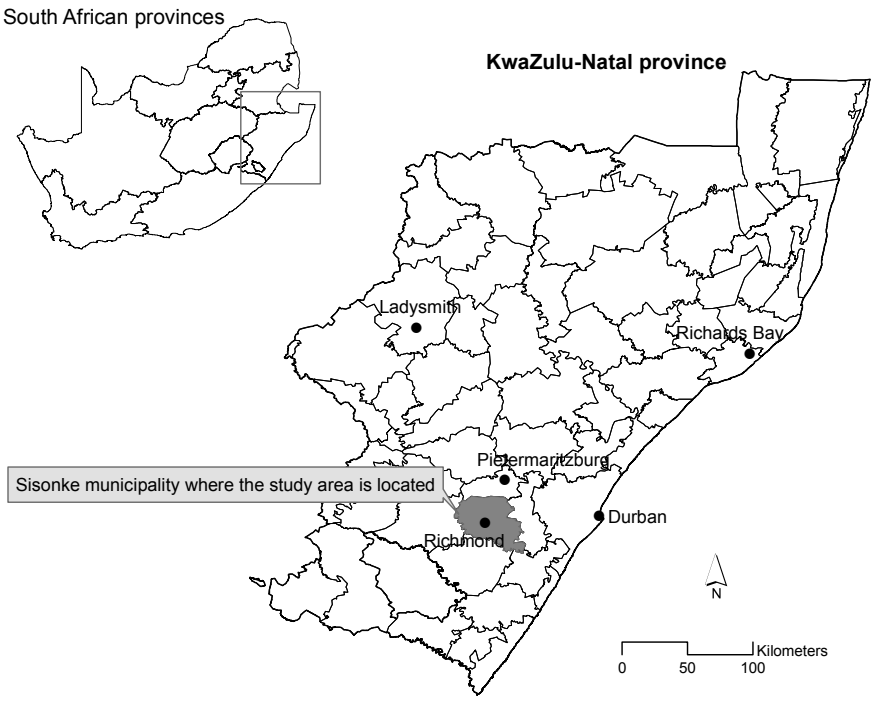

Figure 1.1 Map of the study area located in KwaZulu-Natal, South Africa.

1.6 Outline of the thesis

The thesis is presented as a collection of full length research papers addressing the general objectives listed above. Chapter 2 relates to revision of the literature on forest structural assessment using a suite of remote sensing technologies including optical, lidar, radar, and fused remotely-sensed data. The first three authors of this published paper are all involved in parallel studies towards Ph.D. degrees by focusing on different remote sensing systems. The author of this thesis contributed

to the section on active remote sensing applications in forestry. The latest lidar studies, published since the submission of the paper and that have immediate relevance to the various studies of the thesis, are included in Chapter 1, as well as the respective chapters. Chapter 3 is concerned with estimation of mean tree height and dominant height using lidar data at the plot-level. A distributional approach was used to estimate the attributes. Various lidar points were simulated to assess their effect on height estimations. This chapter has been accepted for publication in the International Journal of Remote Sensing. Chapter 4 investigates the applicability of semi-variogram range and a lidar canopy height model to determine local maxima filter size for estimating stems per hectare. Comparable filtering was performed based on pre-determined tree spacing. The paper of this chapter is in press in the journal ‘Forest Ecology and Management”. The estimation of plot-level mean height, dominant height, and volume were described in Chapter 5. Height attributes were derived based on trees located in Chapter 4, which in combination with stems per hectare, were used to estimate volume. This chapter is under review in a peer reviewed journal. Finally, Chapter 6 provides a general summary and conclusions of the results from the different studies reported in the preceding chapters.

References

Avery, T. E. and Burkhart, H. E. 2001. *Forest Measurements*. 5th edition. McGraw-Hill, New York. 456 pp.

Baltsavias, E. P. 1999. Airborne laser scanning: basic relations and formulas. *ISPRS Journal of Photogrammetry and Remote Sensing*. 54, 199 – 214.

Blair, J. B., Rabine, D. L., and Hofton, M. A. 1999. The Laser Vegetation Imaging Sensor: a medium-altitude, digitisation-only, airborne laser altimeter for mapping vegetation and topography. *ISPRS Journal of Photogrammetry and Remote Sensing*. 54, 115 – 122.

Boyd, D. S. and Danson, F. M. 2005. Satellite remote sensing of forest resources: three decades of research development. *Progress in Physical Geography*. 29, 1 – 26.

Brandtberg, T. and Walter, F. 1998. Automated delineation of individual tree crowns in high spatial resolution aerial images by multiple-scale analysis. *Machine Vision and Applications*. 11, 64 – 73.

Chen, J. M. and Cihlar, J. 1996. Retrieving leaf area index of boreal conifer forests using Landsat TM images. *Remote Sensing of Environment*. 55, 153 – 162.

Chubey, M. S., Franklin, S. E., and Wulder, M. A. 2006. Object-based analysis of IKONOS-2 imagery for extraction of forest inventory parameters. *Photogrammetric Engineering and Remote Sensing*. 72, 383 – 394.

Drake, J. B., Dubayah, R. O., Clark, D. B., Knox, R. G., Blair, J. B., Hofton, M. A., Chazdon, R. L., Weishampel, J. F., and Prince, S. D. 2002. Estimation of tropical forest structural characteristics using large-footprint lidar. *Remote Sensing of Environment*. 79, 305 – 319.

Dralle, K. and Rudemo, M. 1996. Stem number estimation by kernel smoothing of aerial photos. *Canadian Journal of Forest Research*. 26, 1228 – 1236.

Dubayah, R. O. and Drake, J. B. 2000. Lidar remote sensing for forestry. *Journal of Forestry*. 98, 44 – 46.

DWAF. undated. *Strategic plan 2007/08-2009/10*. Department of Water Affairs and Forestry. Pretoria, South Africa.

DWAF. 2008. *Report on commercial timber resources and primary roundwood processing in South Africa 2006/2007*. Department of Water Affairs and Forestry. Pretoria, South Africa.

Foody, G. M. and Curran, P. J. 1994. Estimation of tropical forest extent and regenerative stage using remotely-sensed data. *Journal of Biogeography*. 21, 223 – 244.

Franco-Lopez, H., Ek, A. R., and Bauer, M. E. 2001. Estimation and mapping of forest stand density, volume, and cover type using the k-nearest neighbours method. *Remote Sensing of Environment*. 77, 251 – 274.

Goodwin, N. R., Coops, N. C., and Culvenor, D. S. 2006. Assessment of forest structure with airborne lidar and the effects of platform altitude. *Remote Sensing of Environment*. 103, 140 – 152.

Gougeon, F. A. 1995. A crown-following approach to the automatic delineation of individual tree crowns in high spatial resolution aerial images. *Canadian Journal of Remote Sensing*. 21, 274 – 284.

Hall, R. J., Skakun, R. S., Arsenault, E. J., and Case, B. S. 2006. Modelling forest stand structure attributes using Landsat ETM+ data: application to mapping of aboveground biomass and stand volume. *Forest Ecology and Management*. 225, 378 – 390.

Hall, S. A., Burke, I. C., Box, D. O., Kaufmann, M. R., and Stoker, J. M. 2005. Estimating stand structure using discrete return lidar: an example from low density, fire prone ponderosa pine forests. *Forest Ecology and Management*. 208, 189 – 209.

Harding, D. J., Lefsky, M. A., Parker, G. G., and Blair, J. B. 2001. Laser altimeter canopy height profiles: methods and validation for closed-canopy, broadleaf forests. *Remote Sensing of Environment*. 76, 283 – 297.

Heurich, M. 2008. Automatic recognition and measurement of single trees based on data from airborne laser scanning over the richly structured natural forests of the Bavarian Forest National Park. *Forest Ecology and Management*. 255, 2416 – 2433.

Holmgren, J. 2004. Prediction of tree height, basal area, and stem volume in forest stands using airborne laser scanning. *Scandinavian Journal of Forest Research*. 19, 543 – 553.

Hyde, P., Dubayah, R., Peterson, B., Blair, J. B., Hofton, M., Hunsaker, C., Knox, R., and Walker, W. 2005. Mapping forest structure for wildlife habitat analysis using waveform lidar: validation of montane ecosystems. *Remote Sensing of Environment*. 96, 427 – 437.

Hyyppä, J., Hyyppä, H., Leckie, D., Gougeon, F., Yu, X., and Maltamo, M. 2008. Review of methods of small-footprint airborne laser scanning for extracting forest inventory data in boreal forests. *International Journal of Remote Sensing*. 29, 1339 – 1366.

Hyyppä, J., Hyyppä, H., Litkey, P., Yu, X., Haggrén, H., Rönnholm, P., Pyysalo, U., Pitkänen, J., and Maltamo, M. 2004. Algorithms and methods of airborne laser scanning for forest measurements. *International Archives of Photogrammetry, Remote Sensing, and Spatial Information Sciences*. Vol. 36-8/W2, 82 – 89.

Jensen, J. L. R., Humes, K. S., Vierling, L. A., and Hudak, A. T. 2008. Discrete return lidar-based prediction of leaf area index in two conifer forests. *Remote Sensing of Environment*. 112, 3947 – 3957.

Kwak, D. A., Lee, W. K., Lee, J. H., Biging, G. S., and Gong, P. 2007. Detection of individual trees and estimation of tree height using lidar data. *Journal of Forest Research*. 12, 425 – 434.

Lefsky, M. A., Cohen, W. B., Acker, S. A., Parker, G. G., Spies, T. A., and Harding, D. 1999a. Lidar remote sensing of the canopy structure and biophysical properties of Douglas-fir western Hemlock forests. *Remote Sensing of Environment*. 70, 339 – 361.

Lefsky, M. A., Harding, D., Cohen, W. B., Parker, G., and Shugart, H. H. 1999b. Surface lidar remote sensing of basal area and biomass in deciduous forests of eastern Maryland, USA. *Remote Sensing of Environment*. 67, 83 – 98.

Lefsky, M. A., Cohen, W. B., and Spies, T. A. 2001. An evaluation of alternate remote sensing products for forest inventory, monitoring, and mapping of Douglas-fir forests in western Oregon. *Canadian Journal of Forest Research*. 31, 78 – 87.

Lefsky, M. A., Cohen, W. B., Parker, G. G., and Harding, D. J. 2002. Lidar remote sensing for ecosystem studies. *Bioscience*. 52, 19 – 30.

Lim, K., Treitz, P., Wulder, M., St-Onge, B., and Flood, M. 2003. Lidar remote sensing of forest structure. *Progress in Physical Geography*. 27, 88 – 106.

Lu, D. 2006. The potential and challenge of remote sensing-based biomass estimation. *International Journal of Remote Sensing*. 27, 1297 – 1328.

Mäkelä, H. and Pekkarinen, A. 2001. Estimation of timber volume at the sample plot-level by means of image segmentation and Landsat TM imagery. *Remote Sensing of Environment*. 77, 66 – 75.

Mallet, C. and Bretar, F. 2009. Full-waveform topographic lidar: state-of-the-art. *ISPRS Journal of Photogrammetry and Remote Sensing*. 64, 1 – 16.

Maltamo, M., Eerikäinen, K., Pitkänen, J., Hyyppä, J., and Vehmas, M. 2004. Estimation of timber volume and stem density based on scanning laser altimetry and expected tree size distribution functions. *Remote Sensing of Environment*. 90, 319 – 330.

McAllister, D. M. and Valeo, C. 2007. A robust new method for the remote estimation of LAI in montane and boreal forests. *International Journal of Remote Sensing*. 28, 1891 – 1905.

McCombs, J. W., Roberts, S. D., and Evans, D. L. 2003. Influence of fusing lidar and multispectral imagery on remotely-sensed estimates of stand density and mean tree height in a managed loblolly pine plantation. *Forest Science*. 49, 457 – 466.

Means, J. E., Acker, S. A., Harding, D. J., Blair, J. B., Lefsky, M. A., Cohen, W. B., Harmon, M. E., and McKee, W. A. 1999. Use of large-footprint scanning airborne lidar to estimate forest stand characteristics in the western cascades of Oregon. *Remote Sensing of Environment*. 67, 298 – 308.

Morsdorf, F., Meier, E., Kötz, B., Itten, K. I., Dobbertin, M., and Allgöwer, B. 2004. Lidar-based geometric reconstruction of boreal type forest stands at single tree-level for forest and wildland fire management. *Remote Sensing of Environment*. 92, 353 – 362.

Næsset, E. 2002. Predicting forest stand characteristics with airborne scanning laser using a practical two-stage procedure and field data. *Remote Sensing of Environment*. 80, 88 – 99.

Næsset, E. 2004. Practical large scale forest stand inventory using a small-footprint airborne scanning laser. *Scandinavian Journal of Forest Research*. 19, 164 – 179.

Næsset, E. 2007. Airborne laser scanning as a method in operational forest inventory: status of accuracy assessments accomplished in Scandinavia. *Scandinavian Journal of Forest Research*. 22, 433 – 442.

Næsset, E. 2009. Effects of different sensors, flying altitudes, and pulse repetition frequencies on forest canopy metrics and biophysical stand properties derived from small-footprint airborne laser data. *Remote Sensing of Environment*. 113, 148 – 159.

Nelson, R. 1997. Modelling forest canopy heights: the effects of canopy shape. *Remote Sensing of Environment*. 60, 327 – 334.

Nemani, R. R., Pierce, L., Running, S., and Band, L. 1993. Forest ecosystem processes at the watershed scale: sensitivity to remotely-sensed leaf area index estimates. *International Journal of Remote Sensing*. 14, 2519 – 2534.

Norris-Rogers, M. 2006. *An investigation into using textural analysis and change detection techniques on medium and high spatial resolution imagery for monitoring plantation forestry operations*. Ph.D. Thesis. University of KwaZulu-Natal, Pietermaritzburg, South Africa. 241 pp.

Ozdemir, I. 2008. Estimating stem volume by tree crown area and tree shadow area extracted from pan-sharpened Quickbird imagery in open Crimean juniper forests. *International Journal of Remote Sensing*. 29, 5643 – 5655.

Parker, A. 1995. Structure and microclimate of forest canopies. In: Lowman, M. and Nadkarni, N. (Eds.), *Forest canopies — a review of research on a biological frontier*. Academic Press, San Diego, CA. pp. 73 – 106.

Pollock, R. 1998. Individual tree recognition based on a synthetic tree crown image model. *Proceedings of the International Forum on Automated Interpretation of High Spatial Resolution Digital Imagery for Forestry*. 10–12 February. Pacific Forestry Centre, Canada Forest Service, Natural Resources Canada, Victoria, BC, Canada. pp. 25 – 34.

Popescu, S. C., Wynne, R. H., and Nelson, R. F. 2002. Estimating plot-level tree heights with lidar: local filtering with a canopy height based variable window size. *Computers and Electronics in Agriculture*. 37, 71 – 95.

Popescu, S. C., Wynne, R. H., and Nelson, R. F. 2003. Measuring individual tree crown diameter with lidar and assessing its influence on estimating forest volume and biomass. *Canadian Journal of Remote Sensing*. 29, 564 – 577.

Pouliot, D. A., King, D. J., Bell, F. W., and Pitt, D. G. 2002. Automated tree crown detection and delineation in high resolution digital camera imagery of coniferous forest regeneration. *Remote Sensing of Environment*. 82, 322 – 334.

Reitberger, J. Schnörr, Cl., Krzystek, P., and Stilla, U. In Press. 3D segmentation of single trees exploiting full waveform lidar data. *ISPRS Journal of Photogrammetry and Remote Sensing* (2009), doi:10.1016/j.isprsjprs. 2009.04.002.

Reutebuch, S. E., Anderson, H.-E., and McGaughey, R. J. 2005. Light detection and ranging (lidar): an emerging tool for multiple resource inventory. *Journal of Forestry*. 103, 286 – 292.

Sader, S. A., Waide, R. B., Lawrence, W. T., and Joyce, A. T. 1989. Tropical forest biomass and successional age class relationships to a vegetation index derived from Landsat TM data. *Remote Sensing of Environment*. 28, 143 – 156.

Schreuder, H. T., Gregoire, T. G., and Wood, G. B. 1993. *Sampling methods for multisource forest inventory*. John Wiley and Sons, New York. 464 pp.

Schulze, R. E. 1997. *South African Atlas of Agrohydrology and Climatology*. Water Research Commission, Pretoria, Report TT82/96. 286 pp.

Smith, C. W., Pallett, R. N., Kunz, R. P., Gardner, R. A. W., and du Plessis, M. 2005. A strategic forestry site classification for the summer rainfall region of southern Africa

based on climate, geology, and soils. *ICFR Bulletin 03/2005*. Institute for Commercial Forestry Research, Pietermaritzburg, South Africa. 36 pp.

Soil Classification Working Group. 1991. Soil classification: a taxonomic system for South Africa. *Memoirs on the Agricultural Resources of South Africa No 15.* Department of Agricultural Development, Pretoria, South Africa. 257 pp.

Song, C. and Dickinson, M. B. 2008. Extracting forest canopy structure from spatial information of high resolution optical imagery: tree crown size versus leaf area index. *International Journal of Remote Sensing*. 29, 5605 – 5622.

Spies, T. A. 1998. Forest structure: a key to the ecosystem. *Northwest Science*. 72, 34 – 39.

Steininger, M. K. 1996. Tropical secondary forest regrowth in the Amazon: age, area, and change estimation with thematic mapper data. *International Journal of Remote Sensing*. 17, 9 – 27.

Tickle, P. K., Lee, A., Lucas, R. M., Austin, J., and Witte, C. 2006. Quantifying Australian forest floristics and structure using small-footprint lidar and large scale aerial photography. *Forest Ecology and Management*. 223, 379 – 394.

Thomas, V., Treitz, P., McCaughey, J. H., and Morrison, I. 2006. Mapping stand-level forest biophysical variables for a mixedwood boreal forest using lidar: an examination of scanning density. *Canadian Journal of Forest Research*. 36, 34 – 47.

Turner, D. P., Cohen, W. B., Kennedy, R. E., Fassnacht, K. S., and Briggs, J. M. 1999. Relationship between leaf area index and Landsat TM spectral vegetation indices across three temperate zone sites. *Remote Sensing of Environment*. 70, 52 – 68.

van Aardt, J. A. N., Wynne, R. H., and Oderwald, R. G. 2006. Forest volume and biomass estimation using small-footprint lidar-distributional parameters on a per-segment basis. *Forest Science*. 52, 636 – 649.

von Gadow, K. and Bredenkamp, B. 1992. *Forest management*. Academica, Pretoria. 164 pp.

Wang, L., Gong, P., and Biging, G. S. 2004. Individual tree-crown delineation and treetop detection in high spatial resolution aerial imagery. *Photogrammetric Engineering and Remote Sensing*. 70, 351 – 358.

Wagner, W., Hollaus, M., Briese, C., and Ducic, V. 2008. 3D vegetation mapping using small-footprint full waveform airborne laser scanners. *Internation Journal of Remote Sensing*. 29, 1433 – 1452.

Wehr, A. and Lohr, U. 1999. Airborne laser scanning—an introduction and overview. *ISPRS Journal of Photogrammetry and Remote Sensing*. 54, 68 – 82.

Wu, Y. and Strahler, A. H. 1994. Remote estimation of crown size, stand density, and biomass on the Oregon transect. *Ecological Applications*. 4, 299 – 312.

Wulder, M. 1998. Optical remote-sensing techniques for the assessment of forest inventory and biophysical parameters. *Progress in Physical Geography*. 22, 449 – 476.

Wulder, M., Niemann, K. O., and Goodenough, D. G. 2000. Local maximum filtering for the extraction of tree locations and basal area from high spatial resolution imagery. *Remote Sensing of Environment*. 73, 103 – 114.

Wynne, R. H., Oderwald, R. G., Reams, G. A., and Scrivani, J. A. 2000. Optical remote sensing for forest area estimation. *Journal of Forestry*. 98, 31 – 36.

CHAPTER TWO

LITERATURE REVIEW

Based on

Roberts, J. W., Tesfamichael, S., Gebreslasie, M., van Aardt, J., and Ahmed, F. B. 2007. Forest structural assessment using remote sensing technologies: an overview of the current state of the art. *Southern Hemisphere Forestry Journal*. 69, 183 – 203.

Abstract

The Forestry and Forest Products Research Centre (CSIR), University of KwaZulu-Natal, and MONDI South Africa recently embarked on a remote sensing cooperative. The primary focus of this cooperative is to explore the potential benefits associated with using remote sensing for forestry related activities. A sub-project within the cooperative is exploring the utility of various remote sensing technologies for forest structural assessment. This paper reports on the primary findings of a state of the art review conducted by members of the cooperative and seeks to inform and contribute to the development of focussed research projects. Both active and passive sensors are reviewed at varying spatial scales focussing primarily on accuracies attained. Medium resolution studies focus on area-based forest attributes while high resolution studies focussed on individual tree-based forest attributes. Results from research consulted indicate that while remote sensing has a strong theoretical background, there are several limiting factors that need to be explored within a South African context. These include the saturation of satellite signals in mature forests, underestimation of tree heights using lidar data, and the cost of lidar surveys. The review ends with recommendations for future research activities.

2.1 Introduction

Commercial plantation forests play an important role in South Africa's economy with just over 1.3 million ha currently being cultivated (DWAF, 2005). Forestry products and related services contributed 1.54% to the country's GDP in 2003 (R12.2 billion), employing over 170 000 people in areas where little alternative employment exists (Chamberlain *et al.,* 2005). Products derived from the timber industry include pulp, paper, and solid wood products, earning R270 million in exports in 2003 (DWAF, 2005). Over and above the contribution made to the economy, both natural and commercial forests provide invaluable environmental services. For example, through photosynthesis, forests act as an atmospheric filter replacing carbon dioxide with oxygen (Beedlow *et al*., 2004). Carbon is stored in both above and below ground biomass as well as dead wood and litter. It is reported that over 900 million metric tonnes of carbon is stored in forests within the borders of South Africa (FAO, 2005)

with forestry activities offsetting approximately 3.8% of carbon dioxide emissions each year (Christie and Scholes, 1995).

The sector has come under increasing pressure since the early 1970's and especially after the first democratic elections in 1994 regarding the environmental impacts of timber plantations even though the benefits of the forestry industry in terms of economics and job creation are well-known (Tewari, 2001). Several impacts have been identified, including a loss of biological diversity (Heydenrych, 1995; Richardson, 1998), land degradation and associated soil compaction (Brink, 1990), as well as stream flow reduction (Schonau and Grey, 1987; Scott and Lesch, 1997). The environmental concerns culminated in the replacing of the old forestry permit scheme with a licensing system called the *stream flow reduction activity* (SFRA) regulated under the National Water Act (No 36 of 1998). Currently, afforestation is the only agricultural activity declared an SFRA and is seen as a limiting factor in terms of development within the forestry industry in the Eastern Cape and KwaZulu-Natal (Chamberlain *et al*., 2005). Due to fast growth and high yields the industry has an international competitive advantage. However, cheap imports from emerging growers in Asia and South America threaten to flood the international market and significantly reduce profit margins. Within the context of sustainable and environmentally friendly development the timber industry therefore needs to reduce operating costs while satisfying an ever vigilant environmental lobby seeking to highlight any mismanagement on the part of commercial growers. To achieve this, the industry should explore the potential benefits of using new and emerging technologies to streamline the forestry processing chain and minimise costs where necessary. One such area is that of forest assessment where inventory data relating to the standing population of trees is collected through *in situ* enumeration of forest resources. The process is time consuming and expensive and has long been identified as an area where improved technologies such as remote sensing in conjunction with Geographical Information Systems (GIS) may be used to reduce costs and improve upon inventory estimates (Leckie, 1990a).

Remote sensing is defined as a means of acquiring information about an object of interest without actually coming into contact with the object (Campbell, 2002). This

data is collected using either airborne or satellite borne sensors. In forestry, these objects are usually tree canopies or the gaps between the canopies. Remote sensing systems use either passive or active sensors to scan and record information about an object or area of interest. The most commonly used sensors are passive optical sensors which sample reflected light in the visible, near-, and middle-infrared portions of the electromagnetic spectrum (Hunt, 1980). These sensors can be used for many forestry related activities but are generally seen as providing information on the amount of foliage and the biochemical properties of vegetation. On the other hand, active systems, for example, include sensors that emit microwave pulses and record the backscatter from targets and are better suited to providing information on woody biomass and forest structure (Boyd and Danson, 2005). Synthetic Aperture Radar (SAR) systems are a useful alternative to the standard passive sensors with several advantages. Firstly, due to the active nature of the sensor it is not limited to daytime image capture; secondly, the sensor is impervious to clouds and can operate in almost any weather conditions; finally given the nature of the imaging system it is possible to acquire images at standard time intervals (Rauste, 2005). Both passive and active systems have been used in forestry-related research with passive optical systems seeing limited applications in operational forest inventory (Gjertsen *et al*., 1999; Tomppo and Heikkinen, 1999; Gillis, 2001; Remmel *et al*., 2005; Tomppo, 2005; McRoberts *et al.,* 2006). Another remote sensing system that has seen increased usage in forestry research is an active optical sensor known as Light Detection and Ranging (lidar) (Ackermann, 1999; Baltsavias, 1999). Lidar makes use of high energy laser pulses whereby the sensor measures the distance between the sensor and a target on the Earth (Wehr and Lohr, 1999). The end product is a data set that replicates the three dimensional structure of the area surveyed (Lefsky *et al*., 2002). Operational use of lidar is limited (Næsset, 2004), but while the sensor is recognised as being the future of forest assessment (Lim *et al*., 2003), the lack of imaging systems and the cost associated with performing a lidar survey means that it is still seen as a research, as opposed to an operational, tool (Suárez *et al*., 2005).

Previous reviews conducted by South African researchers have identified remote sensing as a suitable tool for a variety of applications. Lamb *et al.* (1986) reviewed

the use of what was then side-looking radar (now called synthetic aperture radar) for forestry applications and identified this technology as being complementary to passive optical sensors such as Landsat. Later, Thompson and Whitehead (1992) reviewed remote sensing tools for forestry and related activities. The authors noted that remote sensing could play a significant role in natural resource management, but that a lack of local expertise and the ability to integrate the tools into existing management systems has limited its application. Unfortunately, these problems persist and remote sensing tools are still not fully integrated into operational forest inventories. Notable research has also been conducted by Thomas *et al.* (1997), Kätsch and Vogt (1999), Kätsch and van Laar (2002), Ghebremicael *et al*. (2004) and Kätsch and Kunneke (2006), all of whom identify remote sensing as a tool that could be implemented into a variety of activities. However, this research lacks the involvement of commercial timber growing organisations and thus results and findings tend to remain within the academic sphere. What follows is a review of the current state-of-the-art in terms of forest assessment using remote sensing technologies. The review focuses on the published material, in particular the accuracies with which forest parameters are modelled using a variety of sensors and methods. The review seeks to understand and determine the appropriate research focus that should be taken into the 21st century.

2.2 Passive optical systems

2.2.1 Basic system

Optical remotely-sensed data are a result of a complex series of interactions between the electromagnetic radiation emitted by the sun, reflected from the Earth's surface and received by a sensor (Hunt, 1980). Multispectral sensors typically sample reflected radiation at discrete positions within the electromagnetic spectrum (Landgrebe, 1999). An analogue-to-digital converter translates these signals into digital numbers that are then temporarily stored and transmitted to a ground receiving station. The data acquired by passive remote sensing instruments are characterised by its spatial, spectral, radiometric, and temporal resolution (Lillesand *et al*., 2004). Problems of spatial resolution and level of plant recognition in forest

applications were discussed in detail by Wulder (1998), Lefsky *et al.* (2001), and Tomppo *et al.* (2002). By and large, they concluded that spatial resolution is a fundamental concept in remote sensing and plays an important role in determining the type and quality of information that can be extracted from an image. Following spatial resolution, the spectral resolution, which refers to the number and width of discrete wavelength ranges sampled by a sensor, are also of fundamental importance (Lillesand *et al*., 2004). A sensor with less than ten bands is typically known as a multispectral sensor. These sensors image broad regions of the visible, near-, and middle-infrared electromagnetic spectrum. Hyperspectral sensors sample narrow-band contiguous regions of the electromagnetic spectrum and usually have more than 80 bands, on the other hand (Landgrebe, 1999). The radiometric resolution of the sensor refers to the quantisation of each pixel within each band and indicates the sensitivity of the sensor. Essentially, radiometric resolution determines the sensor's ability to detect spectral changes within a given land cover type; the higher the radiometric resolution, the sharper the contrast of an image. Temporal resolution refers to the period of time between successive image acquisitions of the same area (Mather, 2004) and is determined, in part, by the above mentioned parameters. In passive optical remote sensing there is always a trade off between spatial, spectral, and temporal resolution. From the literature one sees that images with high spatial resolution can locate objects with a high degree of accuracy, whereas images with high spectral resolution can be used to identify and discriminate between terrestrial materials.

2.2.2 Area-based forest attributes and passive remote sensing

Area-based attributes refer to forest characteristics representing multiple trees within a given spatial area. Attributes at such a scale can be determined using medium resolution satellite sensors such as Landsat Thematic Mapper (Landsat TM), SPOT HRV, and the Advanced Spaceborne Thermal Emission and Reflection Radiometer (ASTER). These attributes are usually derived at the stand and forest scale, because the spatial resolution of the sensor is not fine enough to discriminate between tree canopies. Various forest structural and biophysical attributes have been assessed using medium resolution passive remote sensing and empirical approaches. Table

2.1 provides an overview of some of the significant publications in this area of research. Maselli *et al.* (2005) used the k-nearest neighbours (k-NN) approach and were able to estimate basal area with a reasonable amount of accuracy (Root Mean Square Error [RMSE] = 4.02 m^2/ha). Ingram *et al*. (2005) also modelled and mapped basal area and stand density but used correlation and artificial neural networks (ANNs). Basal area was found to be correlated with spectral reflectance (r=-0.77, p<0.01: middle-infrared band), while weak relationships were identified between spectral response and stand density (r=-0.21, p<0.01: red band). On the other hand, stand density was strongly correlated with the Normalised Difference Vegetation Index (r=0.69, p<0.01). Further analysis using an ANN (jackknife method) revealed that the ANNs produced strong and significant relationships between *in situ* measures of basal area and predicted measures of the same attribute (r=0.79, p<0.01). The discrepancy between spectral reflectance and vegetation indices is also highlighted in the mapping and modelling of leaf area index (LAI), an important structural parameter that is directly related to rates of energy-mass exchange, biomass partitioning, and productivity (Jensen and Binford, 2004).

Price (1993) originally suggested that LAI should be estimated and mapped using vegetation indices. Several studies have taken place since then with the notable publications mentioned in Table 2.1; most of the researchers report good relationships between LAI and spectral reflectance. Recently, Heiskanen (2006) used ASTER data to estimate tree biomass and LAI. Both spectral reflectance data and vegetation indices returned similar results with differences between the two highlighted only when advanced statistical techniques such as canonical correlation analysis (CCA) and transformed indices were used. The lowest RMSEs reported were 3.45 t/ha (41%) and 0.28 m^2/m^2 (37%) for biomass and LAI, respectively (Heiskanen, 2006). This result highlights the advances made in terms of sensor design and performance. Nearly all published literature on modelling and mapping of LAI use either Landsat TM or ETM+, with the launch of ASTER the research community enters a new age where both high spectral resolution reflectance and vegetation indices can be used. The approach now becomes increasingly important since it determines the outcome and gives researchers the freedom to explore various quantitative procedures. However, critical to forest inventory is the move

from canopy structure to practical inventory-related attributes, e.g. stems per hectare, mean height, and stem volume.

Stem volume is arguably the most important attribute in plantation forestry in South Africa and the ability to model and map the spatial distribution of merchantable timber volume using remote sensing technologies is a central goal of much research. International research such as that described in Table 2.1 focuses on the derivation of timber volume for planning purposes, while Steininger (2000) focussed on deriving timber volume estimates in support of quantifying carbon sequestration in regenerating forests in the Amazon basin. The approach remains fairly standard irrespective of the application; empirical relationships are derived between *in situ* timber volume estimates and spectral reflectance data (Rahman *et al*., 2005). These empirical relationships are then used to derive spatially explicit maps of timber volume, which in turn are used for planning purposes. The accuracy of these methods is tested using reference areas of known volume. Both Franco-Lopez *et al.* (2001) and Mäkelä and Pekkarinen (2001) reported similar results using the k-NN approach (see Table 2.1), while Steininger (2000) reported that relationships between *in situ* forest parameters and remotely-sensed estimations of forest structure tend to saturate in old growth forests. Lu (2005) supports the findings of Steininger (2000) in that regenerating forests return stronger relationships than mature forests. Similar to volume, biomass plays an important role in understanding the function of forests in the carbon cycle. Zheng *et al.* (2004) show that models vary between species and that the combined use of different species in empirical modelling does not necessarily improve estimation. It can be concluded from studies presented in Table 2.1 that it is possible to model and map biomass using remotely-sensed data and *in situ* biomass measures, while Foody *et al.* (2003) illustrated that it is not possible to transfer empirically derived models between sites when using these types of methods.

2.2.3 Individual tree-based forest attributes and passive remote sensing

Individual tree-based attributes refer to forest parameters that are measured for each tree located on the image. High spatial resolution remotely-sensed images, both airborne and space-borne, have been used to measure tree-level structural characteristics. Most applications of high spatial resolution imagery chiefly focus on automated identification of tree location and crown delineation (Larsen and Rudemo, 1998; Wulder *et al*., 2000; Culvenor, 2002; Pouliot *et al*., 2002; Wulder *et al*., 2002; Leckie *et al*., 2005; Pouliot and King, 2005). Furthermore, high spatial resolution imagery has also been used for direct estimation of canopy cover (Lévesque and King, 2003; Furusawa *et al*., 2004; Wang *et al*., 2005a; Xu *et al*., 2006), age (Franklin *et al*., 2001), and predicting various forest structural attributes (Greenberg *et al*., 2005; Kayitakire *et al*., 2006). High spatial resolution data with image pixels smaller than the dimensions of individual tree crowns can provide information on the physical structure of individual trees as well as health and degradation (Goodwin *et al*., 2005; Souza and Roberts, 2005). Table 2.2 provides an overview of various approaches used to quantify forest resources using high spatial resolution imagery. The table highlights three broad approaches typically used, namely image segmentation, textural analysis, and pixel- and object-based approaches.

Table 2.1: Examples of medium resolution studies using passive optical remote sensing

Forest Type	Sensor	Attributes	Methods	Results[a]	Reference
Temperate coniferous forests (USA)	Landsat TM	LAI	Regression analysis	R^2=0.74 Standard error (SE)=0.04	Turner *et al.* (1999)
Boreal Forests: spruce, pine, aspen (Canada)	Landsat TM	LAI	Simple ratio and bivariate regression analysis	R^2=0.51–0.70	Brown *et al.* (2000)
Norway spruce and Scots pine (Sweden)	Landsat ETM+	LAI	Correlation analysis of simple ratio (SR) and NDVI	SR: *r*=0.73 NDVI: *r*=0.77	Eklundh *et al.* (2001)
Long leaf pine, Turkey oak, Sand pine, Pond cypress, Black gum (USA)	Landsat TM	LAI	Multiple regression [1] and ANN [2]	R^2=0.83 [1] RMSE=0.86 [1] R^2=NA [2] RMSE=0.67 [2]	Jensen and Binford (2004)
Boreal forest, black spruce (North America)	Landsat ETM+	LAI	Ordinary least squares regression	R^2=0.82 RMSE=10.41	Cohen *et al.* (2003)
Pine, broad-leaved species (Finland)	Landsat TM	Timber volume	k-NN	RMSE=86.1 m^3/ha	Mäkelä and Pekkarinen (2001)
Aspen, birch, spruce, fir (USA)	Landsat TM	Timber volume	k-NN with empirical bootstrapping	95% confidence interval RMSE=48.68–54.58 m^3/ha	Franco-Lopez *et al.* (2001)
Lodgepole pine, white and black spruce, aspen, poplar (Canada)	Landsat ETM+	Volume and biomass	Stand height and crown closure: inputs to BioSTRUCT model	Volume: RMSE=4 m^3/ha Biomass: RMSE=4 t/ha	Hall *et al.* (2006)
Hardwood, pine, mixed hardwood/pine (USA)	Landsat ETM+	Aboveground biomass	Multiple regression	Hardwood R^2=0.95 Pine R^2=0.86 All R^2=0.67	Zheng *et al.* (2004)
Tropical forests (Malaysia)	Landsat TM	Aboveground biomass	ANN	*r*=0.8	Foody *et al.* (2001)
Tropical forests (Brazilian Amazon)	Landsat TM	Aboveground biomass	Stepwise linear regression Successional forest (SF) Mature forest (MF)	SF R^2=0.76 MF R^2=0.50	Lu (2005)
Conifer (Italy)	Multitemporal Landsat ETM+	Basal area	k-NN	*r*=0.59 RMSE=4.02 m^2/ha	Maselli *et al.* (2005)

[a]The superscripts relate to the corresponding superscripts in Methods

Derivation of individual tree-based attributes from high resolution imagery typically involves some form of image segmentation. Pal and Pal (1993) give a detailed review of image segmentation procedures. Segmentation procedures attempt to segment and identify tree crowns in high resolution multispectral imagery. These algorithms originally attempted to map the location of each individual tree. Gougeon (1995a) used a fairly simple approach that exploited valleys in image brightness seen between tree crowns to segment and then count individual tree crowns within an image (valley following approach). The approach described by the author identified 81% of the trees within the study area correctly. The valley-following approach has also been used by Leckie *et al.* (2003a, 2005) returning accuracies ranging from 50–80%. Pitkänen (2001) also attempted to identify individual trees but used an image smoothing supported by binarisation approach, with accuracies ranging from 70–95%. Culvenor (2002) extended the valley following approach and developed the Tree Identification and Delineation Algorithm (TIDA), an approach that attempts to not only identify individual trees but also delineate individual tree crowns using a top-down spatial clustering approach. The author did not report any quantitative results but noted that the algorithm was developed for applications in native *Eucalyptus* forests. Tree crown delineation algorithms have also been developed by Pinz (1998), Uuttera *et al.* (1998), Pouliot *et al.* (2002), and Pouliot and King (2005). Local maximum filtering techniques have also been employed by Dralle and Rudemo (1996) with Wulder *et el*. (2000, 2002) extending the approach by using variable window sizes based on tree size and species. The authors found that errors of omission and commission were a function of crown radii. In addition to variable size windows, authors have also used region growing techniques supported by fuzzy rule classification to identify and delineate individual trees as well as their crowns (Brandtberg, 2002; Erikson, 2003). Extensions of these algorithms are those designed to locate and classify individual trees in mixed-species forests (Leckie *et al*., 2003a, 2005). The specification of both tree location and species type stems from the need to develop accurate volume assessments of mixed species forests, facilitating effective and sustainable management. These methods of tree detection and tree crown delineation have been used in various forest conditions. An alternative approach to deriving information on the structural characteristics of forests involves the use of image textural attributes.

The increased availability of high spatial resolution imagery, together with improvements in scene processing and interpretation techniques, allows for the extraction of additional information based on image texture (Coops *et al*., 1998). Image texture is an important product of high resolution image analysis as it describes the variation of image tones that are related to the spatial distribution of forest vegetation (Cohen *et al.,* 1990; Franklin *et el*., 2001). The texture of a scene is primarily related to the size of the objects in the scene and the spatial resolution of the remote sensing instrument (van der Sanden and Hoekman, 2005). There are various methods of deriving textural information that can be applied to remotely-sensed data (Tuceryan and Jain, 1998). Semi-variogram modelling and grey-level co-occurrence matrices are two of the methods that have found wide application in the derivation of forest structural information. Semi-variogram modelling has been used for various forest-related activities including damage caused by pollution (Lévesque and King, 1999). The authors identified several relationships between *in situ* measurements of forest structure and various attributes of a semi-variogram model, for example the range and sill of the variogram were strongly related to a visual stress index, while the ranges of all variogram models were also strongly related to crown size and canopy closure. Lévesque and King (1999) concluded that different image resolutions were suited to different tasks, while Treitz (2001) examined spatial resolution but included an analysis of the spatial structure of canopies in the visible and near-infrared reflectance bands. Optimal image resolution for crown delineation was determined by Hyppänen (1996) using semi-variograms and spatial autocorrelation. The range of the semi-variogram was used to measure the autocorrelation of pixels while local variance curves were used to determine the spatial resolution that maximises the variance between adjacent pixels. Variogram modelling has been used for instance by Treitz and Howarth (2000) to investigate spatial scale and ecosystem classifications.

Grey-level co-occurrence matrices (GLCM) have been used to enhance multispectral classification of high resolution satellite imagery. GLCM use filters combined with first and second order measures of variance to determine the grey-level differences within a predefined region. They inform on the general variation or structure of the image which in turn reflects the variation of forest canopies (Haralick *et al*., 1973).

Franklin *et al.* (2000) incorporated textural measures derived from GLCM (homogeneity and entropy) into a classification of forest species composition using airborne multispectral images. Results indicated that the inclusion of the GLCM layer improved classification by between 5 and 12% depending on whether hardwood or softwood stands were analysed. Franklin *et al.* (2001) once again used GLCM in testing first (variance) and second (homogeneity) order textural measures to determine the optimal application for forest age separability using an IKONOS panchromatic image. Findings indicated that second-order texture values derived using larger filter windows returned better results than first-order measures. Further analysis by Kayitakire *et al.* (2006) showed that it was possible to use textural indices derived from a GLCM of an IKONOS-2 image to derive and estimate forest structural attributes such as age, crown circumference, tree height, stand density, and basal area. Empirical relationships were derived between *in situ* measures of forest structure and GLCM features. Coefficients of determination ranged from 0.35 (basal area) to 0.82 (tree height). The authors reported that prediction errors of four out of five attributes were within accepted sampling inventory errors (RMSE of less than 20%).

Finally, in recent years the use of contextual or object-oriented classification procedures such as those implemented in the eCognition (Definiens, 2005) software package have returned interesting results. Contextual classifiers utilise both the spectral and spatial characteristics of a pixel. In these methods, the classification of an individual pixel is influenced by the characteristics of the surrounding pixels (Gong and Howarth, 1992). Sharma and Sarkar (1998) have demonstrated a contextual classification technique that is modifiable for either high or low resolution imagery; Bunting and Lucas (2006) have used object orientated classification procedures to delineate and classify tree crowns in Australian mixed species forests. Wang *et al.* (2004) tested both pixel-based and object-based classification for mapping mangrove forests with IKONOS imagery. Even though both procedures provided adequate results the authors found that they were able to increase the accuracy of the species classification from 80.4% to 91.4% by combining the two in a scale parameter optimisation procedure.

Table 2.2: Examples of high resolution studies using passive optical remote sensing

Forest Type	Sensor	Attributes	Methods	Results	Reference
Douglas-fir (Canada)	IKONOS	Forest age class separability	First- and second-order textural methods (variance and homogeneity)	Larger filters more effective at separating stands and second order texture values for age discrimination	Franklin *et al.* (2001)
Scots pine, Norway spruce, European aspen, Grey alder (Finland)	Compact Imaging System	Individual tree detection	Image smoothing and binarisation	70–95% trees correctly identified	Pitkänen (2001)
Coniferous plantation (Canada)	MEIS-II	Individual tree detection	Local maximum filter	67% overall accuracy	Wulder *et al.* (2002)
Scots pine, Norway spruce, birch, European aspen (Sweden)	Kodak Aerochrome Infrared Film 2443	Individual tree crowns	Region growing supported by fuzzy rules	93% of stems correctly identified	Erikson (2003)
Coastal coniferous species (Canada)	CASI Imaging spectrometer	Individual tree crowns	Valley following (Gougeon 1995) and object orientated ML classification	70–85% trees correctly identified Composition error = 13%	Leckie *et al.* (2003a)
Mangroves (Panama)	IKONOS	Mangrove species classification	Object- and pixel-based classification	Pixel = 88.9% Object = 80.4% Combined = 91.4%	Wang *et al.* (2004)
Western hemlock, amabilis fir, western redcedar (Canada)	CASI Imaging spectrometer	Automated tree recognition	Valley following (Gougeon 1995) and object orientated ML classification	50–60% trees correctly identified Composition error = 20–60%	Leckie *et al.* (2005)
Even-aged spruce stands (Belgium)	IKONOS-2	Age, top height, crown diameter, stand density, and basal area	GLCM (Variance, contrast and correlation)	R^2=0.76–0.82	Kayitakire *et al*. (2006)

2.3 Active synthetic aperture radar systems

2.3.1 Basic system

Radar sensors illuminate off-nadir surfaces using short pulses of electromagnetic energy, part of which is reflected back to the sensor as backscatter (Bergen and Dobson, 1999; Balzter, 2001). The energy used by radar falls within the microwave region of the electromagnetic spectrum with wavelengths ranging from 1 mm to 1 m (Bergen and Dobson, 1999; Campbell, 2002). Sensors operating in these wavelength ranges are not influenced by atmospheric phenomena such as cloud and haze and are also not limited to daytime image capture. Current advanced radar systems for imaging purposes use synthetic aperture radar (SAR – see Figure 2.1). SAR is capable of acquiring high spatial resolution imagery by simulating a long antenna through the sensor's motion (Elachi, 1988; Rees, 1990; Lillesand and Kiefer, 2000). Radar images, in general, are a function of system specifications and surface characteristics. The body of literature in the field of forestry often explore the effects of wavelength, polarisation, and incidence angle in terms of the system specifications. For forestry studies, commonly used radar bands include X (2.4-3.8cm), C (3.9-7.5cm), L (15.0-30.0cm), and P (30.0-100cm) (Jensen, 2000). When transmitted and received, these bands have polarisations that are refined and recorded by the sensor. Two-letter coding is used to define these polarisations: HH, VV, HV, VH where the first letter in each pair represents transmitted and the second received polarisations. Incidence angle refers to the angle subtended by the incident radar signal and normal to the surface at the point of incidence (Jensen, 2000).

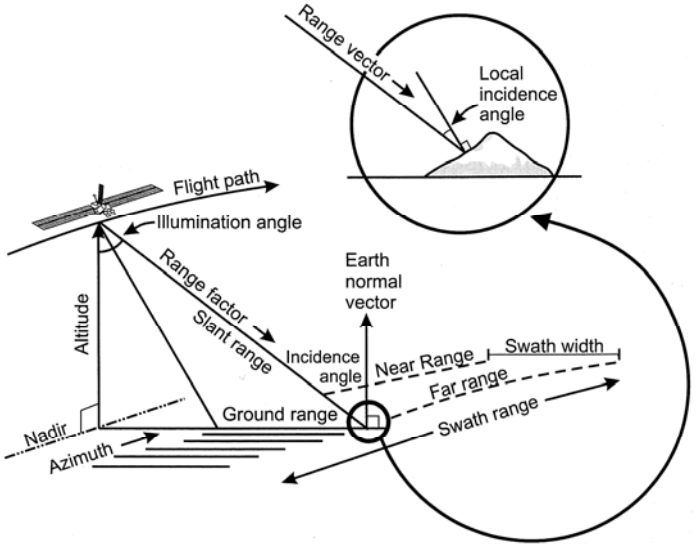

Figure 2.1 Geometry of radar remote sensing (after Pohl *et al*., 2004)

The major target characteristics that affect radar imaging are the dielectric constant and surface roughness. The dielectric property of a surface is the measure of its conductivity, reflectivity, and emissivity (Kasischke *et al*., 2004). This property is related to water content, phase of water, and specific dry density of targets (Bergen and Dobson, 1999), with high moisture content in liquid state having higher dielectric constants (Kasischke *et al*., 2004). The effect of roughness on signal scattering is viewed in relation to wavelength (Simonett and Davis, 1983). A surface might be smooth for a long wavelength while being rough for a short wavelength. A rough surface reflects energy in all directions including significant return towards the radar sensor (diffuse reflection); a smooth surface favours specular reflection, which results in emitted pulses scattering away from the radar sensor, resulting in a loss of data (Lillesand and Kiefer, 2000).

2.3.2 Area-based forest attributes and synthetic aperture radar systems

The accurate estimation and prediction of area-based forest attributes using medium resolution SAR imagery is dependent on several factors. These include the imaging system parameters, e.g., wavelength, polarisation, and incidence angle, and target characteristics, e.g., surface roughness and the dielectric properties. System

parameters such as wavelength determine the penetration capability of the sensor (Paloscia *et al.*, 1999). Shorter wavelengths found on X- and C-band systems interact with the canopy and thus backscatter variation in these images generally contain information on canopy characteristics. Manninen *et al*. (2005) used C-band ENVISAT ASAR to estimate LAI of boreal forests in Finalnd. The authors made use of the dual polarisation capabilities of ENVISAT ASAR and compared ground measured LAI with a ratio of VV/HH polarisations. Results varied according to species with Scots pine returning an R^2 of 0.66 and Norway spruce an R^2 of 0.82. Similarly, the longer wavelengths (L- and P-band), which are larger than the canopy elements and branches, are reflected from the tree trunks and the ground surface (Waring *et al*., 1995; Dobson, 2000; Kasischke *et al*., 2004). The greater penetration capability of P-band SAR allows information acquisition from large stems and underlying ground surface. Therefore, the longer wavelengths have better penetration within forest canopies along the vertical profile than shorter wavelengths (Ferrazzoli *et al*., 1997; Luckman *et al*., 1997; Yanasse *et al*., 1997; Proisy *et al*., 2000). Rauste (2005) was able to accurately define the relationship between backscatter amplitude and boreal forest biomass returning correlation coefficients between 0.63 and 0.89 using multitemporal L-band JERS data. Del Frate and Solimini (2004) used linear, non-linear, and ANNs to determine the relationship between L- and P-band SAR data and forest biomass. Results shown in Table 2.3 suggest that longer wavelengths return lower RMSE. It is also shown that classification procedures may be used to quantify forest structural attributes, with Gaveau *et al.* (2003) and Tansey *et al.* (2004) both stating that it is possible to quantify structural forest resources with a relatively high degree of accuracy.

Following wavelength, polarisation of the SAR signal also plays a significant role in determining the accuracy of derived results. Generally, the information content of backscatter is considered to be higher in cross-polarised (HV and VH) than in co-polarised (HH and VV) configuration (Waring *et al*., 1995) and hence is envisaged to be included in future systems for enhanced structural retrieval capabilities (Townsend, 2002). This was confirmed by Yanasse *et al.* (1997), who undertook forest-nonforest discrimination in Tapajos, Brazil, using SIR-C L- and C-band data and concluded that cross-polarised L-band data contained the highest information

content. Similar observations were reported by Luckman *et al.* (1997). Based on the above illustrations, it is evident that information content increases with the use of more polarisations and based on this, Dobson (2000) suggested that polarimetric (all polarisations) systems would be the ideal choice. It should, however, be noted that it is not always possible to acquire such imagery as the sensors are not readily available, especially in South Africa and that there are few or no satellite based sensors providing polarimetric imagery at this time.

The last of the system parameters influencing image acquisition is incidence angle. In forest structure estimations, higher incident angles often have better capabilities in terms of sensitivity (Elachi, 1988; Townsend, 2002). Wang *et al.* (1998) analysed the difference in sensitivity between C- and L-band among HH, HV, and VV polarisations and incident angles ranging from 20° to 60°. In the incident range of 20°-40° L-HH varied by 5.3-6.9 dB compared to 3.7-4.5 dB for L-VV. For C-HH and C-VV sensitivity was observed between incident angels of between 20°-30° for low biomass levels. The study generalised that sensitivity decreased with increasing incident angle and stand maturity. For example, while discriminating forest type using C-band polarimetric SAR-580 data acquired at 40° and 60°, Touzi *et al.* (2004) reported that better results were obtained with the 60° incident angle. Prior to that Coops (2002) also studied the effect of incidence angle on transmissivity of radiation and illustrated the decrease in transmissivity with increasing incident angle. In general, the effect of incident angle is pronounced with airborne imagery as the incidence angle is generally higher facilitating increased backscatter (Saatchi and Rignot, 1997).

2.3.3 Backscatter saturation in forests

Relationships between forest attributes (e.g., biomass, LAI, stand density) and radar backscatter normally saturate at high biomass levels. Saturation occurs as a result of several factors, of which wavelength is seen as the most important (Ramsey, 1999). Shorter wavelengths are frequently observed to saturate at low levels of biomass (Dobson *et al*., 1992; Rauste *et al*., 1994; Imhoff, 1995; Fransson and Israelsson, 1999). Longer wavelengths, on the other hand, are recommended for use under high

biomass conditions (Townsend, 2002). Forest parameters such as volume and stand density also exhibit varying saturation levels (Castel *et al*., 2002). Variation may also be caused by forest type; however, reports based on direct comparison across species of a single ground data set are lacking. Austin *et al.* (2003), for instance, hinted that the point of saturation could be higher for *Eucalyptus* forests (600 t/ha) as opposed to the work done by Dobson *et al*. (1992) who investigated the relationship between radar backscatter and forest biomass using airborne P-, L-, and C-band data. Results indicated that backscatter sensitivity to biomass increased approximately linearly until a point was reached where the relationship saturated. The saturation limit was found to be dependent on radar frequency with the P-band saturating at 200 t/ha, L-band saturating at 100 t/ha, and the C-band showing much less sensitivity to biomass change. Saturation limits were also investigated by Imhoff (1995) using the NASA/JPL AIRSAR instrument in broadleaf evergreen forests. Saturation limits reported were significantly less than those reported by Dobson *et al.* (1992), with the P-band saturating at approximately 100 t/ha, L-band at 40 t/ha, and the C-band at approximately 20 t/ha.

Other methods must be sought to avoid early saturation in the absence of P- and L-band sensors. One approach could be segmenting into different biomass levels (Gaveau *et al*., 2003; Rauste, 2005). Polarisation type has also been reported to affect saturation levels. Santos *et al.* (2003) analysed the relationship between biomass content and backscatter at HH, HV, and VV polarisations using airborne P-band SAR. The result showed HV to be superior due to its greater dynamic range. van de Griend and Seyhan (1999) observed saturation at low levels of forest density and crown cover for VV polarisation of C-band data. They found relatively small differences among dense, intermediate, and open forest. There is a general consensus that HV polarisation has the strongest sensitivity to forest structural properties for L-band (Kasischke *et al*., 1997; Schmullius and Evans, 1997; Townsend, 2002).

While much is known about the relationships between various radar system parameters and forest structural attributes, it is unclear how radar sensors could integrate into present forestry applications as the sensors have not been used in an

operational environment, and while academic research has taken place the findings have not been applied in operational scenarios. Previous studies by Lamb *et al.* (1986) and Alexander and Inggs (1996) have indicated that SAR, if implemented properly, could provide complementary data for forest inventories as well as other forest activities. Forest inventories and volume assessments are typically undertaken one year prior to planned harvesting when trees reach a mean annual increment culmination, and it is unknown what impact saturation may have and to what extent this will limit SAR applications in South Africa.

Preliminary findings indicate that medium resolution satellite data provide adequate information that may be useful to the forest manager/planner. The resolution of the sensors does not allow for intra-stand analysis, but forest-wide data regarding stem volume, biomass, and LAI can be derived, provided the statistical models are robust and transferable between study areas. Literature furthermore indicates that, in both SAR and passive studies, relationships between satellite measures and ground-based inventory data tend to saturate at high biomass levels (Imhoff, 1995; Turner *et al*., 1999; Austin *et al*., 2003; Castro *et al*., 2003). Changes in stem volume and biomass typically are not replicated in the canopy, and given that passive and radar data essentially measure changes in canopy structure, the models are not able to account for increases in stem volume and aboveground biomass. A concomitant problem associated with saturation is that when models are used to derive spatially explicit maps of LAI, volume, or biomass, they tend to underestimate attributes at high biomass levels and overestimate at low biomass levels. Researchers have recently explored the potential benefits of fusing optical and SAR data for enhanced forest assessment. Studies have shown that by fusing co-located passive and radar data, many of the negative effects associated with each sensor are minimised (Magnusson and Fransson, 2004).

Table 2.3: Examples of medium resolution studies using active synthetic aperture radar systems

Forest Type	Sensor	Attributes	Methods	Results	Reference
Regenerating tropical forests (Brazilian Amazon)	ERS-1, JERS-1, SIR-C	Biomass	Sigmoid function fitted by least squares	Saturation at ±60 t/ha	Luckman *et al.* (1997)
Scots pine, Norway spruce (Sweden)	ERS-1 and 2, SPOT XS	Stem volume	Linear regression	20th Aug 1995 R^2=0.06 12th Mar 1996 R^2=0.87 17th Mar 1996 R^2=0.73 16th Apr 1996 R^2=0.38	Fransson *et al.* (2001)
Pine (Venezuela)	JERS	Volume and stand density	Statistical and semi-empirical models	r=0.92, RMSE=20.6 m^3/ha r=0.90, RMSE=103.5 stems/ha	Castel *et al.* (2002)
Scots pine, Norway spruce, birch (Finland)	ERS-1 and 2	Stem volume	Regression modelling	11th Jun 1995 R^2=0.04 13th Mar 1996 R^2=0.92 21st Apr 1996 R^2=0.74	Santoro *et al.* (2002)
Pine, spruce, larch, cedar birch, aspen (Siberia)	ERS-1 and 2	Biomass classification	Gaussian maximum likelihood classification	Soil/sparse shrub=95% Volume >80 m^3/ha Overall=64%	Gaveau *et al.* (2003)
Conifer, poplar, mangrove (Italy)	Simulated data (L- and P-band, multi-polarisation), NASA/JPL AirSAR	Forest biomass	Linear (LR), non-linear (NLR), and ANNs	P-band (RMSE kg/m^2) LR=5.2 NLR=5.2 ANN=4.4 L-band (RMSE kg/m^2) LR=8.1 NLR=5.9 NN=5.1	Del Frate and Solimini (2004)
Norway spruce, Scots pine, beech (Norway)	CARABAS – II VHF SAR	Forest stem volume	Regression modelling	Tonnersjoheden R^2=0.80 RMSE=20.6% Brattaker R^2=0.52 RMSE=23.1%	Fransson *et al.* (2004)
Boreal (Siberia), Scots and Corsican Pine (UK), Scots pine and Norway spruce (Sweden), Tropical rain forest (Brazil)	ERS and JERS-1	Forest volume	maximum likelihood classification (MLC)	Siberia=86% UK=71.8% Sweden=70.0% Brazil = Not Given	Tansey *et al.* (2004)

2.4 Active optical systems - lidar

2.4.1 Basic system

Acquisition of lidar and SAR data share some basic principles. In lidar, short duration pulses of laser energy are transmitted from which reflected signals are recorded and converted into distance measurements. For accurate location of object position in three dimensional space, the system is integrated with a global positioning system (GPS), inertial navigation system (INS), and angle encoders (Lefsky *et al*., 2002). The GPS records the position of the platform at each signal; INS is used to measure the attitude of the lidar sensor including roll, pitch, and yaw, whereas angle encoders monitor the orientation of the scanning mirror(s) (see Figure 2.2). The final data format of lidar comes as a cloud of points with values in the *x* (longitude), *y* (latitude), and *z* (elevation) dimensions. Accuracy of these values depends mainly on range, position of the laser beam, and direction of the laser beam (Baltsavias, 1999). Lidar sensors can be categorised as small- and large-footprint, based on the size of laser beams used and the method of data capture (Dubayah and Drake, 2000; Drake *et al*., 2002). Small-footprint lidar sensors have at-target beam diameters in the order of centimetres. These sensors are mostly used in discrete return lidar systems. In such a system multiple returns from a single laser pulse are recorded when different portions of the pulse interact with the target at multiple positions along the vertical profile (Reutebuch *et al*., 2005). However, recording two returns only is a common practice for most forest-related studies. In contrast, large-footprint lidar sensors have large at-target beam diameters (mostly 5-25 m) that digitise the entire return signal (Blair *et al*., 1999). The temporal resolution of the returning signal recorded is very high in such systems, resulting in a finely distributed vertical measurement of vegetation structure (Harding *et al*., 2001). This mode of data capture is also called waveform recording. Locating individual trees using this system is, however, difficult due to the size of the footprint (Riaño *et al*., 2004a). Hence, large-footprint lidar data are indicative of multiple forest elements (Lim *et al*., 2003), while small-footprint sensors are indicative of individual crown or non-crown characteristics. Application of lidar remote sensing in estimating structural attributes is fast growing for various reasons. Firstly, it has shown the capability of directly measuring forest structures (Dubayah and Drake, 2000; Lim *et al*., 2003; Kasischke *et al*., 2004); secondly the

range measurements are highly accurate (Lefsky *et al*., 2001); and thirdly the repeatability of surveys is reliable (Lim *et al*., 2003).

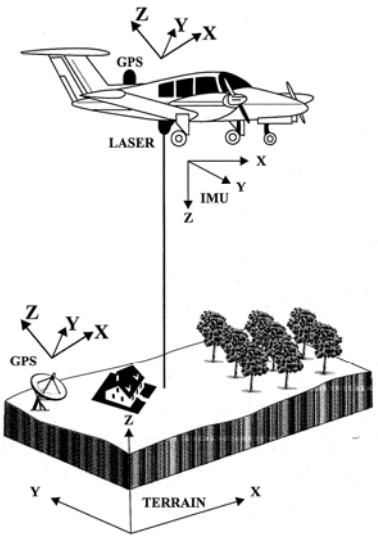

Figure 2.2 Airborne laser scanner (after Pohl *et al*., 2004).

2.4.2 Area-based forest attributes from lidar data (plot-level)

Estimating forest attributes at plot- or stand-level is a routine exercise in forest planning. This is particularly the case for mono-culture, even-aged commercial forestry volume estimates, since homogeneity is maintained at such scales. Riaño *et al.* (2004b) observed more reliable correlations with larger plot sizes when estimating LAI. Lidar data therefore are aggregated over spatial coverages that correspond to field data for extracting structural information from larger areas. The pulse density requirement in this case may not be as high as for tree-level characterisation. Nevertheless, the importance of pulse density in terms of finding sufficient number of tree crowns must not be compromised. This may also be addressed by setting an appropriate plot size (Næsset, 2004). Table 2.4 provides several examples of area-based lidar forest assessment, with both Næsset (1997) and Magnussen and Boudewyn (1998) highlighting established trends using different approaches to aggregation.

Aggregation methods may vary for different forestry organisations (Lovell *et al*., 2005). As a result, models to estimate forest attributes from lidar data must fit specific protocols. The use of quantile-based lidar height metrics is a rather common technique used to estimate canopy height (e.g. Næsset and Bjerknes, 2001; Andersen *et al*., 2005; Næsset and Gobakken, 2005). It is useful, for comparison, to calculate alternative aggregation methods. Næsset (1997), for example, looked at a number of techniques including computation of the mean height of all laser hits, a weighted mean of all canopy heights, and taking the maximum laser height within a grid cell and weighting it by the number of laser hits within the grid cell to estimate height at stand-level (see Table 2.4). The grid-based approach was believed to be less affected by laser sample size since only the largest tree heights were considered. Clark *et al.* (2004) calculated tree height of plots from lidar data in two ways: mean of local maxima from pixels within a plot and mean of all heights (all pixels) within a plot. Lovell *et al.* (2005) related lidar-derived height to predominant trees, which were chosen as 75 tallest trees per hectare. This method is assumed to be less successful in mixed-species forests with each species likely to exhibit different growth characteristics (Patenaude *et al*., 2004). Likewise, canopy density metrics are used to define stems per hectare, crown cover, and volume (Næsset and Bjerknes, 2001; Næsset, 2004). Holmgren *et al.* (2003) calculated tree volume using lidar-derived attributes in two ways: from tree height and crown cover, and tree height and stem density. A comprehensive list of parameters was used by Hall *et al.* (2005) to estimate stand-level forest attributes from lidar data (see Table 2.4).

2.4.3 Individual tree-based forest attributes from lidar data (tree-level)

Structural characterisation of individual trees using lidar data requires the accurate identification of trees. This process involves locating trees and/or delineating the full crown (Hyyppä *et al*., 2004) implying the necessity of having sufficient point density (Holmgren *et al*., 2003). Various techniques have been developed for defining individual trees. Finding local maxima through filtering in a spatial neighbourhood is, perhaps, the most common of all (Popescu *et al*., 2002; Holmgren *et al*., 2003; Maltamo *et al*., 2004a; Takahashi *et al*., 2005a, b). A window that includes a number of spatially coincident lidar points is analysed in this method. Theoretically, the

dimensions of this window should mimic the size of single tree crown; that is, too large a window is likely to consider multiple trees as one (omission error) while a smaller window creates more trees than the actual number (commission error). Popescu *et al.* (2002) developed an algorithm that uses variable window sizes to address this problem. In this method, a direct relationship between tree height and crown size was assumed. The algorithm used larger windows for taller trees and smaller windows for shorter trees. The methodology of Bortolot and Wynne (2005) differed from Popescu *et al.* (2002) in two ways. Firstly, they used multiple parameters to enable the algorithm to adapt to different data and forest types. Secondly, the centre and the crown boundary information was used in the identification process as opposed to the centre information only. However, Bortolot and Wynne (2005) recognised that the two techniques were never tested on the same data set from which comparison could be drawn. Morsdorf *et al.* (2004) used cluster analysis to segment individual trees. However, they picked local maxima from surface models to use them as tree tops to cluster points for each tree rather than from the more difficult point data approach.

Detailed knowledge of individual trees, their heights and crown size can lead to calculation of volume even at large scales (Popescu *et al*., 2003). A two-stage approach was used by Maltamo *et al.* (2004a) to calculate individual stem volume. Firstly, relationships were established between field-measured DBH and field-measured tree height and crown diameter. This relationship was then used to calculate DBH from lidar-derived tree height and crown area. The resulting DBH and the lidar height were then used to calculate volume. The most interesting approach in volume estimation would be to rely on lidar data only to extract dependent attributes. Such an approach was adopted by Holmgren *et al.* (2003) who used a regression equation to relate the field measured stem volume with lidar-derived tree height and lidar-derived crown area. A slight improvement of this approach was employed by Takahashi *et al.* (2005b). These authors used lidar-derived tree height and a number of canopy properties from each tree to predict single stem volume. The comparable field estimates were calculated from height and DBH. After aggregating volumes of individual stems, satisfactory results were obtained despite the difference in type of the prediction attributes.

2.4.4 Underestimation of lidar-derived attributes

Underestimation of tree height is a common problem encountered with small-footprint lidar (e.g. Magnussen and Boudewyn, 1998; Gaveau and Hill, 2003; Clark *et al*., 2004; Maltamo *et al*., 2004b; Suárez *et al*., 2005). This is due primarily to the small-footprint that may not always interact with the top of the tree crown. With high pulse density, however, such a miss is less likely though underestimation is still encountered (Clark *et al*., 2004). Underestimation could also result from laser pulses penetrating below the top crown surfaces and reflected back from lower elements of trees (Gaveau and Hill, 2003; Clark *et al*., 2004). Overestimated digital terrain models (DTMs) are an additional source of tree height underestimation as it reduces the base tree height. This is especially important in areas of heavy understory cover where true ground hits are difficult to retrieve, leading to DTM overestimation (Clark *et al*., 2004).

Patenaude *et al.* (2004) found underestimation to vary directly with tree height whereas canopy density and structural variations were suggested as the main determining factors by Gaveau and Hill (2003). Clark *et al.* (2004) and Maltamo *et al.* (2004b) also noted that old growth forests with typical dense floor cover resulted in overestimated DTMs, which in turn led to underestimation of canopy height. Such a problem can, to an extent, be minimised if results are derived at larger scales (plot/stand) by comparing quantile estimates of field data, such as mean and maximum height to lidar-based quantiles (Magnussen and Boudewyn, 1998; Næsset, 2002). It is suggested that height distribution models may also be used to identify suppressed trees that will eventually improve height estimation (Maltamo *et al*., 2004b). Underestimation of stem volume and stem density is also seen often when a group of trees is considered (Holmgren *et al*., 2003; Maltamo *et al*., 2004a; Takahashi *et al*., 2005b). This can be attributed to the failure to account for the understory canopy, which can be suppressed by dominant trees. Holmgren *et al.* (2003) found that high scanning angles could make crown cover estimation difficult leading to inaccurate volume estimation. The authors furthermore suggested that higher detection rate of trees would give a better estimate of tree height and crown size, which in turn would result in improved volume estimation. Maltamo *et al.*

(2004a) has indicated that adding theoretical distributions to describe small trees can improve the accuracy of estimated volume.

Review findings related to high resolution studies indicate that it is preferable to map and model forest stand parameters at a higher rather than medium spatial resolution. The higher resolution data provides the researcher with the opportunity to analyse intra-stand characteristics using vegetation indices and textural measures such as grey-level co-occurrence matrices (Coops *et al*., 1998). Despite the increase in resolution, satellite sensors such as IKONOS and Quickbird are not suitable for individual tree-based analyses such as tree crown delineation and stem counting, as a resolution of no more than 75 cm is needed to delineate and identify tree crowns (Thomas *et al*., 1997). Segmentation procedures applied to high resolution digital aerial photography are better suited to these applications (Culvenor *et al*., 1998). It furthermore was noted that lidar range measurements were more suited to deriving tree heights, but the sensor tends to underestimate attributes of interest (Magnussen and Boudewyn, 1998; Gaveau and Hill, 2003). As with medium resolution studies, several authors have explored the potential benefits of using co-registered high resolution passive optical data and lidar range measurements for enhanced forest assessments (Coops *et al*., 2004; St-Onge *et al*., 2004; Chen *et al*., 2005; Hill and Thomson, 2005).

Table 2.4: Examples of high resolution studies using active optical systems (lidar)

Forest Type	Sensor	Attributes	Methods	Results[a]	Reference
Scots pine (Sweden)	Waveform	Stand volume Mean tree height	Regression	Stand volume R^2=0.78 Tree height 2.1–3.7 m (underestimation)	Nilsson (1996)
Norway spruce, Scots pine, mixed (Norway)	Small-footprint 0.3 points/m^2	Mean tree height	Mean laser height [1] Weighted mean height [2] Weighted grid approach [3]	Underestimate=4.1–5.5 m [1] Underestimate=2.1–3.6 m [2] Underestimate=0.4–1.9 m [3]	Næsset (1997)
Douglas-fir (Canada)	Small-footprint 0.2 points/m^2	Mean tree height	Quantile based grid approach	Mean laser height R^2=0.62 Max. laser height R^2=0.65 Bias mean height R^2=0.70 Lorey's height R^2=0.49	Magnussen and Boudewyn (1998)
Boreal forest: Norway spruce, Scots pine (Finland)	Small-footprint ±20 points/m^2	Stand volume (m^3/ha) [1] Basal area (m^2/ha) [2] Mean height (m) [3]	Segmentation (Canopy height model)	Standard Error (SE)=35.8 [1] SE=3.4 [2] SE=1.7 [3]	Hyyppä *et al.* (2001)
Trembling aspen, birch, spruce, balsam fir, pine, cedar (Canada)	Small-footprint lidar 1 point/m^2, multispectral imagery	Crown area	Segmentation (TIDA) and regression modelling	Lidar R^2=0.46 Multispectral R^2=0.26	Coops *et al.* (2004)
Scots pine (Spain)	Small-footprint 0.57 points/m^2 (across flight line), ± 9 points/m^2 (along flight line)	Height[1] Crown bulk density[2] Crown volume[3] Foliage biomass[4]	Various lidar-derived metrics inputted into field-developed models	R^2 =0.93 [1] R^2=0.80 [2] R^2=0.92 [3] R^2=0.84 [4]	Riaño *et al.* (2004a)
Ponderosa pine (USA)	Small-footprint 1.23 points/m^2	Height [1] Aboveground biomass [2] Basal area [3] Tree density [4]	Regression models relating lidar-derived metrics to field estimates of structural attributes	R^2=0.87, SE=0.69 [1] R^2=0.74, SE=0.2 [2] R^2=0.79, SE=0.19 [3] R^2=0.67, SE=0.36 [4]	Hall *et al.* (2005)
Loblolly pine plantation (USA)	Small-footprint (density not given)	Forest Biomass	Nelder-Mead simplex optimisation procedure followed by regression modelling	r = 0.59–0.82 RMSE=13.6–140.4 t/ha	Bortolot and Wynne (2005)
Sugi plantation (Japan)	Small-footprint 4.76 points/m^2	Stem Volume	Segmentation and Multiple regression	Adjusted R^2=0.77 SE=23.6%	Takahashi *et al.* (2005b)
Mixed wood boreal (Canada)	Small-footprint (4 points/m^2), large footprint (0.035 points/m^2)	Mean dominant height [1] Basal area [2] Crown closure [3] Biomass [4]	Regression models relating lidar-derived metrics to field estimates	R^2=0.90 [1] R^2=0.91 [2] R^2=0.60 [3] R^2=0.92 [4]	Thomas *et al.* (2006)

[a]The superscripts relate to the corresponding superscripts in Attributes for that given species

2.5 Image fusion for enhanced forest assessment

2.5.1 Basics of image fusion

The objectives of image fusion vary with application but generally the approach is used to combine multisource imagery using advanced image processing techniques that generate an interpretation of the scene not obtainable from a single sensor. Alternatively, the technique may be used to reduce uncertainty associated with the data from individual sensors (Solberg *et al*., 1994). A general example being the identification of military targets using multiple sensors mounted on a tank or armoured vehicle (Lipchen *et al*., 2003). Pohl and van Genderen (1998) identified the following image based applications: image sharpening or pan-sharpening (Wang *et al*., 2005b), improved geometric corrections (Strobl *et al*., 1990), stereo-photogrammetry (Bloom *et al*., 1988), feature enhancement (Leckie, 1990b; Chen *et al*., 2003), improved classification (Fabre and Dherete, 2003), change detection (Duguay *et al*., 1987), substitution of missing data (Aschbacher and Lichtenegger, 1990), and replacement of defective data (Suits *et al*., 1998). Methods used to perform fusion include band selection, colour related techniques, and statistical/numerical techniques, as well as ANNs, Bayesian inference and Dempster-Shafer evidential reasoning, to name but a few.

Image or data fusion is implemented at one of three levels (pixel, feature, and decision) depending on the application and the needs of the user. Pixel-level fusion essentially fuses the physically-measured values using image transformation procedures. Frequency-based image transformations (Ranchin *et al*., 2003) preserve both the spatial and the spectral content of the original data (Ehlers, 2005) and should be used as opposed to the colour (Carper *et al*., 1990; Sanjeevi *et al*., 2001; Hsu and Burke, 2003) and statistical transformations (Zhou *et al*., 1998; Wang *et al*., 2005b). Feature-level fusion procedures fuse independent classifications derived from separate sensors. The procedures used here include parametric templates, attribute-based methods, and ANNs (Pohl and van Genderen, 1998). No one procedure was identified as being more appropriate than another; the technique or algorithm used should be governed by the user's aims and objectives. Finally, decision-level fusion uses both knowledge-based or expert systems and identity

fusion procedures. Essentially, decision-level fusion performs feature identification prior to fusion, whereas feature- and pixel-level fusion perform feature identification after fusion (Hall, 1992). Decision-level fusion primarily makes use of Bayesian inference and evidential reasoning to merge pre-classified geospatial data with a view to improving feature extraction and image characterisation (Solberg *et al*., 1994; Benediktsson and Sveinsson, 1997; Petrakos *et al*., 2001; Benediktsson *et al*., 2004).

2.5.2 Applications of image fusion in forestry

The first and most common application of image fusion is that of pan-sharpening, whereby the high frequency spatial details of a panchromatic image are used to increase the resolution of a spatially coincident multispectral data set. Applications include monitoring forest damage, species identification, and vegetation mapping (Riley *et al*., 2002), along with a more effective use of texture (Kayitakire *et al*., 2006), provided that suitable fusion procedures are used (Shrestha, 2005). Mapping and modelling forest attributes of interest may also benefit from the use of multiple data sources such as SAR, optical, and lidar data. Tanaka *et al.* (1998) showed that by using optical and radar data, they were able to predict both species type and forest structural parameters with a high degree of accuracy (*kappa* > 75%). Moghaddam and Duncan (2001) and Moghaddam *et al*. (2002) have also reported positive results from the combined use of radar and optical sensors, particularly for the estimation of foliage mass and LAI. Furthermore, models were developed to predict foliage biomass at levels that would not be possible if only one sensor was used (RMSE decreased by a factor of two compared to single-sensor analysis). This is a significant finding as it would seem that the combination of the two sensors negated the problem of saturation at high biomass levels. In Sweden, Magnusson and Fransson (2004) reported similar results when assessing the accuracy of combined optical and radar data sets for stem volume estimates. Using regression techniques the authors reported that RMSE improved by up to 15% when compared to results derived from single sensor analysis. An alternative method using k-NN in the same area also reported significant improvements in the estimation of forest attributes (Holmstrom and Fransson, 2003). The authors also found that optical data

provided more robust estimates at lower stem volumes while the inverse was true for radar, hence the combination of both sensors provided robust estimates throughout the age range. The fusion of SAR and passive optical data have also seen increased use in forest classification with several authors reporting improved classifications using combined passive optical and active SAR systems (Keil *et al*., 1999; Le Moigne *et al*., 2001; Miles *et al.,* 2003).

The fusion of lidar and multispectral satellite or airborne imagery typically attempts to reduce the cost of lidar surveys and/or improve upon the derivation of forest inventory data. Hudak *et al.* (2002), for example, were able to predict forest canopy heights with a high degree of accuracy at locations not sampled by the lidar sensor using aspatial statistical models and a combination of lidar and Landsat ETM+ data. Hudak *et al.* (2006) used similar methods to estimate basal area and stand density and were able to explain more than 90% of ground-level variance. The methods used attempt to establish a relationship between the lidar inventory metrics and multispectral reflectance. The models are then applied to multispectral data and used to predict forest metrics at locations not sampled by the lidar sensor. The methods reduce the cost of using lidar sensors as there is no need for a complete lidar survey; managers need only sample a representative portion of the forest. Further applications of combined multispectral and lidar data include the identification of individual trees through the use of high resolution digital airborne imagery and high density lidar range measurements. McCombs *et al*. (2003) used both multispectral and lidar data to identify individual trees and their respective heights. The authors found that the multispectral data were more effective at locating individual trees while the lidar data returned more accurate height estimates. Coops *et al.* (2004) performed a comparable study and returned similar results. Lidar range measurements were suitable for predicting canopy height while high resolution passive data were more suited to tree identification and crown delineation. Spectral characteristics of objects in the passive data set showed strong relationships with vertical positions of lidar points. They concluded that the combination of passive and lidar data in the context of tree crown delineation provided information not available from either source independently. Other procedures described by Leckie *et al.* (2003b), Popescu and Wynne (2004), and Suárez *et al.* (2005) have sought to model

individual tree crowns using interpolated high density lidar range measurements. A key criterion for effective volume estimates is an accurate stem counting algorithm. Leckie *et al.* (2003b) recognised that by using spatially co-registered lidar and multispectral data, tree isolation may be improved. The authors used the well-known valley following approach (Gougeon, 1995b) to extract tree crowns from both data sets, which are then combined to identify individual trees as well as their respective heights. Synergy of passive and lidar imagery resulted in enhanced tree identification.

2.6 Conclusions

The literature indicates that there is strong body of theoretical knowledge supporting the use of remotely-sensed data for forest assessment. Key findings and outcomes support the use of remote sensing for structural forest assessment. Medium resolution optical and SAR systems, when combined with *in situ* measures of forest structure, provide relatively robust models with which to predict forest attributes. Results are dependent on the accurate co-location of sample plots on imagery (Tokola, 2000; Halme and Tomppo, 2001) and suitable statistical approaches (Rahman *et al*., 2005). An established problem with this approach is that relationships tend to saturate in mature forests where canopies become less variable (Imhoff, 1995). While relationships are understood in Europe (Dobson *et al*., 1992; Fransson and Israelsson, 1999), the America's (Luckman *et al*., 1997), and Australia (Austin *et al*., 2003), not much is known about the problem in South Africa. It is therefore necessary to explore and understand this problem and to quantify its potential impact on the assessment procedure for both passive optical sensors and active SAR systems. Several studies in this regard have shown that image fusion could potentially help mitigate the problems associated with saturation. Additional research is requested to ascertain the most appropriate fusion procedure as well as the optimal data combinations. Once the saturation effect is understood and mitigated either through more effective analyses procedures or image fusion, industry can then begin to implement area-based assessment procedures and ultimately streamline management of commercial plantations. High resolution

sensors seem to be more appropriate for individual tree-based (fine scale) studies. These studies seek to model the geometric structure of the forest using either active optical sensor such as lidar or high resolution aerial or spaceborne platforms. It was noted that optical systems may be more adept at identifying and delineating individual tree crowns using segmentation algorithms. These algorithms, although developed under different conditions, could prove to be appropriate for the local forestry industry and should be explored as potential solutions for automated stem counting procedures.

Tree height is an important attribute that is not adept to modelling using passive optical sensors. Lidar has been identified as a potential tool for measuring tree heights (Holmgren *et al.,* 2003; Takahashi *et al.,* 2005b). With a suitable point density it is possible to derive tree location and height with a high degree of accuracy (Hyyppä *et al*., 2001), both of which are needed for volume assessment. Studies also indicate that the accuracy with which lidar measures tree height, location, and associated attributes, such as basal area and diameter at beast height, are comparable to field enumeration techniques (Næsset, 1997; Holmgren and Jonsson, 2004). However, researchers should be cognisant of the fact that lidar may underestimate tree heights leading to an underestimate of volume and other important forestry attributes. Another factor in determining the utility of lidar is cost. Lidar surveys are expensive relative to other remote sensing data sources and do not always serve as cost-effective alternatives. It is therefore imperative that researchers explore various cost saving approaches to the use of lidar data. It is also important to explore a variety of approaches to the quantification of forest resources using lidar data. For example, should interpolated surfaces be used or point cloud analysis? Another important question relates to the lidar point density. An optimal point density for all plantation species should be identified through iterative statistical analysis. It can be concluded that the complementary nature of lidar and high resolution optical data has shown promise. The potential benefits of fusing the two data sources have been explored and presented by various authors, all of whom favour the use of multiple data sources for enhanced forest assessment.

Recommendations emanating from this review are as follows

- Methods for the operational use of medium resolution sensors (including radar) in support of forest enumeration and management should be explored
- The potential impact of signal saturation in mature forests needs to be quantified
- Image fusion should be explored as a means of improving the accuracy of forest structural assessment at both the medium and high spatial resolutions
- Tree counting algorithms developed for high resolution optical imagery should be modified to include lidar-derived top of canopy models
- The cost-effectiveness of remote sensing based inventory and management solutions should be explored

Acknowledgements

The authors would like to acknowledge grant funding provided by the CSIR Parliamentary Grant Committee as well as Mondi South Africa for their monetary and technical contributions made during the preparation of this review paper. Further, the authors would like to acknowledge an anonymous external reviewer.

References

Ackermann, F. 1999. Airborne laser scanning—present status and future expectations. *ISPRS Journal of Photogrammetry and Remote Sensing*. 54, 64 – 67.

Alexander , L. A. and Inggs, M. R. 1996. Synthetic aperture radar for remote sensing. *South African Journal of Science*. 92, 106 – 120.

Andersen, H.-E., McGaughey, R. J., and Reutebuch, S. E. 2005. Estimating forest canopy fuel parameters using lidar data. *Remote Sensing of Environment*. 94, 441 – 449.

Aschbacher, J. and Lichtenegger, J. 1990. Complementary nature of SAR and optical data: a case study in the tropics. *Earth Observation Quarterly*. 31, 4 – 8.

Austin, J. M., Mackey, B. G., and Kimberly, P. V. N. 2003. Estimating forest biomass using satellite radar: an exploratory study in a temperate Australian *Eucalyptus* forest. *Forest Ecology and Management*. 176, 575 – 583.

Baltsavias, E. P. 1999. Airborne laser scanning: basic relations and formulas. *ISPRS Journal of Photogrammetry and Remote Sensing*. 54, 199 – 214.

Balzter, H. 2001. Forest mapping and monitoring with interferometric synthetic aperture radar (InSAR). *Progress in Physical Geography*. 25, 159 – 177.

Beedlow, P. A., Tingey, D. T., Phillips, D. L., Hogsett, W. E., and Olszyk, D. M. 2004. Rising atmospheric CO_2 and carbon sequestration in forests. *Frontiers in Ecology and the Environment*. 2, 315 – 322.

Benediktsson, J. A. and Sveinsson, R. J. 1997. Classification of hyper dimensional data using fusion approaches. *Proceedings of the IEEE International Geoscience and Remote Sensing Symposium, IGARSS '97, 'Remote Sensing – A Scientific Vision for Sustainable Development'*. 3–8 August. Singapore. Vol. 4. IEEE, New York. pp. 1669 – 1671.

Benediktsson, J. A., Palmason, J. A., Sveinsson, R., and Chanussot, J. 2004. Decision-level fusion in classification of hyperspectral data from urban areas. *Proceedings of the IEEE International Geoscience and Remote Sensing Symposium, IGARSS '04.* 20–24 September. Anchorage, Alaska. Vol. 1. IEEE, New York. pp. 73 – 76.

Bergen, K. M. and Dobson, M. C. 1999. Integration of remotely-sensed radar imagery in modelling and mapping of forest biomass and net primary production. *Ecological Modelling*. 122, 257 – 274.

Blair, B. J., Rabine, D. L., and Hofton, M. A. 1999. The Laser Vegetation Imaging Sensor: a medium-altitude, digitisation-only, airborne laser altimeter for mapping vegetation and topography. *ISPRS Journal of Photogrammetry and Remote Sensing*. 54, 115 – 122.

Bloom, A., Fielding, E., and Fu, X. 1988. A demonstration of stereophotography with combined SIR-B and Landsat TM images. *International Journal of Remote Sensing*. 9, 1023 – 1038.

Bortolot, Z. J. and Wynne, R. H. 2005. Estimating forest biomass using small-footprint lidar data: an individual tree-based approach that incorporates training data. *ISPRS Journal of Photogrammetry and Remote Sensing*. 59, 342 – 360.

Boyd, D. S. and Danson, F. M. 2005. Satellite remote sensing of forest resources: three decades of research development. *Progress in Physical Geography*. 29, 1 – 26.

Brandtberg, T. 2002. Individual tree-based species classification in high spatial resolution aerial images of forests using fuzzy sets. *Fuzzy Sets and Systems*. 132, 371 – 387.

Brink, M. P. 1990. The environmental impacts of harvesting as related to soil compaction and erosion. *Wood Southern Africa*. 15, 58 – 68.

Brown, L., Chen, J. M., Leblanc, S. G., and Cihlar, J. 2000. A shortwave infrared modification to the simple ratio for LAI retrieval in boreal forests: an image and model analysis. *Remote sensing of Environment*. 71, 16 – 25.

Bunting, P. and Lucas, R. 2006. The delineation of tree crowns in Australian mixed species forests using hyperspectral Compact Airborne Spectrographic Imager (CASI) data. *Remote Sensing of Environment*. 101, 230 – 248.

Campbell, J. B. 2002. *Introduction to Remote Sensing*. The Guilford Press, New York. 654 pp.

Carper, W. J., Lillesand, T. M., and Kiefer, R. W. 1990. The use of Intensity-Hue-Saturation transform for merging SPOT panchromatic and multispectral image data. *Photogrammetric Engineering and Remote Sensing*. 56, 459 – 467.

Castel, T., Guerra, F. Caraglio, Y., and Houllier, F. 2002. Retrieval biomass of a large Venezuelan pine plantation using JERS-1 SAR data. Analysis of forest structure impact on radar signature. *Remote Sensing of Environment*. 79, 30 – 41.

Castro, K. L., Sanchez-Azofeifa, G. A., and Rivard, B. 2003. Monitoring secondary tropical forests using space-borne data: implications of central America. *International Journal of Remote Sensing*. 24, 1853 – 1894.

Chamberlain, D., Essop, H., Hougaard, C., Malherbe, S., and Walker, R. 2005. *Genesis report: part I. The contribution, costs, and development opportunities of the forestry, timber pulp, and paper industries in South Africa*. Genesis Analytics (Pty) Ltd, Johannesburg, South Africa.

Chen, L., Chiang, T., and Teo, T. 2005. Fusion of lidar and high resolution images for forest canopy modelling. *Proceedings of the 26th Asian Conference on Remote Sensing*. 7–11 November. Hanoi, Vietnam.

Chen, C. M., Hepner, G. F., and Forster, R. R. 2003. Fusion of hyperspectral and radar data using the IHS transformation to enhance urban surface features. *ISPRS Journal of Photogrammetry and Remote Sensing*. 58, 19 – 30.

Christie, S. I. and Scholes, R. J. 1995. Carbon storage in *Eucalyptus* and pine plantations in South Africa. *Environmental Monitoring and Assessment*. 38, 231 – 241.

Clark, M. L., Clark, D. B., and Roberts, D. A. 2004. Small-footprint lidar estimation of sub-canopy elevation and tree height in a tropical rain forest landscape. *Remote Sensing of Environment*. 91, 68 – 89.

Cohen, W. B., Maiersperger, T. K., Gower, S. T., and Turner, D. P. 2003. An improved strategy for regression of biophysical variables and Landsat ETM+ data. *Remote Sensing of Environment*. 84, 561 – 571.

Cohen, W. B., Spies, T. A., and Bradshaw, G. A. 1990. Semi-variograms of digital imagery for analysis of conifer canopy structure. *Remote Sensing of Environment*. 34, 167 – 178.

Coops, N. C. 2002. Eucalypt forest structure and synthetic aperture radar backscatter: a theoretical analysis. *Trees*. 16, 28 – 46.

Coops, N., Culvenor, D., Preston, R., and Catling, P. 1998. Procedures for predicting habitat and structural attributes in eucalypt forests using high spatial resolution remotely-sensed imagery. *Australian Forestry*. 61, 244 – 252.

Coops, N. C., Wulder, M. A., Culvenor, D. S., and St-Onge, B. 2004. Comparison of forest attributes extracted from fine spatial resolution multispectral and lidar data. *Canadian Journal of Remote Sensing*. 30, 855 – 866.

Culvenor, D. S. 2002. TIDA: an algorithm for the delineation of tree crowns in high spatial resolution remotely-sensed imagery. *Computers and Geosciences*. 28, 33 – 44.

Culvenor, D. S., Coops, N., Preston, R., and Tolhurst, K. G. 1998. A spatial clustering approach to automated tree crown delineation. *Proceedings of the International Forum on Automated Interpretation of High Spatial Resolution Digital Imagery for Forestry*. 10–12 February. Pacific Forestry Centre, Canada Forest Service, Natural Resources Canada, Victoria, BC, Canada. pp. 67 – 80.

Definiens. 2005. *eCognition Version 5 Object Orientated Image Analysis User Guide.* Definiens AG, Munich, Germany. 486 pp.

Del Frate, F. and Solimini, D. 2004. On neural network algorithms for retrieving forest biomass from SAR data. *IEEE Transactions on Geoscience and Remote Sensing*. 42, 24 – 34.

Dobson, M. C. 2000. Forest information from synthetic aperture radar. *Journal of Forestry*. 98, 41 – 43.

Dobson, M. C., Ulaby, F. T., Letoan, T., Beaudoin, A., Kasischke, E. S., and Christensen, N. 1992. Dependence of radar backscatter on coniferous forest biomass. *IEEE Transactions on Geoscience and Remote Sensing*. 30, 412 – 415.

Drake, J. B., Dubayah, R. O., Clark, D. B., Knox, R. G., Blair, J. B., Hofton, M. A., Chazdon, R. L. Weishampel, J. F., and Prince, S. D. 2002. Estimation of tropical forest structural characteristics using large-footprint lidar. *Remote Sensing of Environment*. 79, 305 – 319.

Dralle, K. and Rudemo, M. 1996. Stem number estimation by kernel smoothing of aerial photos. *Canadian Journal of Forest Research*. 26, 1228 – 1236.

Dubayah, R. O. and Drake, J. B. 2000. Lidar remote sensing for forestry. *Journal of Forestry*. 98, 44 – 46.

Duguay, G., Holder, G., Howarth, P., and LeDrew, E. 1987. Integrating remotely-sensed data from different sensors for change detection. *Proceedings of the IEEE International Geoscience and Remote Sensing Symposium, IGARSS '87*. 18–21 May. Ann Arbor, USA, IEEE, New York. pp. 333 – 000.

DWAF. 2005. *State of the Forest Report: a pilot report to test the National Criteria and Indicators.* Department of Water Affairs and Forestry. Pretoria, South Africa.

Ehlers, M. 2005. Beyond pan sharpening: advances in data fusion for very high resolution remote sensing data. *Proceedings, ISPRS Workshop on High Resolution Earth Imaging for Geospatial Information*. 17–20 May, Hanover, Germany. 6 pp.

Eklundh, L., Harrie, L., and Kuusk, A. 2001. Investigating relationships between Landsat ETM+ sensor data and leaf area index in a boreal conifer forest. *Remote Sensing of Environment*. 78, 239 – 251.

Elachi, C. 1988. *Spaceborne radar remote sensing: applications and techniques*. IEEE Press, New York. 288 pp.

Erikson, M. 2003. Segmentation of individual tree crowns in colour aerial photographs using region growing supported by fuzzy rules. *Canadian Journal of Forest Research*. 33, 1557 – 1563.

Fabre, S. and Dherete, P. 2003. Data fusion applications: classification and mapping. *Proceedings of the IEEE International Geoscience and Remote Sensing Symposium, IGARSS '03*. 21–25 July. Vol. 2. IEEE, New York. pp. 1053–1055.

FAO. 2005. *Global forest resources assessment 2005: South Africa country report*. Food and Agriculture Organisation of the United Nations, Rome. 41 pp.

Ferrazzoli, P., Paloscia, S., Pampaloni, P., Schiavon, G., Sigismondi, S., and Solimini, D. 1997. Radar sensitivity to tree geometry and woody volume: a model analysis. *IEEE Transactions on Geoscience and Remote Sensing*. 33, 5 – 17.

Foody, G. M., Boyd, D. S., and Cutler, M. E. J. 2003. Predictive relationships of tropical forest biomass from Landsat TM data and their transferability between regions. *Remote Sensing of Environment*. 85, 463 – 474.

Foody, G. M., Cutler, M. E., McMorow, J., Dieter, P., Tangki, H., Boyd, D. S., and Douglas, I. 2001. Mapping the biomass of Bornean tropical rain forests from remotely-sensed data. *Global Ecology and Biogeography*. 10, 107 – 120.

Franco-Lopez, H., Ek, A. R., and Bauer, M. E. 2001. Estimation and mapping of forest stand density, volume, and cover type using the k-nearest neighbour method. *Remote Sensing of Environment*. 77, 251 – 274.

Franklin, S. E., Hall, R. J., Moskal, L. M., Maude, A. J., and Lavigne, M. B. 2000. Incorporating texture into classification of forest species composition from airborne multispectral images. *International Journal of Remote Sensing*. 21, 61 – 79.

Franklin, S., Wulder, M., and Gerylo, G. 2001. Texture analysis of IKONOS panchromatic data for Douglas-fir forest age class separability in British Columbia. *International Journal of Remote Sensing*. 22, 2627 – 2632.

Fransson, J. E. S. and Israelsson, H. 1999. Estimation of stem volume in boreal forests using ERS-1 C- and JERS-1 L-band SAR data. *International Journal of Remote Sensing*. 20, 123 – 137.

Fransson, J. E. S., Smith, G., Askne, J., and Olsson, H. 2001. Stem volume estimation in boreal forests using ERS-1/2 coherence and SPOT XS optical data. *International Journal of Remote Sensing*. 22, 2777 – 2791.

Fransson, J. E. S., Smith, G., Walter, F., Gustavsson, A., and Ulander, L. M. H. 2004. Estimation of forest stem volume in sloping terrain using CARABAS-II VHF SAR data. *Canadian Journal of Remote Sensing*. 30, 651 – 660.

Furusawa, T., Pahari, K., Umezaki, M., and Ohtsuka, R. 2004. Impacts of selective logging on New Georgia Island, Solomon Islands evaluated using very high resolution satellite (IKONOS) data. *Environmental Conservation*. 31, 349 – 355.

Gaveau, D. L. A. and Hill, R. A. 2003. Quantifying canopy height underestimation by laser pulse penetration in small-footprint airborne laser scanning data. *Canadian Journal of Remote Sensing*. 29, 650 – 657.

Gaveau, D. L. A., Balzter, H., and Plummer, S. 2003. Forest woody biomass classification with satellite-based radar coherence over 900 000 km^2 in central Siberia. *Forest Ecology and Management*. 174, 65 – 75.

Ghebremicael, S. T., Smith, C. W., and Ahmed, F. B. 2004. Estimating the leaf area index (LAI) of black wattle from Landsat ETM+ satellite imagery. *Southern African Forestry Journal*. 201, 3 – 12.

Gillis, M. D. 2001. Canada's National Forest Inventory (responding to current information needs). *Environmental Monitoring and Assessment.* 67, 121 – 129.

Gjersten, A. K., Tomppo, E., and Tomter, S. 1999. National forest inventory in Norway: using sample plots, digital maps, and satellite images. *Proceedings of the IEEE International Geoscience and Remote Sensing Symposium, IGARSS '99.* 28 June–2 July, Hamburg, Germany. Vol. 2. IEEE, New York. pp. 729 – 731.

Gong, P. and Howarth, P. 1992. Frequency based contextual classification and grey-level vector reduction for land use identification. *Photogrammetric Engineering and Remote Sensing*. 58, 423 – 437.

Goodwin, N., Coops, N. C., and Stone, C. 2005. Assessing plantation canopy condition from airborne imagery using spectral mixture analysis and fractional abundances. *International Journal of Applied Earth Observation*. 7, 11 – 28.

Gougeon, F. A. 1995a. A crown-following approach to the automatic delineation of individual tree crows in high spatial resolution aerial images. *Canadian Journal of Remote Sensing*. 21, 274 – 284.

Gougeon, F. A. 1995b. Comparison of possible multispectral classification schemes for tree crowns individually delineated on high spatial resolution MEIS images. *Canadian Journal of Remote Sensing*. 21, 1 – 9.

Greenberg, J. A., Dobrowski, S. Z., and Ustin, S. L. 2005. Shadow allometry: estimating tree structural parameters using hyperspatial image analysis. *Remote Sensing of Environment*. 97, 15 – 25.

Hall, D. L. 1992. *Mathematical techniques in multisensor data fusion*. Artech House, Norwood, MA. 326 pp.

Hall, S. A., Burke, I. C., Box, D. O., Kaufmann, M. R., and Stoker, J. M. 2005. Estimating stand structure using discrete return lidar: an example from low density, fire prone ponderosa pine forests. *Forest Ecology and Management*. 208, 189 – 209.

Hall, R. J., Skakun, R. S., Arsenault, E. J., and Case, B. S. 2006. Modelling forest stand structure attributes using Landsat ETM+ data: application to mapping of aboveground biomass and stand volume. *Forest Ecology and Management*. 225, 378 – 390.

Halme, M. and Tomppo, E. 2001. Improving the accuracy of multisource forest inventory estimates by reducing plot location error – a multicriteria approach. *Remote Sensing of Environment*. 78, 321 – 327.

Haralick, R. M., Shanmugam, K., and Dinstein, I. 1973. Textural features for image classification. *IEEE Transactions on Systems, Man, and Cybernetics*. 3, 610 – 621.

Harding, D. J., Lefsky, M. A., Parker, G. G., and Blair, J. B. 2001. Laser altimeter canopy height profiles: methods and validation for closed-canopy, broadleaf forests. *Remote Sensing of Environment*. 76, 283 – 297.

Heiskanen, J. 2006. Estimating aboveground tree biomass and leaf area index in a mountain birch forest using ASTER satellite data. *International Journal of Remote Sensing*. 27, 1135 – 1158.

Heydenrych, B. 1995. Forestry plantations vs. biodiversity. *Veld and Flora*. 81, 20 – 21.

Hill, R. A. and Thomson, A. G. 2005. Mapping woodland species composition and structure using airborne spectral and lidar data. *International Journal of Remote Sensing*. 26, 3763 – 3779.

Holmgren, J. and Jonsson, T. 2004. Large scale airborne laser-scanning of forest resources in Sweden. *International Archives of Photogrammetry, Remote Sensing, and Spatial Information Sciences*. Vol. 36-8/W2, 157 – 160.

Holmgren, J., Nilsson, M., and Olsson, H. 2003. Estimation of tree height and stem volume on plots using airborne laser scanning. *Forest Science*. 49, 419 – 428.

Holmstrom, H. and Fransson, J. E. S. 2003. Combining remotely-sensed optical and radar data in k-NN estimation of forest variables. *Forest Science*. 49, 409 – 418.

Hsu, S. M. and Burke, H. K. 2003. Multisensor fusion with hyperspectral imaging data: detection and classification. *Lincoln Laboratory Journal*. 14, 145 – 158.

Hudak, A. T., Crookston, N. L., Evans, J. S., Falkowski, M. J., Smith, A. M. S., Gesseler, P. E., and Morgan, P. 2006. Regression modelling and mapping of coniferous forest basal area and tree density from discrete return lidar and multispectral satellite data. *Canadian Journal of Remote Sensing*. 32, 126 – 138.

Hudak, A. T., Lefsky, M. A., Cohen, W. B., and Berterretche, M. 2002. Integration of lidar and Landsat ETM+ data for estimating and mapping forest canopy height. *Remote Sensing of Environment*. 82, 397 – 416.

Hunt, G. R. 1980. Electromagnetic radiation: the communication link in remote sensing. In: Siegal, G. S. and Gillespie, A. R. (Eds.), *Remote sensing in geology*. John Wiley and Sons, New York. pp. 5 – 45.

Hyppänen, H. 1996. Spatial autocorrelation and optimal spatial resolution of optical remote sensing data in boreal forest environment. *International Journal of Remote Sensing*. 17, 3441 – 3452.

Hyyppä, J., Hyyppä, H., Litkey, P., Yu, X., Haggrén, H., Rönnholm, P., Pyysalo, U., Pitkänen, J., and Maltamo, M. 2004. Algorithms and methods of airborne laser scanning for forest measurements. *International Archives of Phtogrammetry, Remote Sensing, and Spatial Information Sciences*. Vol. 36-8/W2, 82 – 89.

Hyyppä, J., Kelle, O., Lehikoinen, M., and Inkinen, M. 2001. A segmentation-based method to retrieve stem volume estimates from 3-D tree height models produced by laser scanners. *IEEE Transactions on Geoscience and Remote Sensing*. 39, 969 – 975.

Imhoff, M. L. 1995. Radar backscatter and biomass saturation: ramifications for global biomass inventory. *IEEE Transactions on Geoscience and Remote Sensing*. 33, 511 – 518.

Ingram, J. C., Dawson, T. P., and Whittaker, R. J. 2005. Mapping tropical forest structure in south-eastern Madagascar using remote sensing and artificial neural networks. *Remote Sensing of Environment*. 94, 491 – 507.

Jensen, J. R. 2000. *Remote sensing of the environment: an Earth resource perspective*. Prentice-Hall, New Jersey. 336 pp.

Jensen, R. R. and Binford, M. W. 2004. Measurement and comparison of leaf area index estimators from satellite remote sensing techniques. *International Journal of Remote Sensing*. 25, 4251 – 4265.

Kasischke, E. S., Melack, J. M., and Dobson, M. C. 1997. The use of imaging radars for ecological applications – a review. *Remote Sensing of Environment*. 59, 141 – 156.

Kasischke, E. S., Goetz, S., Hansen, M. C., Ustin, S. L., Ozdogan, M., Woodcock, C. E., and Rogan, J. 2004. Temperate and boreal forests. In: Ustin, S. L. (Ed.), *Remote sensing for natural resource management and environmental monitoring*. *Manual of remote sensing*. John Wiley and Sons, New York. pp. 147 – 238.

Kätsch, C. and Kunneke, A. 2006. Forest inventory in the digital remote sensing age. *Southern African Forestry Journal*. 206, 43 – 49.

Kätsch, C. and van Laar, A. 2002. The estimation of the growing stock of eucalypt plantation forests, based on spectral signatures of satellite imagery, in South Africa. *Southern African Forestry Journal*. 194, 65 – 70.

Kätsch, C. and Vogt, H. 1999. Remote sensing from space – present and future applications in forestry, nature conservation, and landscape management. *Southern African Forestry Journal*. 185, 14 – 26.

Kayitakire, F., Hamel, C., and Defourny, P. 2006. Retrieving forest structure variables based on image texture analysis and IKONOS-2 imagery. *Remote Sensing of Environment*. 102, 390 – 401.

Keil, M., Akgoz, E., Carl, S., Forster, B., Hausler, T., Johlige, A., Lautner, M., and Martin, K. 1999. Use of SIR-C/X-SAR and Landsat TM data for vegetation mapping in the Bavarian Forest National Park and the Ore Mountains. *Proceedings of the IEEE International Geoscience and Remote Sensing Symposium, IGARSS '99*. 28 June–2 July, Hamburg, Germany. Vol. 1. IEEE, New York. pp. 293 – 295.

Lamb, A. D., Mönnig, N. H., and van der Zel, D. W. 1986. Side-looking radar – a remote sensing application in South African forestry plantations. *Southern African Forestry Journal*. 139, 54 – 59.

Landgrebe, D. 1999. Information extraction principles and methods for multispectral and hyperspectral image data. In: Chen, C. H. (Ed.), *Information processing for remote sensing.* World Scientific Publishing, New Jersey. pp. 1 – 30.

Larsen, M. and Rudemo, M. 1998. Optimising templates for finding trees in aerial photographs. *Pattern Recognition Letters*. 19, 1153 – 1162.

Leckie, D. G. 1990a. Advances in remote sensing technologies for forest surveys and management. *Canadian Journal of Forest Research*. 20, 464 – 483.

Leckie, D. G. 1990b. Synergism of SAR and visible/infrared data for forest type discrimination. *Photogrammetric Engineering and Remote Sensing.* 56, 1237 – 1246.

Leckie, D., Gougeon, F., Hill, D., Quinn, R., Armstrong, L., and Shreenan, R. 2003b. Combined high-density lidar and multispectral imagery for individual tree crown analysis. *Canadian Journal of Remote Sensing*. 29, 633 – 649.

Leckie, D. G., Gougeon, F. A., Tinis, S., Nelson, T., Burnett, C. N., and Paradine, D. 2005. Automated tree recognition in old growth conifer stands with high resolution digital imagery. *Remote Sensing of Environment*. 94, 311 – 326.

Leckie, D. G., Gougeon, F. A., Walsworth, N., and Paradine, D. 2003a. Stand delineation and composition estimation using semi-automated individual tree crown analysis. *Remote Sensing of Environment.* 85, 355 – 369.

Lefsky, M. A., Cohen, W. B., and Spies, T. A. 2001. An evaluation of alternate remote sensing products for forest inventory, monitoring, and mapping of Douglas-fir forests in western Oregon. *Canadian Journal of Forest Research*. 31, 78 – 87.

Lefsky, M. A., Cohen, W. B., Parker, G. G., and Harding, D. J. 2002. Lidar remote sensing for ecosystem studies. *Bioscience*. 52, 19 – 30.

Lévesque, J. and King, D. J. 1999. Airborne digital camera image semi-variance for evaluation of forest structural damage at an acid mine site. *Remote Sensing of Environment*. 68, 112 – 124.

Lévesque, J. and King, D. J. 2003. Spatial analysis of radiometric fractions from high resolution multispectral imagery for modelling individual tree crown and forest canopy structure and health. *Remote Sensing of Environment*. 84, 589 – 602.

Le Moigne, J., Laporte, N., and Netanyahu, N. S. 2001. Enhancement of tropical land cover mapping with wavelet-based fusion and unsupervised clustering of SAR and Landsat image data. *Proceedings of SPIE – the 8th International Symposium on Remote Sensing*. Toulouse, France. pp. 190 – 198.

Lillesand, T. M. and Kiefer, R. W. 2000. *Remote sensing and Image Interpretation*. 4th edition. John Wiley and Sons, New York. 736 pp.

Lillesand, T. M., Kiefer, R. W., and Chipman, J. W. 2004. *Remote Sensing and Image Interpretation*. 5th edition. John Wiley and Sons, New York. 784 pp.

Lim, K., Treitz, P., Wulder, M., St-Onge, B., and Flood, M. 2003. Lidar remote sensing of forest structure. *Progress in Physical Geography*. 27, 88 – 106.

Lipchen, A. C., Der, S. Z., and Nasrabadi, N. M. 2003. Dualband FLIR fusion for automatic target recognition. *Information Fusion*. 4, 35 – 45.

Lovell, J. L., Jupp, D. L. B., Newnham, G. J., Coops, N. C., and Culvenor, D. S. 2005. Simulation study for finding optimal lidar acquisition parameters for forest height retrieval. *Forest Ecology and Management*. 214, 398 – 412.

Lu, D. 2005. Aboveground biomass estimation using Landsat TM data in the Brazilian Amazon. *International Journal of Remote Sensing*. 26, 2509 – 2525.

Luckman, A., Baker, J., Kuplich, T. M., Yanasse, C. C. F., and Frery, A. C. 1997. A study of the relationship between radar backscatter and regenerating tropical forest biomass for spaceborne SAR instruments. *Remote Sensing of Environment*. 60, 1 – 13.

Magnussen, S. and Boudewyn, P. 1998. Derivations of stand heights from airborne laser scanner data with canopy-based quantile estimators. *Canadian Journal of Forest Research*. 28, 1016 – 1031.

Magnusson, M. and Fransson, J. E. S. 2004. Combining airborne CARABAS-II VHF SAR data and optical SPOT-4 satellite data for estimation of forest stem volume. *Canadian Journal of Remote Sensing*. 30, 661 – 670.

Mäkelä, H. and Pekkarinen, A. 2001. Estimation of timber volume at the sample plot-level by means of image segmentation and Landsat TM imagery. *Remote Sensing of Environment*. 77, 66 – 75.

Maltamo, M., Eerikäinen, E., Pitkänen, J., Hyyppä, J., and Vehmas, M. 2004a. Estimation of timber volume and stem density based on scanning laser altimetry and expected tree size distribution functions. *Remote Sensing of Environment*. 90, 319 – 330.

Maltamo, M., Mustonen, K., Hyyppä, J., Pitkänen, J., and Yu, X. 2004b. The accuracy of estimating individual tree variables with airborne laser scanning in a boreal nature reserve. *Canadian Journal of Forest Research*. 34, 1791 – 1801.

Manninen, T., Stenberg, P. R., Voipio, P., and Smolander, H. 2005. Leaf area index estimation of boreal forest using ENVISAT ASAR. *IEEE Transactions on Geosicence and Remote Sensing*. 43, 2627 – 2635.

Maselli, F., Chirici, G., Bottai, L., Corona, P., and Marchetti, M. 2005. Estimation of Mediterranean forest attributes by the application of k-NN procedures to multitemporal Landsat ETM+ images. *International Journal of Remote Sensing*. 26, 3781 – 3796.

Mather, P. M. 2004. *Computer processing of remotely-sensed images: an introduction*. 3rd edition, John Wiley and Sons, New York. 442 pp.

McCombs, J. W., Roberts, S. D., and Evans, D. L. 2003. Influence of fusing lidar and multispectral imagery on remotely-sensed estimates of stand density and mean tree height in a managed loblolly pine plantation. *Forest Science*. 49, 457 – 466.

McRoberts, R. E., Holden, G. R., Nelson, M. D., Liknes, G. C., and Gormanson, D. G. 2006. Using satellite imagery as ancillary data for increasing the precision of estimates for Forest Inventory and Analysis program of the USDA Forest Service. *Canadian Journal of Forest Research*. 36, 2968 – 2980.

Miles, V. V., Bobylev, L. P., Maximov, S. V., Johannessen, O. M., and Pitulko, V. M. 2003. An approach for assessing boreal forest conditions based on combined use of satellite SAR and multispectral data. *International Journal of Remote Sensing*. 24, 4447 – 4466.

Moghaddam, M. and Duncan, J. L. 2001. Estimating forest variables from fusion of SAR and TM data and analytical scattering and reflectance models. *Proceedings of the IEEE International Geoscience and Remote Sensing Symposium, IGARSS '01.* 9–13 July. Sydney, Australia. Vol. 2. IEEE, New York. pp. 885 – 887.

Moghaddam, M., Duncan, J. L., and Acker, S. 2002. Forest variable estimation from fusion of SAR and multispectral optical data. *IEEE Transactions on Geoscience and Remote Sensing*. 40, 2176 – 2187.

Morsdorf, F., Meier, E., Kötz, B., Itten, K. I., Dobbertin, M., and Allgower, B. 2004. Lidar-based geometric reconstruction of boreal type forest stands at single tree-level for forest and wildland fire management. *Remote Sensing of Environment*. 92, 353 – 362.

Næsset, E. 1997. Determination of mean tree height of forest stands using airborne laser scanner data. *ISPRS Journal of Photogrammetry and Remote Sensing*. 52, 49 – 56.

Næsset, E. 2002. Predicting forest stand characteristics with airborne scanning laser using a practical two-stage procedure and field data. *Remote Sensing of Environment*. 80, 88 – 99.

Næsset, E. 2004. Accuracy of forest inventory using airborne laser scanning: evaluating the first Nordic full-scale operational project. *Scandinavian Journal of Forest Research*. 19, 554 – 557.

Næsset, E. and Bjerknes, K. O. 2001. Estimating tree heights and number of stems in young forest stands using airborne laser scanner data. *Remote Sensing of Environment*. 78, 328 – 340.

Næsset, E. and Gobakken, T. 2005. Estimating forest growth using canopy metrics derived from airborne laser scanner data. *Remote Sensing of Environment*. 96, 453 – 465.

Nilsson, M. 1996. Estimation of tree heights and stand volume using an airborne lidar system. *Remote Sensing of Environment*. 56, 1 – 7.

Pal, N. R. and Pal, S. K. 1993. A review of image segmentation techniques. *Pattern Recognition*. 26, 1277 – 1294.

Paloscia, S., Macelloni, G., Pampaloni, P., and Sigismondi, S. 1999. The Potential of C- and L-band SAR in estimating vegetation biomass: the ERS-1 and JERS-1 experiments. *IEEE Transactions on Geoscience and Remote Sensing*. 37, 2107 – 2110.

Patenaude, G., Hill, R. A., Milne, R., Gaveau, D. L. A., Briggs, B. B. J., and Dawson, T. P. 2004. Quantifying forest aboveground carbon content using lidar remote sensing. *Remote Sensing of Environment*. 93, 368 – 380.

Petrakos, M., Benediktsson, J. A., and Kanellopoulos, I. 2001. The effect of classifier agreement on the accuracy of the combined classifier in decision-level fusion. *IEEE Transactions on Geoscience and Remote Sensing*. 39, 2539 – 2546.

Pinz, A. 1998. Tree isolation and species classification. *Proceedings of the International Forum on Automated Interpretation of High Spatial Resolution Digital Imagery for Forestry,* 10–12 February. Pacific Forestry Centre, Canada Forest Service, Natural Resources Canada, Victoria, BC. pp. 127 – 139.

Pitkänen, J. 2001. Individual tree detection in digital aerial images by combining locally adaptive binarisation and local maxima methods. *Canadian Journal of Forest Research*. 31, 832 – 844.

Pohl, C. and van Genderen, J. L. 1998. Multisensor image fusion in remote sensing: concepts, methods, and applications. *International Journal of Remote Sensing*. 19, 823 – 854.

Pohl, C., Tempfli, K., and Huureman, G. C. 2004. Active sensors. In: Kerle, N., Janssen, L. L. F., and Huurmen, G. C. (Eds.), *Principles of remote sensing: an introductory textbook.* 3rd edition. The International Institute for Geo-Information Science and Earth Observation (ITC). Enschede. pp. 95 – 119.

Popescu, S. C. and Wynne, R. H. 2004. Seeing the trees in the forest: using lidar and multispectral data fusion with local filtering and variable window size for estimating tree height. *Photogrammetric Engineering and Remote Sensing*. 70, 589 – 604.

Popescu, S. C., Wynne, R. H., and Nelson, R. F. 2002. Estimating plot-level tree heights with lidar: local filtering with a canopy height based variable window size. *Computers and Electronics in Agriculture*. 37, 71 – 95.

Popescu, S. C., Wynne, R. H., and Nelson, R. F. 2003. Measuring individual tree crown diameter with lidar and assessing its influence on estimating forest volume and biomass. *Canadian Journal of Remote Sensing*. 29, 564 – 577.

Pouliot, D. and King, D. 2005. Approaches for optimal automated individual tree crown detection in regenerating coniferous forests. *Canadian Journal of Remote Sensing*. 31, 255 – 267.

Pouliot, D. A., King, D. J., Bell, F. W., and Pitt, D. G. 2002. Automated tree crown detection and delineation in high resolution digital camera imagery of coniferous forest regeneration. *Remote Sensing of Environment*. 82, 322 – 334.

Price, J. C. 1993. Estimating leaf area index from satellite data. *IEEE Transactions of Geoscience and Remote Sensing*. 31, 727 – 734.

Proisy, C., Mougin, E., Fromard, F., and Karam, M. A. 2000. Interpretation of polarimetric radar signatures of mangrove forests. *Remote Sensing of Environment*. 71, 56 – 66.

Rahman, M. M., Csaplovics, E., and Koch, B. 2005. An efficient regression strategy for extracting forest biomass information from satellite sensor data. *International Journal of Remote Sensing*. 26, 1511 – 1519.

Ramsey, E. J. 1999. Radar remote sensing of wetlands. In: Lunetta, R. S. and Elvidge, C. D. (Eds.), *Remote sensing change detection: environmental monitoring methods and applications*. Taylor and Francis, London. pp. 211 – 243.

Ranchin, T., Aiazzi, B., Alparone, L., Baronti, S., and Wald, L. 2003. Image fusion – the ARSIS concept and some successful implementation schemes. *ISPRS Journal of Photogrammetry and Remote Sensing*. 58, 4 – 18.

Rauste, Y. 2005. Multitemporal JERS SAR data in boreal forest biomass mapping. *Remote Sensing of Environment*. 97, 263 – 275.

Rauste, Y., Hame, T., Pulliainen, J., Heiska, K., and Hallikainen, M. 1994. Radar-based forest biomass estimation. *International Journal of Remote Sensing*. 15, 2797 – 2808.

Rees, W. G. 1990. *Physical principles of remote sensing*. Cambridge University Press, UK. 372 pp.

Remmel, T. K., Csillag, F., Mitchell, S., and Wulder, M. A. 2005. Integration of forest inventory and satellite imagery: a Canadian status assessment and research issues. *Forest Ecology and Management*. 207, 405 – 428.

Reutebuch, S. E., Andersen, H.-E., and McGaughey, R. J. 2005. Light detection and ranging (lidar): an emerging tool for multiple resource inventory. *Journal of Forestry*. 103, 286 – 292.

Riaño, D., Chuvieco, E., Condes, S., Gonzalez-Matesanz, J., and Ustin, S. L. 2004a. Generation of crown bulk density for *Pinus sylvestris* L. from lidar. *Remote Sensing of Environment*. 92, 345 – 352.

Riaño, D., Valladares, F., Condes, S., and Chuvieco, E. 2004b. Estimation of leaf area index and covered ground from airborne laser scanner (lidar) in two contrasting forests. *Agricultural and Forest Meteorology*. 124, 269 – 275.

Richardson, D. M. 1998. Forestry trees as invasive aliens. *Conservation Biology*. 12, 18 – 26.

Riley, M., Schwind, B., Daliparthi, P., and Warbington, R. 2002. A comparison of cover type delineations from automated image segmentation of Independent and merged IRS and Landsat TM image based data sets. *USDA Forest Service.* Available at: http://www.fs.fed.us/r5/rsl/publications/rsmapping/compare-irs-tm.pdf [Accessed 30 June 2006].

Saatchi, S. S. and Rignot, E. 1997. Classification of boreal forest cover types using SAR images. *Remote Sensing of Environment*. 60, 270 – 281.

Sanjeevi, S., Vani, K., and Lakshmi, K. 2001. Comparison of conventional and wavelet transform techniques for fusion of *IRS-1C LISS-III* and pan images. *Proceedings of the 22nd Asian Conference on Remote Sensing*. 5–9 November. Singapore. Vol. 1. CRISP, SISV, and AARS. pp. 140 – 145.

Santoro, M., Askne, J., Smith, G., and Fransson, J. E. S. 2002. Stem volume retrieval in boreal forests from ERS-1/2 interferometry. *Remote Sensing of Environment*. 81, 19 – 35.

Santos, J. R., Freitas, C. C., Araujo, L. S., Dutra, L. V., Mura, J. C., Gama, F. F., Soler, L. S., and Sant'Anna, S. J. S. 2003. Airborne P-band SAR applied to the aboveground biomass studies in the Brazilian tropical rainforest. *Remote Sensing of Environment*. 87, 482 – 493.

Schonau, A. P. G. and Grey, D. C. 1987. Site requirements of exotic tree species. In: von Gadow, K., van der Zel, D. W., and van Laar, A. (Eds.), *Forestry Handbook.* Southern African Institute of Forestry, Pretoria. pp. 82 – 94.

Schmullius, C. C. and Evans, D. L. 1997. Review article: synthetic aperture radar (SAR) frequency and polarisation requirements for applications in ecology, geology, hydrology, and oceanography: a tabular status quo after SIR-C/X-SAR. *International Journal of Remote Sensing*. 18, 2713 – 2722.

Scott, D. F. and Lesch, W. 1997. Streamflow responses to afforestation with *Eucalyptus grandis* and *Pinus patula* and to felling in the Mokobulaan experimental catchments, South Africa. *Journal of Hydrology*. 199, 360 – 377.

Sharma, K. and Sarkar, A. 1998. A modified contextual classification technique for remote sensing data. *Photogrammetric Engineering and Remote Sensing*. 64, 273 – 280.

Shrestha, H. L. 2005. Comparative evaluation of different spatial resolution data for timber volume estimation. *ISPRS workshop on High Resolution Earth Imaging for Geospatial Information.* July 2005. Hanover, Germany.

Simonett, D. S. and Davis, R. E. 1983. Image analysis – active microwave. In: Colwell R. N. (Ed.), *Manual of remote sensing*. American Society of Photogrammetry, Virginia. pp. 1125 – 1181.

Solberg, A. H., Jain, A. K., and Taxt, T. 1994. Multisource classification of remotely-sensed data: fusion of Landsat TM and SAR Images. *IEEE Transactions on Geoscience and Remote Sensing*. 32, 768 – 778.

Souza, C. M. and Roberts, D. 2005. Mapping forest degradation in the Amazon region with IKONOS images. *International Journal of Remote Sensing*. 26, 425 – 429.

Steininger, M. K. 2000. Satellite estimation of tropical secondary forest aboveground biomass: data from Brazil and Bolivia. *International Journal of Remote Sensing*. 21, 1139 – 1157.

St-Onge, B., Jumelet, J., Cobello, M., and Vega, C. 2004. Measuring individual tree height using a combination of stereophotogrammetry and lidar. *Canadian Journal of Forest Research*. 34, 2122 – 2130.

Strobl, D., Raggam, J., and Buchroithner, M. F. 1990. Terrain correction geocoding of a multi-sensor image data set. *Proceedings of the 10th EARseL Symposium*. 5–8 June. European Space Agency, Toulouse, France. pp. 98 – 107.

Suárez, J. C., Ontiveros, C., Smith, S., and Snape, S. 2005. Use of lidar and aerial photography in the estimation of individual tree heights in forestry. *Computers and Geosciences*. 31, 253 – 262.

Suits, G., Malila, W., and Weller, T. 1998. Procedures for using signals from one sensor as substitutes for signals of another. *Remote Sensing of Environment*. 25, 395 – 408.

Takahashi, T., Yamamoto, K., Senda, Y., and Tsuzuku, M. 2005a. Estimating individual tree heights of sugi (*Cryptomeria japonica* D. Don) plantations in mountainous areas using small-footprint airborne lidar. *Journal of Forest Research*. 10, 135 – 142.

Takahashi, T., Yamamoto, K., Senda, Y., and Tsuzuku, M. 2005b. Predicting individual stem volumes of sugi (*Cryptomeria japonica* D. Don) plantations in mountainous areas using small-footprint airborne lidar. *Journal of Forest Research*. 10, 305 – 312.

Tanaka, S., Sugimura, T., Senoo, T., and Nishi, T. 1998. Forest stand structure analysis in Mt. Fuji area with OPS and SAR Data. *Advances in Space Research*. 22, 685 – 688.

Tansey, K. J., Luckman, A. J., Skinner, L., Balzter, H., Strozzi, T., and Wagner, W. 2004. Classification of forest volume resources using ERS tandem coherence and JERS backscatter data. *International Journal of Remote Sensing*. 25, 751 – 768.

Tewari, D. D. 2001. Is commercial forestry sustainable in South Africa? The changing institutional and policy needs. *Forest Policy and Economics*. 2, 333 – 353.

Thomas, M., Everard, D. A., and van Wyk, G. F. 1997. An evaluation of two-metre resolution black and white satellite image for woodland remote sensing applications. *Southern African Forestry Journal*. 180, 33 – 36.

Thomas, V., Treitz, P., McCaughey, J. H., and Morrison, I. 2006. Mapping stand-level forest biophysical variables for a mixedwood boreal forest using lidar: an examination of scanning density. *Canadian Journal of Forest Research*. 36, 34 – 47.

Thompson, M. W. and Whitehead, K. 1992. An overview of remote sensing in forestry and related activities: its potential applications in South Africa. *Southern African Forestry Journal*. 161, 59 – 69.

Tokola, T. 2000. The influence of field sample data location on growing stock volume estimation in Landsat TM-based forest inventory in eastern Finland. *Remote Sensing of Environment*. 74, 422 – 431.

Tomppo, E. 2005. The Finnish multi-source inventory. *Proceedings of ForestSat 2005*. 31 May–3 June. National Board of Forestry, Borås. Sweden. pp. 27 – 34.

Tomppo, E. and Heikkinen, J. 1999. National forest inventory of Finland – past, present, and future. In: Alho, J. (Ed.), *Statistics, registries, and science – experiences from Finland*. Statistics Finland, Helsinki. pp. 89 – 108.

Tomppo, E., Nilsson, M., Rosengren, M., Aalto, P., and Kennedy, P. 2002. Simultaneous use of Landsat-TM and IRS-1c WiFS data in estimating large area tree stem volume and aboveground biomass. *Remote Sensing of Environment*. 82, 156 – 171.

Touzi, R., Landry, R., and Charbonneau, F. J. 2004. Forest type discrimination using calibrated C-band polarimetric SAR data. *Canadian Journal of Remote Sensing*. 30, 543 – 551.

Townsend, P. A. 2002. Estimating forest structure in wetlands using multitemporal data. *Remote Sensing of Environment*. 79, 288 – 304.

Treitz, P. 2001. Variogram analysis of high spatial resolution remote sensing data: an examination of boreal forest ecosystems. *International Journal of Remote Sensing*. 22, 3895 – 3900.

Treitz, P. and Howarth, P. 2000. High spatial resolution remote sensing data for forest ecosystem classification: an examination of spatial scale. *Remote Sensing of Environment*. 72, 268 – 289.

Tuceryan, M. and Jain, A. K. 1998. Texture analysis. In: Chen, C. H., Pau, L. F., and Wang, P. S. P. (Eds.), *Handbook of pattern recognition and computer vision*. 2nd edition. World Scientific Publishing, Singapore. pp. 207 – 248.

Turner, D. P., Cohen, W. B., Kennedy, R. E., Fassnacht, K. S., and Briggs, J. M. 1999. Relationships between leaf area index and Landsat TM spectral vegetation indices across three temperate zone sites. *Remote Sensing of Environment*. 70, 52 – 68.

Uuttera, J., Haara, A., Tokola, T., and Maltamo, M. 1998. Determination of the spatial distribution of trees from digital aerial photographs. *Forest Ecology and Management*. 110, 275 – 282.

van de Griend, A. A. and Seyhan, E. 1999. Multitemporal analysis of ERS-1 and EMISAR C-band VV backscattering properties of forest and lake surfaces in the NOPEX region. *Agricultural and Forest Meteorology*. 98, 363 – 374.

van der Sanden, J. J. and Hoekman, D. H. 2005. Review of relationships between grey-tone co-occurrence, semi-variance, and autocorrelation based image texture analysis approaches. *Canadian Journal of Remote Sensing*. 31, 207 – 213.

Wang, L., Sousa, W. P., and Gong, P. 2004. Integration of object-based and pixel-based classification for mapping mangroves with IKONOS imagery. *International Journal of Remote Sensing*. 25, 5655 – 5668.

Wang, Q., Adiku, S., Tenhune, J., and Granier, A. 2005a. On the relationships of NDVI with leaf area index in a deciduous forest site. *Remote Sensing of Environment*. 94, 244 – 255.

Wang, Y., Day, J. L., and Davis, F. W. 1998. Sensitivity of modelled C- and L-band radar backscatter to ground surface parameters in loblolly pine forest. *Remote Sensing of Environment*. 66, 331 – 342.

Wang, Z., Ziou, D., Armenakis, C., Li, D., and Li, Q. 2005b. A comparative analysis of image fusion methods. *IEEE Transactions on Geosceince and Remote Sensing*. 43, 1391 – 1402.

Waring, R. H., Way, J. B., Hunt, E. R., Jr, Morrissey, L., Ranson, K. J., Weishampel, J. F., Oren, R., and Franklin, S. E. 1995. Imaging radar for ecosystem studies. *Bioscience*. 45, 715 – 723.

Wehr, A. and Lohr, U. 1999. Airborne laser scanning—an introduction and overview. *ISPRS Journal of Photogrammetry and Remote Sensing*. 54, 68 – 82.

Wulder, M. 1998. Optical remote-sensing techniques for the assessment of forest inventory and biophysical parameters. *Progress in Physical Geography*. 22, 449 – 476.

Wulder, M., Niemann, K. O., and Goodenough, D. G. 2000. Local maximum filtering for the extraction of tree locations and basal area from high spatial resolution imagery. *Remote Sensing of Environment*. 73, 103 – 114.

Wulder, M., Niemann, K. O., and Goodenough, D. G. 2002. Error reduction methods for local maximum filtering of high spatial resolution imagery for locating trees. *Canadian Journal of Remote Sensing*. 28, 621 – 628.

Xu, Y., Prather, J. W., Hampton, H. M., Aumack, E. N., Dickson, B. G., and Sisk, T. D. 2006. Advanced exploratory data analysis for mapping regional canopy cover. *Photogrammetric Engineering and Remote Sensing*. 72, 31 – 38.

Yanasse, C. C. F., Sant'Anna, S. J. S., Frery, A. C., Renno, C. D., Soares, J. V., and Luckman, A. J. 1997. Exploratory study of the relationship between tropical forest regeneration stages and SIR-C L and C data. *Remote Sensing of Environment*. 59, 180 – 190.

Zheng, D., Rademacher, J., Chen, J., Crow, T., Bresee, M., Moine, J. L., and Ryu, S. R. 2004. Estimating aboveground biomass using Landsat 7 ETM+ data across a managed landscape in northern Wisconsin, USA. *Remote Sensing of Environment*. 93, 402 – 411.

Zhou, J., Civco, D. L., and Silander, J. A. 1998. A wavelet transform method to merge Landsat TM and SPOT panchromatic data. *International Journal of Remote Sensing*. 19, 743 – 757.

CHAPTER THREE

ESTIMATING PLOT-LEVEL MEAN AND DOMINANT TREE HEIGHT USING DISTRIBUTIONAL METRICS

Based on

Tesfamichael, S. G., Ahmed, F. B., and van Aardt, J. A. N. Accepted. Investigating the impact of discrete return lidar point density on estimations of mean and dominant plot-level tree height in *Eucalyptus grandis* plantations. *International Journal of Remote Sensing*.

Abstract

The accuracy of lidar remote sensing in characterising three dimensional forest structural attributes has encouraged foresters to integrate lidar approaches in routine inventories. However, lidar point density is an important consideration when assessing forest biophysical parameters, given the direct relationship between higher spatial resolution and lidar acquisition and processing costs. The aim of this study was to investigate the effect of point density on mean and dominant tree height estimates at plot-level. The study was conducted in an intensively-managed *Eucalyptus grandis* plantation. High point density (8 points/m^2) discrete return, small-footprint lidar data were used to generate point density simulations averaging 0.25 points/m^2, 1 point/m^2, 2 points/m^2, 3 points/m^2, 4 points/m^2, 5 points/m^2, and 6 points/m^2. Field surveyed plot-level mean and dominant heights were regressed against metrics derived from lidar data at each simulated point density. Stepwise regression was used to identify which lidar metrics produced the best models. Mean height was estimated at accuracy of R^2 ranging between 0.93 and 0.94 while dominant height was estimated with an R^2 of 0.95. Root mean square error was also similar at all densities for mean height (~1.0 m) and dominant height (~1.2 m); the relative RMSE compared to field-measured mean was constant at approximately 5%. Analysis of bias showed that the estimation of both attributes did not vary with density. The results indicated that all lidar point densities resulted in reliable models. It was concluded that plot-level height can be estimated with reliable accuracy using relatively low density lidar point spacing. Additional research is required to investigate the effect of low point density on estimation of other forest biophysical attributes.

3.1 Introduction

The application of lidar remote sensing for estimating forest structural attributes has grown in popularity due to the direct sampling of the three dimensional structure of forests that it offers (Dubayah and Drake, 2000; Lim *et al*., 2003; Reutebuch *et al*., 2005). Lidar sensors transmit short burst laser pulses and record the returning signals. The total traveling time between the emittance and receipt at the sensor is converted to distance (range) between the sensor and the reflecting object on the ground (Wehr and Lohr, 1999). Accurate geographical positioning of each return in the *x* (longitude) and *y* (latitude) directions is effected by a differential global positioning system (DGPS) and inertial management unit (IMU) integrated into the sensor system (Wehr and Lohr, 1999). Recent advances in lidar technology have resulted in sensors that have the capability to sample at high frequencies (approximately 200 kHz) (Ackermann, 1999; Lim *et al*., 2003; Reutebuch *et al*., 2005; Hyyppä *et al*., 2008). These properties make lidar sensors an ideal tool for structural assessment of vegetated areas (Lefsky *et al*., 2002), of which stand height is one such an attribute.

Stand height is a key component of forest inventories and requires accurate in-field measurements as it is used to calculate site quality and timber yield, among other stand attributes (von Gadow and Bredenkamp, 1992). Although the quantification of stand height using manual methods is relatively accurate, it is time consuming and costly in commercial forestry. Studies have shown that lidar remote sensing provides a more efficient alternative to traditional inventory, particularly in attaining the accuracy sought by foresters (Næsset, 1997; Magnussen and Boudewyn, 1998; Means *et al*., 2000; Næsset, 2002; Næsset and Økland, 2002; Clark *et al*., 2004). The variations in field-measured height explained by lidar data in these studies often exceed 90%.

Despite high accuracies, the inclusion of lidar as part of an operational forest inventory has seen limited application with the exception of Næsset *et al.* (2004). One of the reasons for this is the cost of data acquisition which needs to be addressed in relation to a wide range of variables, as well as accuracy and quality of

end products (Flood, 2001). From a systems perspective, acquisition cost is dependent on the area sampled, instrument cost, and density of point returns per unit area (Baltsavias, 1999a; Lovell *et al*., 2005), among other things. High point density acquisition, which translates into increased costs, has been regarded by some as desirable to improve accuracy in forested areas (Reutebuch *et al*., 2003). Therefore, balancing cost and accuracy becomes an important consideration when planning a lidar-based forest inventory (Lovell *et al*., 2005). While cost is a complex term that varies for different reasons, there is a need for rigorous research to examine the effect of lidar point density on the accuracy of structural estimates.

Lovell *et al*. (2005) investigated the effect of point density on estimation of predominant height by using simulated lidar data and crown shapes and including conical and ellipsoidal shapes, which approximate pine and *Eucalyptus* plantations, respectively. It was observed that both simulated shapes were estimated at error levels that increased linearly with increasing mean lidar point spacing. The study also found lower estimation errors for ellipsoidal shapes. Holmgren (2004) simulated lidar densities of 4.29 points/m^2, 0.55 points/m^2, 0.17 points/m^2, and 0.1 points/m^2 and estimated plot-level basal area and weighted mean tree height for Norway spruce, Scots pine, and birch. Models were developed on 10 m radius plots from a set of variables (percentiles) extracted from the lidar data at two sites. Height estimations using the models returned correlation coefficients (r) of approximately one and root mean square error (RMSE) values ranging between 0.59 and 0.99 m at stand-level. A comparison based on relative RMSE resulted in the conclusion that results for the various densities were similar. Thomas *et al*. (2006) compared mean height and mean dominant height from lidar data acquired at density levels of 4 points/m^2 and 0.035 points/m^2 by varying flight altitude in a mixed forest species area, consisting of fir, birch, aspen, and spruce. Plots (11.3 m radius) were split between model development and validation subsets. The models developed from first return points of high lidar point density had correlation accuracies of R^2=0.67 (RMSE=1.78 m) and R^2=0.89 (RMSE=1.62 m) for mean height and mean dominant height, respectively. Application of the models on the validation subset returned R^2=0.83 and 0.84 (mean and mean dominant height, respectively; RMSE not reported). At the lower density level, the model developed to explain mean height

resulted in R^2=0.68 (RMSE=1.75 m). Two models were developed from the first return and all return points for mean dominant height and resulted in R^2=0.92 (RMSE=1.37 m) and R^2=0.94 (RMSE=1.18 m), respectively. For the validation subset of plots, correlation of the models for mean height returned R^2=0.80. The models for estimating mean dominant height based on the first return and all return points, on the other hand, resulted in R^2=0.90 and 0.78, respectively. Stand-level estimation by Magnusson *et al*. (2007) found a decrease in RMSE of 1.1 to 0.7 m for densities ranging between 0.004 to 2.5 points/m^2 (~40 to 25 000 points/ha).

Most of the preceding studies were based on tree species with a conical canopy shape, which is different to the canopy shape of *Eucalyptus* species. Such variation has been shown to have an effect on lidar point return and thereby height estimation (Nelson, 1997). Goodwin *et al*. (2006) analysed the effects of platform altitude on estimations of structural attributes, including mean height and maximum height, in managed regrowth and plantation forests dominated by *Eucalyptus grandis*, *E. pilularis*, *Corymbia maculata*, and *E. microcorys*. Lidar data at three altitudes of 1000 m, 2000 m, and 3000 m were acquired over three plots of 3600 m^2 each. These flight altitudes resulted in respective average point spacings of 1.1 m, 1.55 m, and 1.9 m, respectively. Corresponding average plot-level densities were about 1 point/m^2, 0.4 points/m^2, and 0.2 points/m^2. In addition, the lowest flight altitude also provided a higher density data set with a point spacing of 0.9 m (1.4 points/m^2). The field plots represented regrowth sites with stockings of 139 stems/ha and 156 stems/ha, and a plantation with open canopy and low stocking (83 stems/ha). Plot-level mean and maximum height estimates of lidar data at all densities were in close agreement with corresponding field observations.

However, a study by Goodwin *et al*. (2006) put more emphasis on attributes other than tree height. Although a plantation forest was included in the study, it is unlikely to be representative of short rotation plantations of *Eucalyptus* trees grown for fast return (five to ten years) timber and pulp yields. Such plantations are often characterised by significant stocking densities, which results in potential attainment of near-complete canopy closures at a relatively early age after planting, depending on site characteristics. Canopy closure typically favours reliable point returns from

the upper section of canopies. Nevertheless, the lack of sufficient points returning from the underlying structural layers (e.g., lower growth, ground, etc.) may undermine the accuracy of estimation (Popescu *et al*., 2002; Clark *et al*., 2004; Thomas *et al*., 2006). The extent to which the overall penetration rate is affected by varying lidar point densities in even-aged short rotation *Eucalyptus* species plantations still requires in-depth investigation. Findings of such studies will have important implications for the bias associated with lidar-based height estimation, as well for the inventory cost associated with a given precision and accuracy. The objective of this study therefore was to assess the effect of simulated point density on the estimation of plot-level mean and dominant heights of *E. grandis*. The approach used in the study was to compare height estimates from models developed at various densities, utilising lidar data that were collected in a single survey and with fixed lidar acquisition properties. Point densities considered in this study were varied to correspond to nominal cost rating systems frequently used by lidar data providers.

3.2 Methods

3.2.1 Field data

Field data were collected during spring (October) of 2006. The age of the trees at the time of the survey ranged from four to nine years. Spacing between and within rows of the stands were approximately 3 and 2 m, respectively, at time of planting. Management of the plantations uses a sample size of 5% of the total area of a stand while our sampling achieved more than this figure in each stand. A total of 63 plots were sampled in 19 selected stands. The distance between plots in the same stand was not less than 50 m, thereby capturing as much variability within the compartment as possible. A 15 m radius was specified to delineate a circular plot from the centre tree. The geographical coordinates of an open location outside of a stand and closest to a plot was recorded using a differential global positioning system (DGPS) within a sub-meter accuracy level. The centre tree of the plot was then referenced to the GPS-located spot using bearing and distance measurements. Plot area was then adjusted for slope since this has an implication on the measurement of stems per hectare (SPHA).

Selective height and diameter at breast height (DBH) measurements were made. These inventory data subsequently were used to make statistical inferences about the population of trees within a stand (von Gadow and Bredenkamp, 1992). Such inference is usually achieved by relating measured height with corresponding DBH. Following this approach, DBH at 1.3 m above the ground was measured for all trees in each plot using a DBH tape (von Gadow and Bredenkamp, 1992). Only trees with a DBH thicker than 5 cm were considered for analysis and measurement. Tree height was measured on a sample of trees using a Vertex III hypsometer® (Haglöf, Sweden). The sample selected was based on the distribution of DBH measurements, thereby ensuring a representative sample of the entire DBH range. Relationships between DBH and corresponding height were established at plot-level using regression analysis with R^2 above 80% for the majority of plots and up to 98% (p<0.01) for a selection of plots. Heights of all trees within a plot were estimated using the resulting regression equations. Subsequently, two area-based definitions of height were applied: mean height and mean dominant height. Mean height was calculated as the arithmetic mean of all trees. Dominant height can be defined as the mean height of a selected number of trees per hectare (García, 1998). The selection of these trees could be based on DBH or height. Following the forest mensuration protocol of the forestry company managing the study area, dominant height was derived as the mean of the top 20% tallest trees. Results of these computations as well as DBH and SPHA are summarised in Table 3.1.

Table 3.1: Summary of field data (n=63)

Attribute	Range	Mean ± SD	Median
Mean Height (m)	14.59 – 31.64	21.31 ± 4.18	20.46
Dominant height (m)	14.51 – 40.77	25.15 ± 5.82	23.99
SPHA	602 – 1614	1138 ± 238	1177
DBH (cm)	12.2 – 24.8	16.9 ± 3.1	16.2

3.2.2 Lidar data

A lidar survey of the study area was carried out on November 8, 2006 using the Optech ALTM 3033 sensor mounted on a Cessna Caravan 206 aircraft (Airborne Laser Solutions, ALS; www.alsafrica.com). The system uses a discrete return mode

and was configured to record first and last return points. Performance characteristics of the sensor and the survey are listed in Table 3.2. Lidar points were classified as ground and non-ground using Terrasolid's TerraScan® software prior to delivery. The process involves an initial automated classification using the software, which attains 60 to 80% accuracy depending on terrain variation. This is followed by a manual editing processes supported by 15 cm resolution orthophoto images. Accuracy of the final digital terrain model (DTM) is compared with ground control points. Based on this, error of DTM was reported as +0.031 m (range: -0.017 to +0.078 m). The data were referenced to a local coordinate system (WGS 84 with Gauss Conform projection at longitude of 31°E). The geographical reference system of the ground data and associated GIS maps were, therefore, converted to the same projection.

Table 3.2: Flight and sensor characteristics of lidar survey of the study area

Parameter	**Value**
Average flying height	550 m (aboveground)
Flight side overlap	25%
Wavelength	1064nm
Pulse rate	33 kHz
Scan angle	10 degrees
Scan width	40 Hz
Beam divergence	0.2 mrad
Footprint	< 20 cm
Vertical accuracy	15 cm
Horizontal accuracy	28 cm
Nominal pulse density	5 points/m^2
Actual pulse density	Approximately 8 points/m^2

3.2.3 Lidar metrics extraction

Ground and non-ground points were extracted for each plot, with a buffer of one meter used to include point returns from crowns that extend beyond plot boundaries. Labelling of ground and non-ground was assigned to each point in the attribute tables of both data sets to keep track of their original class. The points subsequently were combined into a data set representing all returns. The spatial coverage of the points was divided into 1 m^2 rectangular plots using a freeware ArcGIS extension,

namely Hawth's Analysis Tools (Beyer, 2004), in order to analyse point density within each plot. Points were subsequently assigned to their geographically co-incident sub-plots. A preliminary analysis of the spatial distribution of the densities showed that all plots exhibited relatively normal distributions, which suggested that the mean was representative of the centre value. Although the data provider was contracted to acquire a mean point density of 5 points/m^2, 59 plots had equal to or greater than 6 points/m^2; further analysis of the data therefore focussed on these 59 plots. The highest mean density of these plots was 10.1 points/m^2, while the mean was 8.2 points/m^2. The first and third quartiles were 7.6 points/m^2 and 8.8 points/m^2, respectively, indicating a higher point density than the nominal figure of 5 points/m^2.

Seven mean density levels were simulated for each plot in this study (Table 3.3). The lowest level of 0.25 points/m^2 was chosen to obtain a single point return from a tree, given an in field inter-tree spacing of about 2 m. An assumption was made that the mean density levels would represent the true centre of normally distributed densities. The total number of points required to generate a simulated average point density was calculated as a percentage of the ratio of a simulated density to the original point density. Points were then extracted using the resulting percentage values for a given density level. Previous studies have demonstrated that extraction can be carried out based on time of laser returns (Holmgren, 2004) and minimum horizontal distance between adjacent returns (Magnusson *et al*., 2007). While all approaches strive towards depiction of density levels that have variations in simulated densities, as achieved under real lidar surveying conditions, Magnusson *et al*. (2007) acknowledged that artificial density reduction could best be described as theoretical. In this study, extraction was implemented using a random selection approach available in Hawth's Analysis Tools (Beyer, 2004). It was also deemed critical that the spatial distribution of points at a reduced density level is similar to that at the original level. Hence this characteristic was confirmed for the resulting points at all simulated density levels using histogram analysis. A summary of the number of points per plot extracted for the selected density levels is also presented in Table 3.3. The mean number of points ranged between 209 (0.25 points/m^2) and 5026 (6 points/m^2). Consequently, these points were separated as ground and non-ground following the original class labels assigned before combining the two sets of

points. The mean penetration rate was approximately 24%, indicating similarity in the number of ground vs. non-ground returns across density levels (Table 3.3).

Table 3.3: Simulated mean density levels and respective returns (n=59)

Density (points/m^2)	**No of points per plot**			**% Rate of ground returns**		
	Range	*Mean*	*SD**	*Range*	*Mean*	*SD**
0.25	122-219	209	17	11.4-38.9	23.9	6
1	487-870	838	67	12.6-35.7	24.1	5.3
2	973-1741	1675	133	13.0-34.2	23.7	5
3	1460-2608	2513	200	13.5-33.1	23.8	5.2
4	1950-3475	3350	267	15.0-33.9	23.8	5.1
5	2437-4349	4188	333	14.2-34.5	23.7	5.1
6	2924-5216	5026	400	14.3-33.9	23.7	5.2

*SD: standard deviation

Since both ground and non-ground points were measured relative to the same reference datum, the next step was computation of non-ground height values. A digital elevation model (DEM) was created by interpolating the ground points using ordinary kriging (Oliver, 1990). The pixel size was selected based on the minimum horizontal (*x* and *y* directions) distance between neighbouring points in order to utilise a maximum of available ground points. A minimum pixel size finally was specified at 10 cm in order to minimise the burden on computational requirements; this limit applied specifically to a density level of 6 points/m^2. There was a corresponding increase in pixel cell size as the density level decreased, with the maximum specified at 50 cm for the lowest density level. Additionally, whenever there were two or more points within a specified pixel size the point with the lowest elevation (*z* direction) value was used, since it was argued that this point more likely came from the ground. This was done to avoid instances where the interpolation algorithm encountered more than one representative lidar point per pixel.

Elevation values from the pixels of the DEM were registered to corresponding non-ground points that fell within the horizontal plane of the pixels (Beyer, 2004). DEM pixel values were then subtracted from non-ground point values. Visual assessment of the results showed points that were relatively close to the ground. It was decided

to exclude points below 5 m based on the field data, resulting in only points above or equal to 5 m in height being used in further analyses. A total of 28 independent variables, which will be referred to hereafter as metrics (Table 3.4), were computed from these points. The choice of these metrics follows their well documented applications in literature (Popescu *et al*., 2002; Holmgren, 2004; Næsset, 2004). Note from Table 3.4 that while percentiles are taken up to the 99th level, no mean values are derived above the 95th and 99th percentiles, due to the small number of returns above these percentiles for low density levels. Table 3.5 summarises the available number of points for all points above 5 m as well as above the indicated percentiles for each point density level. Clearly, the number of points decreased as the percentile cut-off increased. For example, there were on average 16 ± 2 points per plot above the 90% cut-off, compared to 116 ± 13 above the 25% and 156 ± 17 for all points in the 0.25 points/m^2 density data set.

Table 3.4: Independent variable metrics extracted from lidar points

Metrics*	**Label**
Mean of points	Mean
Standard deviation of points	SD
Coefficient of variation of points	CV
Skewness of points	Skewness
Kurtosis of points	Kurtosis
Percentiles at 25%, 50%, 75%, 80%, 90%, 95%, 99%	P_{25}…P_{99}
Mean of points above percentiles: 25%, 50%, 75%, 80%, 90%	Mean_P_{25} …Mean_P_{90}
Standard deviation above percentiles: 25%, 50%, 75%, 80%, 90%	SD_P_{25} …SD_P_{90}
Coefficient of variation above percentiles: 25%, 50%, 75%, 80%, 90%	CV_P_{25} …CV_P_{90}

*Derived from all points > 5 m aboveground

3.2.4 Statistical analyses

Stepwise regression was used to develop the single best model, in terms of R^2 and RMSE values, for each density level. The procedure operates by selecting independent variable(s) that provide the best estimation accuracy. Variables are included or excluded from a model based on specified criteria. The process involves fitting the model and iteratively removing and including variables until such time as the model has identified the variables which fulfil the predefined statistical criteria.

Here, a significance level of 0.1 was set for entry while significance level for retention in the model was specified as 0.05. Coefficients of determination and RMSE statistics were noted for comparison of models from the various densities. Relative RMSE was also calculated as the ratio of RMSE to field mean in order to relate the error to field measurements. Subsequent estimations were performed using the developed models. Residuals of estimates were used to assess the fitness of the models by computing signed and mean absolute errors (Kozak and Kozak, 2003). Further analysis was performed to test whether there were significant differences between observed and estimated means as well as among estimated means using analysis of variance (ANOVA).

Although model development was not the goal of this study, an attempt was made to compare prediction abilities of models from the various lidar point densities. Developing a model for prediction purposes involves testing its reliability based on samples not included in the model (Kozak and Kozak, 2003). While validation on independently gathered data is highly recommended, it is often expensive. An alternative approach is sub-setting the sample into modelling and validation sets, but this method requires a large sample size (Yang *et al*., 2004). The simplest and most widely used approach is cross-validation, which omits a subset of samples from the modelling effort and predicts the value(s) of the validation sample(s). The leave-one-out cross-validation method was adopted in this study, whereby each sample was removed iteratively and its value predicted using a model developed from the remaining samples. Error of prediction is then computed for the sample not used in developing the model. This process continues until all samples are predicted in a similar manner and the sum of the errors of prediction is commonly presented as the PRESS statistic (prediction residual sum of squares) (Allen, 1974). A model with a small PRESS value may be selected as the most reliable, while in this study the approach was extended to density comparison.

Table 3.5: Number of points counted above percentiles per density level

Density (points/m^2)		All > 5 m	>25%	>50%	>75%	>80%	>90%
0.25	Minimum	92	69	46	23	19	10
	Maximum	187	140	92	47	38	19
	mean	156	116	77	39	31	16
	SD	17	13	8	4	3	2
1	Minimum	365	273	182	90	73	36
	Maximum	721	540	360	180	144	72
	Mean	619	463	309	154	123	62
	SD	63	47	32	16	12	6
2	Minimum	728	546	363	101	146	73
	Maximum	1440	1078	718	360	287	144
	Mean	1246	933	621	307	248	124
	SD	124	93	62	41	25	12
3	Minimum	1103	826	549	274	220	109
	Maximum	2174	1631	1085	542	434	217
	Mean	1866	1402	930	465	372	186
	SD	191	141	95	48	38	19
4	Minimum	1429	1070	714	354	286	143
	Maximum	2866	2148	1430	716	570	286
	Mean	2490	1866	1242	620	496	248
	SD	253	190	127	64	51	25
5	Minimum	1845	1381	917	461	365	185
	Maximum	3609	2706	1803	902	720	358
	Mean	3116	2334	1554	776	620	310
	SD	315	236	158	78	63	31
6	Minimum	2197	1646	1095	549	439	220
	Maximum	4310	3231	2154	1077	860	426
	Mean	3739	2801	1865	931	744	372
	SD	378	283	189	94	75	37

3.3 Results

Model properties for estimating mean and dominant height from lidar metrics are summarised in Table 3.6. Two independent variables were used to develop models for mean height, except at a point density level of 0.25 points/m^2, which had only one independent variable. On the other hand, dominant height could be explained by a single independent variable at all density levels. All models were also comprised of higher order percentiles, with P_{95} being the most prevalent. Model performance in explaining the variability (R^2-values) in mean height was 0.94 for all models, except where a density level of 0.25 points/m^2 was used (R^2=0.93). Models explaining

dominant height had R^2-values of 0.95 for all density levels. Estimation error of the respective models was given as RMSE. The RMSE for mean height was close to 1 m for all density levels, while relative RMSE to the observed mean was consistently less than 5%. RMSE was slightly larger for dominant height at approximately 1.2 m; however, in all cases its relative value to the observed mean was approximately 5% (Table 3.6). Scatterplots relating field and estimated values are illustrated for three density levels (0.25 points/m^2, 3 points/m^2, and 6 points/m^2) in Figure 3.1. There was no evidence of serious systematic over- or underestimation of mean and dominant height. In addition, most estimations fell within the 95% confidence interval as illustrated by the selected density levels in the graph.

Table 3.6: Summary of model properties for estimating height at various point density levels

	Independent variable	***R^2**	**RMSE**	**RMSE (%)**
Mean height	P_{95}, Kurtosis	0.94	1.0 m	5%
Dominant height	P_{95}	0.95	1.2 m	5%

*p<0.01

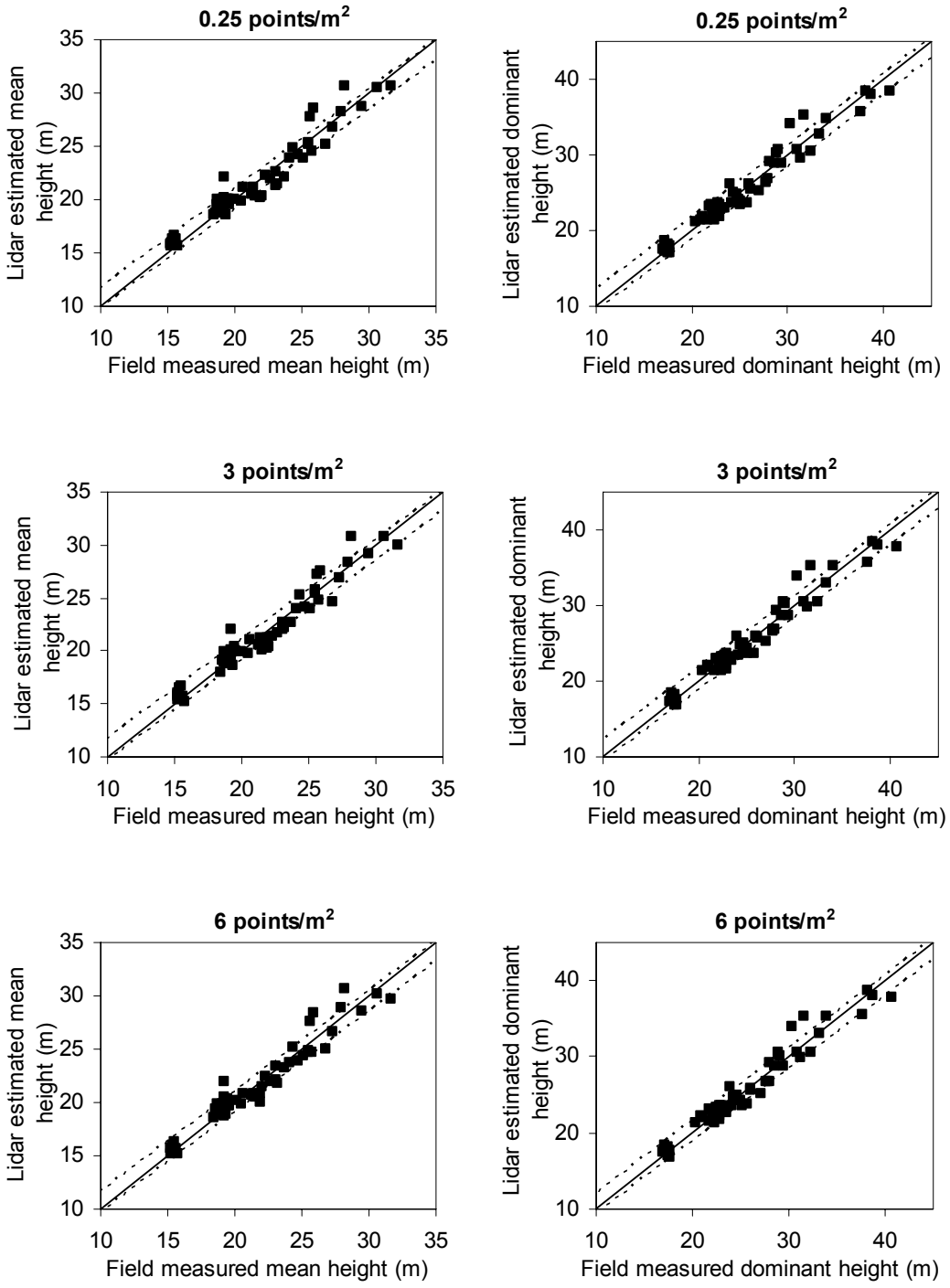

Figure 3.1 Scatterplots of lidar estimated vs. field measured heights. Solid lines indicate a 1:1 fit; dashed lines show the 95% confidence interval.

Means of the estimated values were compared among point density approaches and with the observed mean in each case. Estimated mean height across densities varied between 21.20 and 21.42 m. None of the estimates exhibited significant differences with the observed mean (21.41 m) and with each other (α=0.05, p<0.0001). Similarly, there was no significant difference between observed mean dominant height (25.27 m) and estimated means for dominant height which ranged from 25.27 to 25.28 m (α=0.05, p<0.0001). Various bias statistics of the models are presented in Table 3.7. Mean height and dominant height estimates had at least one sample with distinct overestimation at all density levels, based on the extreme values (range statistic). Mean signed error was close to zero for both mean height and dominant height estimations. There was less variability in the error for mean height (SD: 0.99 to 1.07 m) than for dominant height (SD: 1.23 to 1.26 m) across all densities (Table 3.7). Mean absolute error (MAE) for mean height ranged between 0.75 and 0.84 m, with a point density of 0.25 points/m^2 exhibiting the highest value. This statistic was higher for dominant height than for mean height and varied between 0.93 and 0.97 m (Table 3.7).

Although the above assessments indicated an overall similarity in bias among densities, closer observation at corresponding values was performed graphically by plotting the signed biases. The corresponding biases of estimation for mean height were nearly equal for densities of 2 points/m^2, 4 points/m^2, 5 points/m^2, and 6 points/m^2 (Figure 3.2). A similar comparison for dominant height showed that densities 2 points/m^2, 3 points/m^2, 4 points/m^2, 5 points/m^2, and 6 points/m^2 could be considered as identical (Figure 3.2).

Assessment of model performance for prediction purpose, based on observations not used for modelling, was performed using the PRESS statistic (Table 3.8). For mean height, density levels 0.25 points/m^2 and 1 point/m^2 had almost similar values at 74.48 and 76.56, respectively, while the remaining densities had PRESS values ranging between 65.50 and 66.68. This statistic varied between 97.72 and 102.37 across densities for dominant height (Table 3.8).

Table 3.7: Bias of estimations at various point density levels

Density (points/m^2)	Mean height				Dominant height			
	Range (m)	*Mean (m)*[a]	*SD (m)*[b]	*MAE (m)*[c]	*Range (m)*	*Mean (m)*	*SD (m)*	*MAE (m)*
0.25	-1.78 – 2.90	0.0011	1.07	0.84	-2.38 – 3.83	0.0012	1.25	0.96
1	-2.34 – 2.78	-0.0004	0.99	0.75	-3.67 – 3.71	-0.0010	1.23	0.93
2	-1.94 – 2.69	-0.0001	1.00	0.75	-3.12 – 3.69	-0.0002	1.26	0.97
3	-2.22 – 2.78	0.0002	1.00	0.79	-3.01 – 3.68	-0.0008	1.24	0.96
4	-1.86 – 2.65	0.0015	1.00	0.76	-3.07 – 3.68	-0.0004	1.24	0.95
5	-1.95 – 2.76	0.0010	1.00	0.76	-3.18 – 3.68	-0.0006	1.25	0.95
6	-1.89 – 2.68	0.0016	1.00	0.76	-3.08 – 3.68	0.0012	1.25	0.96

[a]Mean: mean signed error; [b]SD: standard deviation; [c]MAE: mean absolute error

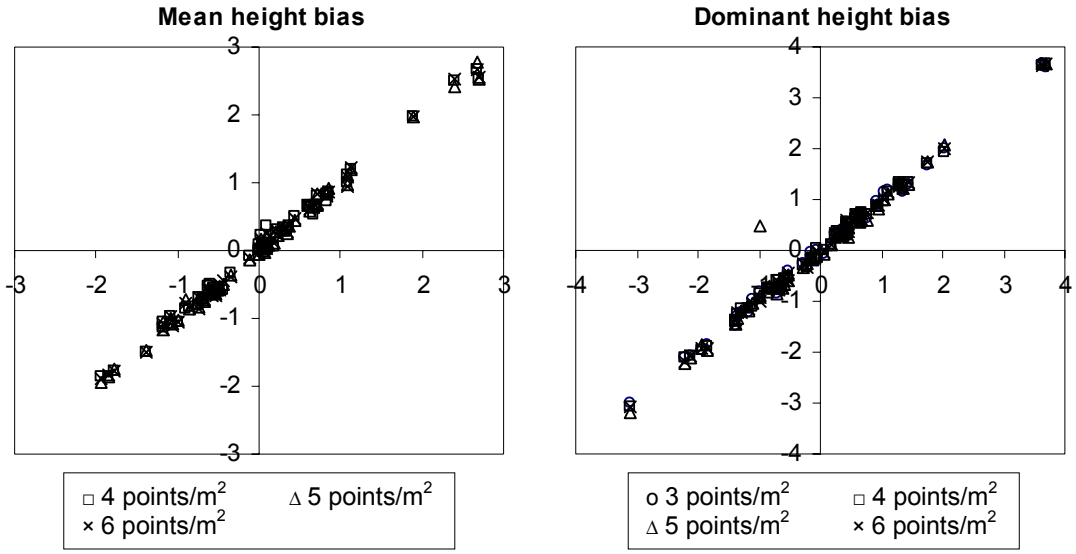

Figure 3.2 Similarity of bias of corresponding samples for various point density levels. The reference density is 2 points/m^2 for both attributes.

Table 3.8: PRESS values at various point density levels

Density (points/m^2)	Mean height (m)	Dominant height (m)
0.25	74.48	99.49
1	76.56	97.72
2	65.77	102.37
3	66.68	99.33
4	65.51	99.45
5	65.95	101.02
6	66.31	100.60

3.4 Discussion

The objective of this study was to investigate the effect of simulated lidar point density on the estimation of mean and dominant heights of *E. grandis* tree height at the plot-level. Comparisons were made using height prediction models developed from the lidar point densities of interest. Model results indicated that each of the attributes could be estimated with acceptable and similar accuracies at all density levels. The prevalent independent variable for most models came from the higher percentiles. Moreover, the comparable magnitudes of coefficients of determination for the percentiles confirmed the similarity of the models that explain the relevant dependent-independent relationships (Table 3.6). The agreement between higher percentile lidar metrics (independent variables) with field measured height previously has been demonstrated by researchers such as Means *et al*. (2000), Næsset (2002), and Holmgren (2004). Given the relative homogeneity of height and foliage structure of the target forests, a one-to-one relationship between lidar and field measured height values was expected. Selection of similar independent variables at all point densities indicated that there was a fairly equal proportion of lidar point returns across the vertical dimension.

Accuracy of height estimation has become a distinguishing strength of lidar application in forestry (e.g. Means *et al*., 2000; Næsset, 2002; Næsset and Økland, 2002). The model accuracy level at all densities was high in this study, with R^2-values ranging between 0.93 and 0.94 for mean height and 0.95 for dominant height (Table 3.6). Error of estimation (relative RMSE) was also low compared to field values (5% or less) (Table 3.6). Although regression analysis removes systematic

errors, it is important to note the absence of serious underestimation at all density levels (see Figure 3.1). This is in contrast to what is commonly mentioned as a characteristic of lidar, namely underestimation of plot-level tree height (Næsset, 1997; Magnussen and Boudewyn, 1998; Næsset, 2002; Clark *et al*., 2004; Holmgren, 2004). Although point density has been suggested as a potential cause of underestimation of tree heights (Lefsky *et al*., 2002), this did not seem to be the case in this study. This was attributed to the size of the plots, relative to the number of trees per plot, being large enough to have sufficient number of points from the upper canopy at all densities considered. Secondly, there might have been enough point representation even at the tree-level. It is hypothesised that the larger number of lidar points available when a larger spatial area is inventoried, as is often the case in operational inventories of commercial forests, will lead to improved accuracies based on these outcomes. However, this will be subject to intra-stand height homogeneity as well.

Results indicated that estimates of height variables and corresponding biases among the point density levels resulted in insignificant differences among lidar point density approaches in this forest environment. In fact, comparison of field mean and all estimated means have shown significant relationships. Error analyses also proved the absence of overall variation among densities (Table 3.7). While the overall similarity of the densities based on generalised bias is evident, a detailed look at corresponding estimates by plotting the errors revealed that some density levels could be described as nearly identical. The higher densities (mostly 4 points/m^2, 5 points/m^2, and 6 points/m^2), in general, were found to have such characteristics (Figure 3.2). This may hint at the potential of obtaining very similar bias or accuracy values for a given sample at the higher point densities.

Cross-validation of the models using the leave-one-out approach resulted in improved PRESS statistics and stronger similarities among densities of 2 points/m^2, 3 points/m^2, 4 points/m^2, 5 points/m^2, and 6 points/m^2 for mean height, while models developed at all point densities were similar for dominant height prediction. This indicated that a model developed at any level of the evaluated point densities could be regarded as reliable for future estimations outside of the model development

scenario. It should be stressed that this may only be used as an indicator of a general trend, rather than a complete picture, since the models were not originally intended for prediction purposes.

The results agree with the findings of Holmgren (2004) and Thomas *et al*. (2006), who reported similarity of height estimates irrespective of point density. Holmgren (2004) implemented a similar approach to this study in that densities were simulated from lidar data acquired at fixed flight parameters. Similarity of the results for the density levels was attributed to the relatively large footprint size (1.8 m diameter) of each pulse. The author concluded that increasing the point density might only result in overlapping of footprints that would have little impact on estimation. Thomas *et al*. (2006), on the other hand, compared two lidar densities acquired at two flight altitudes that resulted in two different footprint sizes. Low density point spacing performed slightly better than the higher density approach, which was attributed to the improved canopy penetration of points in the latter case as a result of the smaller footprint size. Given the scenarios related to structural geometry and the lidar data properties of this study, it is unlikely that the above reasons hold true. Instead, one probable conclusion could be related to the nature of *Eucalyptus* canopy structure. Variability in height of the upper canopy portion is relatively low and as a result points returning from this layer have comparable height measures (Lovell *et al*., 2005). Coupled with this, the closure of canopy may also play an important role. Nelson (1997) showed that closed canopies are amenable to accurate height estimations. The fact that the plantations used in this study have similar genetic material implies that growth and canopy closure is attained at approximately the same age across stands, provided similar site characteristics. However, canopy closure should not hinder point penetration to the extent that affects DEM accuracy as this would, in turn, bias tree height. The footprint size in the case of this study likely was small enough (Table 3.2) to enable penetration rates that are acceptable for accurate DEM generation.

The results of this study indicate that *E. grandis* plantations or other forests of similar canopy structure, height homogeneity, and subject to similar silvicultural practices, may not require high density lidar data for accurate height estimation. This will have

a significant influence on the cost of forest lidar surveying, which is considered one of the main constraints to operational use of lidar sensing. However, caution must be exercised when choosing the mode of acquisition towards a required point density level. One approach is by increasing flying height (e.g. Goodwin *et al*., 2006; Thomas *et al*., 2006). This method, however, influences important scanning properties such as increasing scanning angle and footprint size based on at-sensor beam divergence (Baltsavias, 1999b) and thus its effect on canopy penetration needs to be considered. Based on results of a simulation model, Holmgren *et al*. (2003) recommend that large scanning angles for characterising tree height and canopy returns be avoided. Moreover, a higher flying altitude, which leads to low rate of returns, potentially could affect the detection of individual trees. This could in turn diminish the accuracy of variable estimation at such a scale (Goodwin *et al*., 2006). A more preferable approach to reduce point density is by increasing the flying speed, which does not have a significant effect on penetration rate, provided that other system characteristics, e.g., beam divergence, pulse rate, and scan angle remain constant (Magnusson *et al*., 2007). Current results showed that the number of points from the upper canopy was sufficient for accurate height estimation, even for such a small footprint size, which may suggest that there was near-complete canopy closure in this study. Hence, increasing footprint size by increasing flying height may reduce the canopy penetration rate, which could cause insufficient ground sampling. While this may not pose a challenge in areas with flat topography, it will have a serious effect on applications in areas with an undulating ground surface.

This study focussed on intensively-managed plantations used for producing timber resources. Management of tree spacing in the plantations is a crucial factor for attaining an optimal harvest. Any decision to apply lidar technology in the plantation requires a careful study into the choice of specific lidar data acquisition parameters. Given that the target species of the study has received little attention in the research community, it was deemed useful to investigate the response of the species to various point densities of the lidar survey. Point densities selected in this study can be considered as having a narrow range (0.25 points/m^2 to 6 points/m^2). Similar approaches were also followed by Holmgren (2004) (0.1 points/m^2 to 4.29 points/m^2), Lovell *et al*. (2005) (spacing: 0.25 m to 1.3 m), Goodwin *et al*. (2006) (0.18 points/m^2

to 1.76 points/m^2), and Thomas *et al*. (2006) (0.035 points/m^2 to 4 points/m^2). In contrast, Magnusson *et al*. (2007) progressively thinned lidar points from 2.5 points/m^2 to 0.004 points/m^2. However, the authors reported only a slight decrease in the accuracy of height estimation in the range of 2.5 points/m^2 to 0.008 points/m^2 whereas better accuracies could still be achieved even at lower point densities than alternative approaches, such as aerial photo interpretation. However, the notion of surveying at very low point densities could be undesirable for inventories aimed at individual tree characterisation. This is particularly critical in plantations with high stocking such as the study area targeted in this paper.

3.5 Conclusion

Mean and dominant plot-level tree heights were estimated with high accuracy and low error at all the considered lidar point density levels in this study. Regression models developed for each density level exhibited strong linear relationships between field measured and lidar estimated mean height and dominant height. The commonly used model indices (R^2 and RMSE) showed that all densities resulted in similar model fit statistics. Comparison based on estimation errors (range, mean and SD of signed error, and mean absolute error) confirmed a strong similarity among densities for both dependent variables. Furthermore, models developed from all the densities were shown to be comparable in terms of prediction ability.

This study has shown that low point density acquisitions have significant potential for operational use in *E. grandis* plantations or forests of similar structures when the objective of a lidar survey is estimation of height at plot or larger scales. The range of density levels applied in this study theoretically results in at least one lidar point return from each tree. This provides an opportunity for further studies that may require the characterisation of individual trees, or their aggregation towards more detailed structural parameters, e.g., volume and biomass.

Results and interpretations refer to height estimations only, given the scope of the study. Comparable studies (Holmgren, 2004; Goodwin *et al*., 2006; Thomas *et al*., 2006; Magnusson *et al*., 2007) have shown that other attributes also can be

accurately estimated using low point density lidar data. Additional research is required on studies that investigate the application of lidar technology for multiple and alternative dependent variable prediction in intensively-managed *Eucalyptus* plantations, given the high cost of lidar surveys. Outcomes of such studies will be beneficial in terms of indicating to what extent low point density lidar data can be used as stand-alone data source for complete forest inventories.

Acknowledgments

This study was conducted under a Remote Sensing Cooperative project sponsored by the Council for Scientific and Industrial Research (CSIR) and Mondi South Africa. The authors would also like to thank members of the Cooperative for reviewing and adding constructive comments.

References

Ackermann, F. 1999. Airborne laser scanning—present status and future expectations. *ISPRS Journal of Photogrammetry and Remote Sensing*. 54, 64 – 67.

Allen, D. M. 1974. The relationship between variable selection and data augmentation and a method of prediction. *Technometrics*. 16, 125 – 127.

Baltsavias, E. P. 1999a. A comparison between photogrammetry and laser scanning. *ISPRS Journal of Photogrammetry and Remote Sensing*. 54, 83 – 94.

Baltsavias, E. P. 1999b. Airborne laser scanning: basic relations and formulas. *ISPRS Journal of Photogrammetry and Remote Sensing*. 54, 199 – 214.

Beyer, H. L. 2004. Hawth's Analysis Tools for ArcGIS®. Available at: http://www.spatialecology.com/htools [Accessed 03 December 2008].

Clark, M. L., Clark, D. B., and Roberts, D. A. 2004. Small-footprint lidar estimation of sub-canopy elevation and tree height in a tropical rain forest landscape. *Remote Sensing of Environment*. 91, 68 – 89.

Dubayah, R. O. and Drake, J. B. 2000. Lidar remote sensing for forestry. *Journal of Forestry*. 98, 44 – 46.

Environmental Systems Research Institute® (ESRI). ArcGIS® v. 9.1, 1999 – 2005, Redlands, CA, USA.

Flood, M. 2001. Laser altimetry: from science to commercial lidar mapping. *Photogrammetric Engineering and Remote Sensing*. 67, 1209 – 1217.

García, O. 1998. Estimating top height with variable plot sizes. *Canadian Journal of Forest Research*. 28, 1509 – 1517.

Golden software, Inc., Surfer® v. 8.06.39, 2006, CO, USA.

Goodwin, N. R., Coops, N. C., and Culvenor, D. S. 2006. Assessment of forest structure with airborne lidar and the effects of platform altitude. *Remote Sensing of Environment*. 103, 140 – 152.

Holmgren, J. 2004. Prediction of tree height, basal area, and stem volume in forest stands using airborne laser scanning. *Scandinavian Journal of Forest Research*. 19, 543 – 553.

Holmgren, J., Nilsson, M., and Olsson, H. 2003. Simulating the effects of lidar scanning angle for estimation of mean tree height and canopy closure. *Canadian Journal of Remote Sensing*. 29, 623 – 632.

Hyyppä, J., Hyyppä, H., Leckie, D., Gougeon, F., Yu, X., and Maltamo, M. 2008. Review of methods of small-footprint airborne laser scanning for extracting forest inventory data in boreal forests. *International Journal of Remote Sensing*. 29, 1339 – 1366.

Kozak, A. and Kozak, R. 2003. Does cross-validation provide additional information in the evaluation of regression models? *Canadian Journal of Forest Research*. 33, 976 – 987.

Lefsky, M. A., Cohen, W. B., Parker, G. G., and Harding, D. J. 2002. Lidar remote sensing for ecosystem studies. *Bioscience*. 52, 19 – 30.

Lim, K., Treitz, P., Wulder, M., St-Onge, B., and Flood, M. 2003. Lidar remote sensing of forest structure. *Progress in Physical Geography*. 27, 88 – 106.

Lovell, J. L., Jupp, D. L. B., Newnham, G. J., Coops, N. C., and Culvenor, D. S. 2005. Simulation study for finding optimal lidar acquisition parameters for forest height retrieval. *Forest Ecology and Management*. 214, 398 – 412.

Magnussen, S. and Boudewyn, P. 1998. Derivations of stand heights from airborne laser scanner data with canopy-based quantile estimators. *Canadian Journal of Forest Research*. 28, 1016 – 1031.

Magnusson, M., Fransson, J. E. S., and Holmgren, J. 2007. Effects on estimation accuracy of forest variables using different pulse density of laser data. *Forest Science*. 53, 619 – 626.

Means, J. E., Acker, S. A., Fitt, B. J., Renslow, M., Emerson, L., and Hendrix, C. J. 2000. Predicting forest stand characteristics with airborne scanning lidar. *Photogrammetric Engineering and Remote Sensing*. 66, 1367 – 1371.

Næsset, E. 1997. Determination of mean tree height of forest stands using airborne laser scanner data. *ISPRS Journal of Photogrammetry and Remote Sensing*. 52, 49 – 56.

Næsset, E. 2002. Predicting forest stand characteristics with airborne scanning laser using a practical two-stage procedure and field data. *Remote Sensing of Environment*. 80, 88 – 99.

Næsset, E. 2004. Effects of different flying altitudes on biophysical stand properties estimated from canopy height and density measured with a small-footprint airborne scanning laser. *Remote Sensing of Environment*. 91, 243 – 255.

Næsset, E. and Økland, T. 2002. Estimating tree height and tree crown properties using airborne scanning laser in a boreal nature reserve. *Remote Sensing of Environment*. 79, 105 – 115.

Næsset, E., Gobakken, T., Holmgren, J., Hyyppä, H., Hyyppä, J., Maltamo, M., Nilsson, M., Olsson, H., Persson, Å., and Söderman, U. 2004. Laser scanning of forest resources: the Nordic experience. *Scandinavian Journal of Forest Research*. 19, 482 – 499.

Nelson, R. 1997. Modelling forest canopy heights: the effects of canopy shape. *Remote Sensing of Environment*. 60, 327 – 334.

Oliver, M. A. 1990. Kriging: a method of interpolation for Geographical Information Systems. *International Journal of Geographic Information Systems*. 4, 313 – 332.

Popescu, S. C., Wynne, R. H., and Nelson, R. F. 2002. Estimating plot-level tree heights with lidar: local filtering with a canopy height based variable window size. *Computers and Electronics in Agriculture*. 37, 71 – 95.

Reutebuch, S. E., Andersen, H.-E., and McGaughey, R. J. 2005. Light detection and ranging (lidar): an emerging tool for multiple resource inventory. *Journal of Forestry*. 103, 286 – 292.

Reutebuch, S. E., McGaughey, R. J., Andersen, H.-E., and Carson, W. W. 2003. Accuracy of a high resolution lidar terrain model under a conifer forest canopy. *Canadian Journal of Remote Sensing*. 29, 527 – 535.

SAS® Institute, Inc., v. 9.1.3, 2002 – 2003, Cary, NC, USA.

Thomas, V., Treitz, P., McCaughey, J. H., and Morrison, I. 2006. Mapping stand-level forest biophysical variables for a mixedwood boreal forest using lidar: an examination of scanning density. *Canadian Journal of Forest Research*. 36, 34 – 47.

von Gadow, K. and Bredenkamp, B. 1992. *Forest management*. Academica, Pretoria. 164 pp.

Wehr, A. and Lohr, U. 1999. Airborne laser scanning—an introduction and overview. *ISPRS Journal of Photogrammetry and Remote Sensing*. 54, 68 – 82.

Yang, Y., Monserud, R. A., and Huang, S. 2004. An evaluation of diagnostic tests and their roles in validating forest biometric models. *Canadian Journal of Forest Research*. 34, 619 – 629.

CHAPTER FOUR

ESTIMATING STEMS PER HECTARE USING LIDAR HEIGHT DATA

Based on

Tesfamichael, S. G., Ahmed, F. B., van Aardt, J. A. N., and Blakeway, F. In Press. A semi-variogram approach for estimating stems per hectare in *Eucalyptus grandis* plantations using discrete return lidar height data. *Forest Ecology and Management*.

Abstract

Estimating stems per hectare (SPHA) for a given forest area from high spatial resolution remotely-sensed data usually follows the identification of individual trees. A common method of tree identification is through local maxima filtering, which in the context of a lidar canopy height model (CHM), seeks to locate the highest value within a specified neighbourhood of pixels. Hence, specifying an appropriate window size is a critical consideration. This study investigated the potential of the semi-variogram range towards defining an average window size for a given plot within *Eucalyptus* species plantations. The analysis also included comparisons of CHMs with three lidar point densities (1 point/m^2, 3 points/m^2, and 5 points/m^2) and three pixel sizes (spatial resolutions) (0.2 m, 0.5 m, and 1 m) at 5 points/m^2. These variations were introduced to study the effect of interpolated height surface resolution and lidar point density, respectively, on the identification of trees. Semi-variogram analysis yielded range values that varied distinctly with spatial resolution and point density. Computation of SPHA based on the semi-variogram range values resulted in overall accuracies of 73%, 56%, and 41% for 0.2 m, 0.5 m, and 1 m resolutions, respectively. A comparative approach, that defines window size based on pre-determined tree spacing, yielded corresponding accuracies of 82%, 82%, and 68% at the respective CHM resolutions. Point density comparisons based on interpolated CHM of 0.2 m resolution and the semi-variogram approach resulted in similar results between 5 points/m^2 (73%) and 3 points/m^2 (70%), whereas 1 point/m^2 returned the lowest accuracy (56%). Similar trends with superior accuracies were observed using the pre-determined tree spacing approach from the same resolution CHM: 82% (5 points/m^2), 80% (3 points/m^2), and 74% (1 point/m^2). While all estimates were negatively biased, the CHM with a 0.2 m spatial resolution at a point density of 3 points/m^2 resulted in a reasonable level of accuracy, negating the need for high density (>3 points/m^2) lidar surveys for this purpose. It was concluded that the semi-variogram approach showed promise for estimation of SPHA, particularly due to its independence from *a priori* knowledge regarding the tree stocking of the plantation.

4.1 Introduction

Measurement of the structural attributes of vegetation is an essential component of forest inventory. Currently, most forest inventories involve traditional methods that require intensive field efforts. The sampling design of such field visits are dependent on accuracy and precise specifications, areal coverage, and the budget of the inventory. Sampling strategy is an integral part of this method, since covering vast forest tracts is challenging (Schreuder *et al.*, 1993; Avery and Burkhart, 2001). A need exists to reduce inventory cost while maintaining coverage, given the high costs coupled to acceptable levels of accuracies that are achieved through existing field-based methods. The lack of accessibility, particularly in structurally and topographically complex forests, may further influence the sampling strategy. The introduction of remote sensing technologies has shown great promise towards addressing the above problems through significant cost reduction and synoptic coverage of large tracts of land (Wulder, 1998). This has resulted in remote sensing technology being increasingly applied to deliver information at the levels of detail demanded by operational forest management (Wulder, 1998; Boyd and Danson, 2005).

Lidar is a remote sensing technology that has seen growing application in forestry over the past few decades (Lefsky *et al.*, 2002; Lim *et al.*, 2003; Reutebuch *et al.*, 2005). Lidar is an active system that generates its own electromagnetic energy, usually in the near-infrared region of the light spectrum (Baltsavias, 1999a). The system emits high frequency bursts of laser pulses and records the time elapsed between emittance and sensor detection, following interaction with a target within the laser pulse's path. The elapsed time is used to calculate the distance between the lidar sensor and the reflecting object and is translated into elevation above mean sea level (Wehr and Lohr, 1999). Because lidar pulses are emitted at very short time intervals, they are able to penetrate relatively dense vegetation canopies and capture a large volume of information about the underlying ground surface (Ackermann, 1999). Given such information, it has now become possible to estimate canopy height at accuracy levels that are rarely matched by other remote sensing methods (Lefsky *et al.*, 2001; McCombs *et al.*, 2003). In fact, research has shown

accuracies to be equivalent to or better than those derived from traditional methods based on manual surveys (e.g., Coops *et al*., 2004; Holmgren, 2004). Other attributes that have been estimated using lidar include volume (Holmgren, 2004; Chen *et al*., 2007; Heurich, 2008), basal area (Holmgren, 2004; Hall *et al.*, 2005; Thomas *et al*., 2006; Chen *et al*., 2007), leaf area index (Riaño *et al*., 2004; Roberts *et al*., 2005; Jensen *et al*., 2008), canopy cover (Thomas *et al.*, 2006; Lee and Lucas, 2007; Heurich, 2008), etc. The focus of this paper, however, will be on the estimation of stems per hectare, which is an attribute that is critical to assessment of forest stocking and is required as an independent variable to a host of other forest attribute models (Avery and Burkhart, 2001).

Stems per hectare (SPHA) thus has other important implications in forest planning. For example, in homogenous stands, basal area can be calculated from SPHA. SPHA is also used as a multiplicative factor in conjunction with volume of an average tree for estimating an aggregate volume per unit area. This advantage, in particular, is critical in commercial forestry since economic return is measured in terms of timber volume. Estimation of SPHA from remotely-sensed data generally follows one of two approaches: (i) counting individual trees, which usually involves tree identification and/or crown segmentation for trees with known locations on the ground (Wulder *et al.*, 2000; Maltamo *et al*., 2004) and (ii) estimating aggregate number of trees per given area (stand-level) based on sampling plots (Holmgren *et al.*, 2003; Pouliot *et al*., 2005).

Regression analysis is the most common method for estimating aggregate SPHA while disregarding the location of individual trees. Hall *et al.* (2005) used an information-theoretic approach to select variables for predicting trees/ha in montane forests. The best model returned an R^2-value of 0.67, with canopy-related metrics as the independent variables. While comparing various remotely-sensed data, Lefsky *et al.* (2001) used lidar data derived from the full-waveform SLICER system (Scanning Lidar Imager of Canopies by Echo Recovery) to estimate coniferous forest attributes, including SPHA. A stepwise regression approach relating SLICER-derived canopy metrics with SPHA returned the best estimation accuracy when compared to other remote sensing data in terms of coefficient of determination (R^2=0.85). However, it

should be noted that waveform lidar data are still very much in a research and development phase, are costly to acquire, and result in large data volumes. Numerous studies have also been undertaken in developing and standardising models across the Scandinavian region for use in operational forest inventories (e.g., Næsset, 2002, 2004, 2007). Discrete return lidar data inputs in these studies included various statistical metrics such as maximum, mean, coefficient of variation, and percentiles of canopy height. Næsset (2007) stated that the error of estimates of these studies were within 11.6-29.3% of ground observations. This approach could be advantageous in that it does not require complex algorithms and returns relatively quick results. Reutebuch *et al.* (2005) also mentioned the relevance of lidar-based regression methods for assessing vertically complex forests, as well as their applicability at low point density levels. For example, Hall *et al.* (2005) used an average density of 1.23 points/m^2, while Næsset (2007) applied an average of 0.7-0.8 points/m^2. The main constraint of the noted studies is the dependence on regression-based models, which are developed using field-based model fitting and calibration sites. This becomes problematic if the target area is large, since the corresponding field sample size increases in order to represent the potential variability (Schreuder *et al.*, 1993). In addition, SPHA estimates that are obtained using regression-based methods do not contain any spatial information.

Estimation of SPHA through individual tree counting, on the other hand, is preceded by identification of potential trees or delineation of individual tree crowns. Techniques to accomplish this have been developed for high resolution imagery and have been adopted in the analysis of lidar data for similar objectives (Hyyppä *et al.*, 2004). Widely applied delineation algorithms include valley-following, which seeks to join minimum values in imagery and ideally create crown boundaries (Gougeon, 1995), identifying crown edges formed at multiple imagery scales (Brandtberg and Walter, 1998), template matching that relates crown models to image data (Pollock, 1998), and watershed segmentation, in which case a tree is simulated as an inverted mountainous topography to allow ‘flow’ from crown edges (upper areas) to the canopy top (lowest point) (Persson *et al.*, 2002; Heurich, 2008). However, most crown delineation applications using lidar data have adopted a region growing

approach whereby a region initiation point is identified first (Maltamo *et al.*, 2003; Hyyppä *et al.*, 2004; Morsdorf *et al.*, 2004; Kwak *et al.*, 2007).

Local maxima filtering is perhaps the most widely used approach for individual tree identification. In high spatial resolution optical imagery, a local maximum is defined as a pixel having the maximum reflectance within a given window or pixel neighbourhood that represents the individual tree crown size (Wulder *et al.*, 2000). This principle has been extended to lidar data to identify a pixel with the highest value (Popescu *et al.*, 2002; McCombs *et al.*, 2003; Maltamo *et al.*, 2004; Chen *et al*., 2006). A critical step in local maxima filtering is the selection of an appropriate window size for which the maximum value is determined (Wulder *et al.*, 2000; Popescu *et al.*, 2002). For fixed-size windows, size is often determined based on field-assessed canopy diameter of individual trees (Zimble *et al.*, 2003; Morsdorf *et al*., 2004; Roberts *et al.*, 2005). McCombs *et al.* (2003) used a window size based on the minimum spacing between trees in a loblolly pine plantation and reported correctly identifying trees with accuracies of approximately 65% and 87% for high and low planting densities, respectively. When erroneously committed (but not existing on the ground) trees were included, corresponding overall accuracies for the densities were 67% and 93%, respectively. Popescu *et al.* (2002) varied window size based on lidar height, an approach based on the relationship between canopy diameter and tree height established from field data. While this approach is applicable in predominantly natural forests, it may have limited application in homogenous stands grown for commercial purposes. The main reason for this is that the intensive management in commercial plantations is aimed at maximising merchantable tree volume, irrespective of canopy diameter. Although crown structures play an important role in photosynthesis and resultant trunk expansion, their effect is considerably diminished by the fixed tree spacing and thus the relationship between height and canopy diameter is relatively poor (Schreuder *et al.*, 1993). Moreover, field measurement of canopy diameter is a difficult task due to the irregularity of its projected area on the ground (Schreuder *et al.*, 1993; Pouliot *et al*., 2002). These aspects have resulted in yet undetermined lidar-based SPHA estimation algorithms in homogeneous, non-coniferous forest stands. This is

especially true where reliance on *a priori* field data needs to be limited in order to minimise inventory cost.

The objectives of this study were (i) to estimate stems per hectare using lidar data and a local maxima filtering approach in homogeneous, even-aged *Eucalyptus* plantations and (ii) to investigate the applicability of lidar-derived semi-variogram range and known tree spacing, as window size determinants for local maxima filtering. Two secondary objectives were targeted, namely evaluating the effects of canopy height model (CHM) pixel size and simulated lidar point density, as these interpolation inputs impact the CHM derivation. Local maxima filtering using the semi-variogram range sought to calculate an average range that could be used as a window size for a given plot. A second approach applied a fixed window size for all plots based on known tree spacing, given that trees were planted at the same regular interval. This study also assumed that the use of a fixed window size for a given plot has strong relevance in even-aged and homogenous stands.

4.2 Methods

4.2.1 Field data

Field data were collected during spring (October) of 2006. The age of the trees at the time of the survey ranged from four to nine years. Spacing between and within rows of the stands were approximately 3 m and 2.4 m, respectively. A total of 63 plots were sampled in 19 selected stands. A minimum distance of 50 m was maintained between adjacent plots wherever possible, thereby capturing as much variability within the compartment as possible. Management of the forest plantations in the area uses circular plots of 10 m radius; however, a 15 m radius was specified for this study in order to include more trees and thereby strengthen the statistical reliability of the results. The geographical coordinates of an open location outside of a stand and closest to a plot was recorded using a differential global positioning system (DGPS) within a sub-meter accuracy level. The centre tree of the plot was then referenced to the GPS-located spot using bearing and distance measurements. Plot area was then

adjusted for slope, since this has an implication on the conversion of tree count to stems per hectare (SPHA).

In each plot, only trees with a diameter at breast height (DBH) greater than 5 cm were considered for enumeration. This approach is commensurate to the inventory protocol of the forestry company that manages the plantations and has also been followed by other studies (e.g. Holmgren, 2004; Maltamo *et al.*, 2004). Trees that appeared to be damaged, dead, or dying were excluded from the inventory process for two main reasons. Firstly, the commercial industry rarely includes such trees in an accounting scheme and secondly, the number of lidar returns from trees devoid of canopies was deemed less significant. Tree counts in each plot were then converted to SPHA based on the area of the respective plot. Results of computed SPHA are summarised in Table 4.1. Distribution of SPHA indicates that more than a half of the total number of plots has greater than 1000 SPHA (Figure 4.1). Trees across the range of the DBH values were also selected for height measurement. DBH-height regression relations were developed within each plot, upon which the height estimation of all trees was based. A summary of plot-level arithmetic mean height and associated statistics are given in Table 4.1. This summary is intended to provide information on the extent of plot-level height variability that can have a significant impact on the stratification of the vertical structure (Latham *et al.*, 1998; Zimble *et al.*, 2003). Standard deviation (SD) and coefficient of variation (CV) values for height indicate the presence of a fair degree of variability in vertical structure, even though the study is based on even-aged plantations.

Table 4.1: Summary of SPHA and plot height field data

	SPHA (count)	**Height (m)**
Minimum	529	8 – 18
Maximum	1504	17 – 43
Mean	1024	15 – 32
SD	211	2 – 8
CV (%)	21	7 – 30

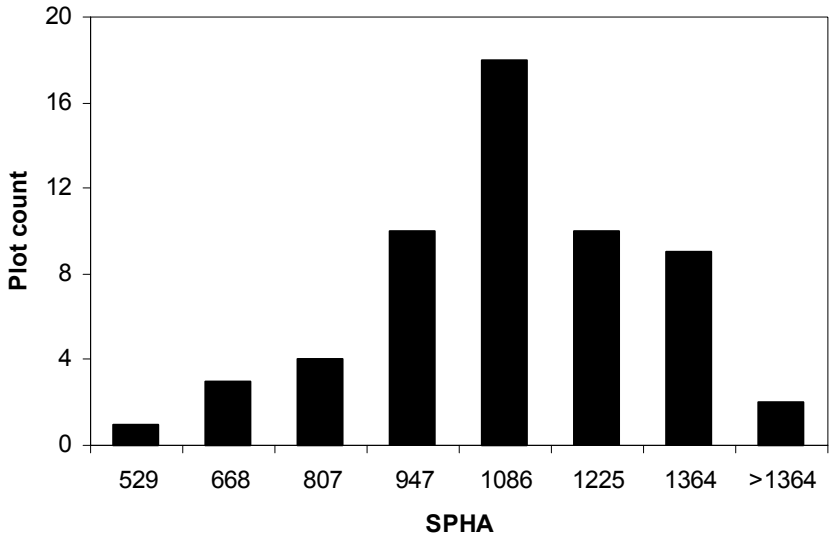

Figure 4.1 Distribution of SPHA across sample plots.

4.2.2 Lidar data

A lidar survey of the study area was carried out on November 8, 2006 using the Optech ALTM 3033 sensor mounted on a Cessna Caravan 206 aircraft (Airborne Laser Solutions, ALS; www.alsafrica.com). The system uses discrete return near-infrared laser pulses (wavelength 1064 nm) with a pulse rate of 33 kHz and was configured to record first and last returns per pulse with a density of five points per square meter (points/m^2). The aircraft was flown at an average height of 550 m above the ground with scan angle of 10° and beam divergence of 0.2 mrad to achieve the stated point density. The overlap between successive flight lines was set to 25%. At such specifications the resulting ground footprint size theoretically should not exceed 0.2 m. The vertical and horizontal accuracies of the point height and *x*,*y* coordinate values were 0.15 m and 0.28 m, respectively.

The data provider classified the points as ground and non-ground using Terrasolid's TerraScan® software. Briefly, the process involved an initial automated classification using the software, which attained accuracies between 60-80% depending on terrain variation. This was followed by a manual editing process aided by 0.15 m resolution orthophoto images. Accuracy of the final digital terrain model (DTM) was assessed using ground control points. Based on this, a mean error for the DTM was reported

as +0.031 m (range: -0.017 m to +0.078 m). The data were referenced to a local coordinate system (WGS 84 with Gauss Conform projection at longitude of 31°E).

4.2.3 Creating a canopy height model (CHM) at three spatial resolutions

An assessment of point density for the sample plots indicated that 61 plots had a density of at least 5 points/m^2, thus further analysis focused on these plots. A stand-level digital elevation model (DEM) was created from the lidar ground return layer. Since original lidar points were irregularly spaced, a continuous surface was created by estimating values for non-sampled areas using the ordinary kriging interpolation approach (Oliver, 1990) in Surfer 8.0 (Golden Software, Inc., Golden, CO, USA). A pixel size of 1 m was used in the interpolation, with at most one point used for generating a pixel height value. Whenever two or more points occurred within a pixel, the minimum point was utilised for the interpolation. The selection of these points was based on the assumption that they theoretically were closest to the 'true' ground value for that pixel.

Subtracting the digital elevation model from the original non-ground lidar returns resulted in normalised, aboveground height values for all non-ground returns. These normalised non-ground returns were then interpolated using ordinary kriging to generate a canopy height model (CHM). Although the plantations are even-aged and considered to be homogeneous, tree height variation within each plot does exist and is likely to be explained by the height of lidar returns. It should furthermore be noted that identification of trees from such lidar data may need to utilise all points, mainly because screening points based on height can remove a considerable number of adjacent points that might have returned from smaller trees. Thus all non-ground points, except those with zero height or less, as well as extremely large values, were employed in the interpolation. Point heights smaller than zero and substantially larger than observed tree height were regarded as errors. The interpolation created canopy height models (CHMs) at pixel sizes of 0.2 m, 0.5 m, and 1 m in order to address the spatial resolution objective of the study. For convenience, the term 'spatial resolution' is used in place of pixel size in this study (Atkinson and Aplin, 2004). Accordingly, the inverse relationship between spatial resolution and pixel size applies. Only the maximum point height was considered for interpolation whenever

two or more points were located in the same pixel. It was deemed highly probable that the surface interpolated from these points would constitute an outline of the upper surface of adjacent tree crowns. Plot-level CHM values subsequently were extracted for each CHM spatial resolution.

4.2.4 Simulating point densities

Three densities were compared in order to assess the effect of point density on estimation of stems per hectare: 1 point/m^2, 3 points/m^2, and 5 points/m^2. Lidar point density is a function of factors such as scanning angle, flying height, and flying speed (Baltsavias, 1999b) and may require several surveys at various densities to depict actual variations (e.g., Hirata, 2004; Thomas *et al.*, 2006). However, conducting separate surveys to obtain different densities was not feasible in this study, given the high cost of lidar campaigns. This necessitated the simulation of densities from a single survey. A similar approach has been used previously by Hirata (2004), Holmgren (2004), and Magnusson *et al.* (2007). Here, original ground and non-ground sets of points were uniquely labelled based on their ground-return class and then combined into a single data set. A grid with 1 m^2 cells was laid over each plot and point density calculated for each cell. Descriptive statistics of the resultant densities showed a normal distribution, which implied that the mean could be regarded as a representative value.

The total number of points required to generate a simulated average point density was calculated as a percentage of the ratio of a simulated average density to the original average density. It was assumed that the simulated point densities would display similar statistics in terms of distribution and representativeness of the mean. Points were then extracted using the resulting percentage values for a given density level. Previous studies have demonstrated that extraction can be carried out based on the time of laser returns (Holmgren, 2004) and minimum horizontal distance between adjacent returns (Magnusson *et al*., 2007). While all approaches strive towards depiction of simulated density levels with spatial density variations, as is achieved under actual lidar surveying conditions, Magnusson *et al.* (2007) acknowledged that artificial density reduction could best be described as theoretical. Extraction in this study was implemented using a random selection approach (Beyer,

2004). It was also deemed critical that the spatial distribution of points at a reduced density level is similar to that of the original data. Hence, this characteristic was confirmed for the resulting points at both simulated reduced density levels using histogram analysis. The resultant points were reclassified into ground and non-ground based on the labels attached to them prior to creating the combined data set.

A CHM was created for each density level using the same procedures described above. It was assumed in this study that comparison of pixel size is applicable across density levels. While this assumption was deemed logical, there could, however, be the possibility that it may not necessarily hold true. The density reduction process was therefore not repeated for each pixel size. Instead, the pixel size that provided the best result from the comparison based on the original density was applied to each of the three densities. This study also did not seek to evaluate the effect of the interaction between pixel size and point density on the estimation of SPHA.

4.2.5 Local maxima filtering

The process of local maxima filtering was performed on the respective CHMs using a window size determined by semi-variance analysis and pre-determined (*a priori* planting information) tree spacing. The semi-variance quantifies the degree of similarity/dissimilarity of a continuously varying attribute between a pair of samples separated by a certain distance (Isaaks and Srivastava, 1989). This concept has found a wide range of applications in the analysis of remotely-sensed data, given its spatial nature (Curran, 1988; Franklin *et al.*, 1996; Curran and Atkinson, 1998; Lévesque and King, 1999). Equation 4.1 shows that the semi-variance, $\gamma(h)$, for pixels separated by distance *h*, called *lag*, is defined as the average of the squared difference of an attribute between all pairs of pixels (Curran and Atkinson, 1998).

$$\gamma(h) = \frac{1}{2m(h)} \sum_{i=1}^{m(h)} \left[z(x_i) - z(x_i + h) \right]^2 \quad \text{.....(4.1)}$$

where $m(h)$ is the number of pairs of pixels separated by the same lag and $z(x_i)$ is the digital number of pixel x. Typically, the semi-variance increases at a decreasing rate as the lag increases and gradually reaches its 'maximum' at a certain limit called the *sill* (St-Onge and Cavayas, 1997). The lag (ground distance or number of pixels) where the sill is reached is dubbed the *range* and marks a threshold where pixels within that range are correlated to each other, whereas pixels at a lag beyond the range are uncorrelated (Curran and Atkinson, 1998). Consequently, pixels with strong correlation as specified by the range are considered to be spatially related. The range is often regarded as indicative of object size based on this principle, with an object in forestry terms seen as defining an individual tree canopy diameter (e.g. Woodcock *et al.*, 1988a, b; Wulder *et al.*, 2000).

It is proposed in this study that a continuous CHM, which represents heights of tree components, exhibits characteristics that can be modelled by variography. Although the canopy shape of *Eucalyptus* can be visualised as an ellipsoid (Lovell *et al*., 2005), a conical shape is still widely accepted in both coniferous and young hardwoods (Schreuder *et al*., 1993). Components of a tree therefore should have heights that progressively increase or decrease between canopy 'base' and 'top', respectively, assuming a smooth and solid crown geometry. Sampling the height of these components using lidar non-ground points provides useful information in defining the within-tree structural progression. However, given the nature of lidar sampling, some of these points pass through or penetrate the canopy resulting in irregular height variations. To minimise the influence of such variations, non-ground points can be converted into a surface of equal area and continuous pixels while removing a substantial number of points that degrade the smooth continuity of upper canopy geometry. The resulting pixels can serve as building sheets by factoring out continuously varying heights, since they outline individual tree canopies from the 'top' to the 'base'. The more a point deviates from a straight, continuous surface from canopy top to bottom of a tree the less likely it is to come from that tree. Certain studies have shown that the application of a smoothing filter to the CHM, prior to

local maxima filtering, improves the distinctiveness of trees (e.g. Hyyppä *et al*., 2001; Persson *et al*., 2002; Maltamo *et al*., 2004; Koch *et al*., 2006). However, smoothing, evaluated for a sample of plots, reduced the detection rate considerably; this was attributed to the loss of variability in height for closely spaced trees (Koch *et al*., 2006; Reitberger *et al*., In Press). As a result, smoothing was not applied here.

A sample variogram was first derived during the course of the analysis using the height values of pixels for each plot. This was followed by fitting a theoretical canopy model constructed using a weighted least squares approach (Cressie, 1985). A spherical canopy model is generally preferred to other models (e.g., St-Onge and Cavayas 1997; Lévesque and King, 1999); in this study, however, a choice was made based on comparison between circular and spherical models (ESRI®, ArcMap™ 9.1, Redlands, CA, USA). Visual observation of the graphs indicated strong similarities between the two models, while the difference in height RMSE between the two models for a plot was relatively small at an average of 0.01 m (range: 0.00-0.06 m). However, the range for the circular model was consistently smaller in size, which was more comparable to the nominal spacing between adjacent trees. Another distinct advantage of semi-variogram analysis is the ability to indicate the presence/absence of variability due to directionality of samples. Previous studies have shown the importance of direction in textural characterisation using digital imagery (Woodcock *et al.*, 1988a; Cohen *et al.*, 1990; St-Onge and Cavayas, 1997). Directionality was assessed at 0°, 45°, 90°, and 135°, while each direction was buffered with 30° tolerance in order to include a sufficient number of paired samples. Thus, if rows of the plantations have any effect in creating directional variability, the selected directions are deemed capable of identifying this feature. Results indicated that there was no difference among all directions in the computed parameters, including the range value. This was not unexpected given that the focus was on height variability within a crown, which is generally characterised by a circular shape. Moreover, the attribute of interest is height rather than spectral information, with the latter being influenced by shadow effects, especially in open forests (St-Onge and Cavayas, 1997). An omni-directional variogram with large directional tolerance therefore was used (Isaaks and Srivastava, 1989).

User intervention is needed for the computation of a variogram, specifically when fitting the theoretical model to the sample model. Inputs include specifying the lag size, the number of lags, and adjusting the nugget effect. Since the spatial information of the data was regularised in the form of pixels, the pixel size was used as spacing between samples (Isaaks and Srivastava, 1989). The unit of this distance was expressed in meters, the same as the ground distance unit. The number of lags was determined such that when multiplied with the lag size, the product approximated half the largest distance of all pairs (ESRI®, ArcMap™ 9.1, Redlands, CA, USA). In this case, the largest distance was equivalent to the diameter of the plot. Unlike the above two inputs, which followed widely accepted specifications of values, adjustment of the nugget effect requires careful visual inspection and thus is likely to depend on the user's judgment. The adjustment essentially seeks to align the theoretical variogram so that it optimally fits the sample variogram towards the smaller lags. Nugget is introduced into the variogram mainly if there is variation between samples that could not be captured by the sampling scale and/or is due to sampling error (Isaaks and Srivastava, 1989). A combination of all these inputs resulted in a range value which was taken as the window size to filter local maxima.

The second approach of local maxima filtering utilised actual, pre-determined spacing between adjacent trees. According to the database of the plantations, trees are planted at a spacing of 2.4 m within a row and 3 m between rows in most timber plantations of the study area. It should be noted that there could be a decrease in stocking due to mortality as a result of drought spells and competition in the area during the growing period (Smith *et al*., 2005). However, this does not preclude the possibility of the original spacing being maintained even at a rare occurrence. Considering a circular shape of canopies, a tree was then assumed to have a canopy diameter of approximately 2.4 m, which was in turn used as the window size for local maxima filtering.

The next step in the analysis involved determining the shape of the roving window, as this can play an important role in the filtering. Wulder *et al.* (2000), for example, translated the semi-variogram range into square window. McCombs *et al.* (2003) used circular windows to identify trees in a loblolly plantation using spectral imagery

and lidar data. Usually, a circle should generalise the shape of a tree crown on the horizontal plane (Schreuder *et al.*, 1993) and hence is a more appropriate shape than a square for local maxima filtering (Popescu and Wynne, 2004). We therefore chose a circular window for the analysis. The range of a variogram subsequently was taken as the mean diameter of a single tree canopy for a given plot while a diameter of 2.4 m was used for all plots in the tree spacing approach. The window was then moved across the CHM in order to identify the pixel with the maximum value within its respective local neighbourhood. The number of per-plot maximum values, identified by using each of the local maxima filtering approaches, spatial resolutions, and lidar point densities were counted as the number of trees for that specific plot. Plot-level counts were then converted to the standard inventory unit of SPHA using plot area.

4.2.6 Accuracy assessment

The intention of this study was to compute the aggregate number of trees rather than locating individual trees, even though an alternative approach to map trees exists and utilises the information on the rows (Pouliot *et al.*, 2002). Although the silvicultural practices include row planting, the latter method was not strictly followed since there were noticeable deviations from spacing design within rows. The common accuracy indices of omission and commission errors that respectively define exclusion and addition of trees were therefore not applicable. This necessitated accuracy assessment based on aggregated values. First, the total number of trees, as identified by local maxima, was converted to SPHA based on the area of analysis. Accuracy was subsequently calculated as a percentage of the lidar-derived SPHA versus field-observed SPHA. Various accuracy-related statistics were also computed. Residuals were analysed using common descriptive statistics. Absolute error was preferred to signed error, since the goal was to investigate accuracy irrespective of omission and commission errors. Root mean square error was calculated to quantify the distance between estimated and observed means. Analysis of variance of mean SPHA was used to determine whether lidar estimates differed with each other and from field observations significantly.

4.3 Results

4.3.1 SPHA at various spatial resolutions

From the total of 61 plots, two had range values that exceeded the respective plot sizes at all spatial resolutions. This is attributed to the lack of spatial correlation between samples spaced at distances up to the equivalent of plot diameter. Further, additional two plots returned an unrealistically large number of trees for the 0.2 m resolution due to very small range values that in turn could have stemmed from significant degree of variability between samples over short distances. Such variability must have resulted in the identification of more than one local maximum from a considerable number of individual trees. These four plots were therefore excluded and all results presented here are based on analysis of the remaining 57 plots. It is believed that the exclusion of the plots would not constitute as removal of outlier. Table 4.2 summarises local maxima filtering window size results per spatial resolution, as determined by the semi-variogram range. Mean window sizes for 0.2 m, 0.5 m, and 1 m spatial resolutions were 3.0 m, 3.9 m, and 5.2 m, respectively. The differences in mean range were significant (α=0.05, p<0.001). Fitness of model variogram was measured by RMSE for all plots at each spatial resolution. Summary statistics (Table 4.2) showed a marginal improvement in RMSE as spatial resolution decreased. For example, the mean RMSEs of model variograms for all plots were 0.635 m, 0.502 m, and 0.436 m at 0.2 m, 0.5 m, and 1 m spatial resolutions, respectively. Figure 4.2 illustrates model variograms from a sample plot for comparing the three spatial resolutions. The position of the range (open circles) on the lag distance confirmed the results presented in Table 4.2. The sill, i.e., where the variance starts to level off, was largest for the 0.2 m resolution, followed by the 0.5 m and 1 m spatial resolutions.

Table 4.2: Summary of semi-variogram range and model fitness results for the three CHM spatial resolutions

	CHM spatial resolution					
	0.2 m		0.5 m		1 m	
	Range (m)	*RMSE (m)*	*Range (m)*	*RMSE (m)*	*Range (m)*	*RMSE (m)*
Minimum	2.0	0.173	2.1	0.240	3.2	0.251
Maximum	5.4	1.411	6.0	0.986	7.8	0.908
Mean*	3.0[a]	0.635	3.9[b]	0.502	5.2[c]	0.436
SD	0.7	0.294	0.8	0.202	1.0	0.140

*Different letters indicate significant differences at α=0.05

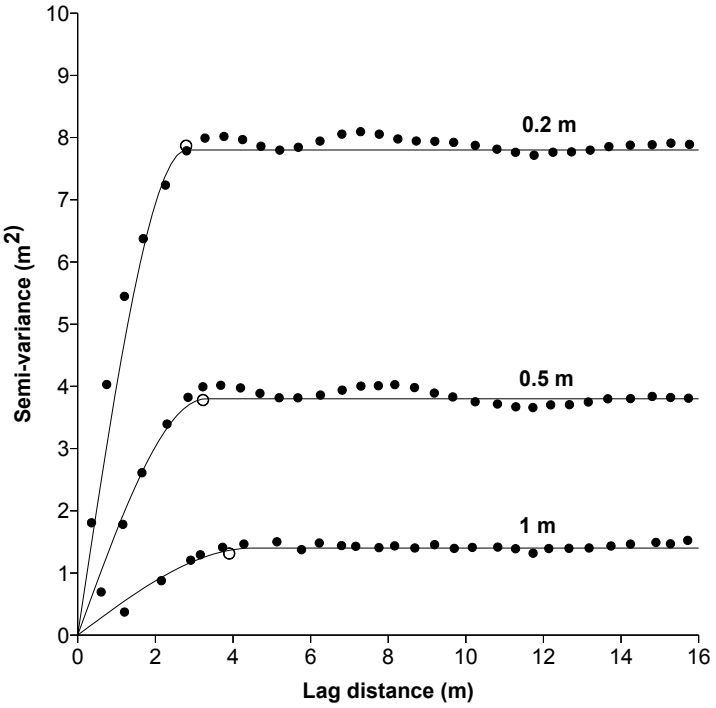

Figure 4.2 Variograms of the three spatial resolutions for a random sample plot. Open circles indicate the range size on the x-axis (lag).

Accuracies of estimated SPHA using both local maxima filtering approaches are summarised in Table 4.3. In the case of the approach based on the semi-variogram range, 0.2 m spatial resolution resulted in the highest overall mean accuracy (73%), followed by resolutions of 0.5 m (56%) and 1 m (41%). Quartile distributions showed that 75% of the plots had accuracies greater than 56% for 0.2 m resolution, while accuracies in the same range were observed for 50% of the plots when a 0.5 m

resolution was used. Similar statistical measures for SPHA estimation using a window size based on pre-determined tree spacing returned better accuracies at each resolution, although accuracies at 0.2 m and 0.5 m resolutions were similar.

Table 4.3: Accuracies of SPHA estimated at three CHM spatial resolutions using the semi-variogram range and tree spacing approaches

SPHA statistic	**CHM spatial resolution**					
	0.2 m		**0.5 m**		**1 m**	
	Variogram	*Spacing*	*Variogram*	*Spacing*	*Variogram*	*Spacing*
Minimum (%)	36	50	32	46	18	35
Maximum (%)	99	100	97	100	98	98
Mean (%)	73	82	56	82	41	68
SD (%)	17	14	15	14	17	17
Quartile 1 (%)	56	74	44	71	28	57
Quartile 2 (%)	77	85	54	83	38	67
Quartile 3 (%)	88	91	64	93	45	78

Results for absolute error assessment are presented in Table 4.4. As expected, following the accuracy results in Table 4.3, the error of estimation increased as spatial resolution decreased. Mean absolute errors of estimation were 295 SPHA, 464 SPHA, and 621 SPHA for 0.2 m, 0.5 m, and 1 m resolutions, respectively. Standard deviations of errors were equal for 0.2 m and 0.5 m resolutions, amounting to 20% of the field mean with a slightly larger value for the 1 m resolution case (24%). In contrast, there was a considerable increase in RMSE values as the spatial resolution decreased. Local maxima filtering based on tree spacing resulted in mean absolute errors of 206 SPHA, 208 SPHA, and 360 SPHA for 0.2 m, 0.5 m, and 1 m, respectively. Standard deviations were comparable to the approach that utilised the semi-variogram range. However, RMSE was considerably lower at each spatial resolution for the approach that followed tree spacing. Similar to the accuracy assessment (shown in Table 4.3), results exhibited a strong similarity between 0.2 m and 0.5 m spatial resolutions. Table 4.4 also provides the number of plots overestimated by the different resolutions. Overestimation decreased as spatial resolution decreased. A cursory comparison between methods showed a larger

overestimation for the tree spacing approach than the semi-variogram range approach within each spatial resolution.

Table 4.4: Absolute error of estimation at the three spatial resolutions. Figures in parentheses indicate proportion to observed mean

SPHA statistic	**CHM spatial resolution**					
	0.2 m		**0.5 m**		**1 m**	
	Variogram	*Spacing*	*Variogram*	*Spacing*	*Variogram*	*Spacing*
Minimum (SPHA)	12	0	38	0	25	12
Maximum (SPHA)	774	682	995	765	1128	916
Mean (SPHA)	295	206	464	208	621	360
SD (SPHA)	210 (20%)	172 (17%)	208 (20%)	180 (18%)	249 (24%)	229 (22%)
RMSE (SPHA)	361 (35%)	267 (26%)	507 (50%)	274 (27%)	668 (65%)	426 (42%)
Overestimated plots (n)	10	25	1	18	3	6

The mean estimates using the semi-variogram approach were 866 SPHA, 558 SPHA, and 432 SPHA for resolutions of 0.2 m, 0.5 m, and 1 m, respectively. Corresponding estimates using filtering based on tree spacing were 997 SPHA, 904 SPHA, and 711 SPHA. For all resolutions, mean values were less than the observed mean of 1024 SPHA. Except for the estimate using tree spacing and 0.2 m CHM, analysis of variance between observed and estimated SPHA at each spatial resolution using both approaches showed that the mean difference was significant (α=0.05, p<0.001) (Figure 4.3). The variation was also significant between the semi-variogram range and tree spacing approaches within each resolution. The ANOVA did not confirm the reported similarity between 0.2 m and 0.5 m spatial resolutions in terms of accuracy and error assessments for the same approach. Similarly, ANOVA among spatial resolutions also indicated significant variation for estimated SPHA.

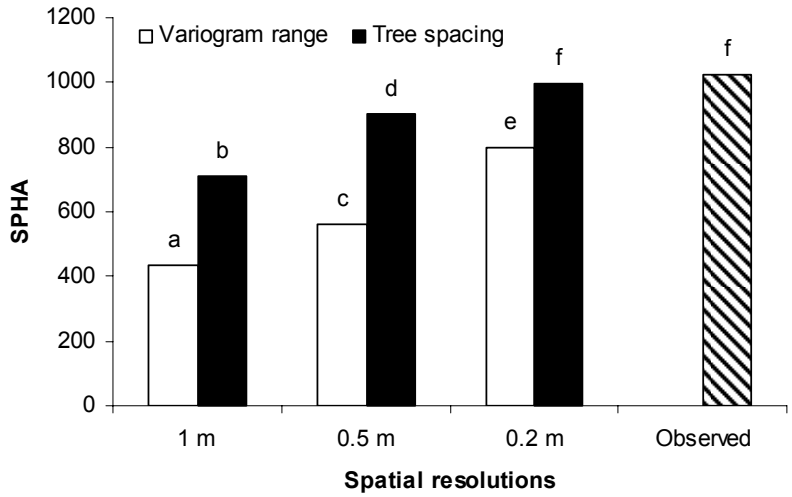

Figure 4.3 A comparison of the means between lidar estimates and field-observed values for the three spatial resolutions. Different letters indicate significant differences at α=0.05.

4.3.2 SPHA at various point densities

Based on the results of pixel comparisons presented above, the 0.2 m spatial resolution was chosen to construct a CHM for each of the density levels. Hence, it should be noted that all the results relating to the highest density level (5 points/m^2) will remain the same as the results for 0.2 m spatial resolution reported above. Table 4.5 provides a summary of the semi-variogram range values computed for each density. Range increased with a decrease in point density. However, the increases were not as large as those observed in the comparisons of spatial resolutions with mean values of 3.0 m, 3.1 m, and 3.6 m for 5 points/m^2, 3 points/m^2, and 1 point/m^2, respectively. Densities of 5 points/m^2 and 3 points/m^2 exhibited a similar mean range, while both were significantly different from range at 1 point/m^2 (α=0.05, p<0.001). Variogram model goodness-of-fit (RMSE) indicated a decreasing trend with a decrease in lidar point density. Sample and fitted models of a sample plot showed that higher densities were similar, especially in variance (sill), whereas a density of 1 point/m^2 resulted in the lowest variance (Figure 4.4).

Table 4.5: Summary of semi-variogram range and model fitness results for CHMs derived from three lidar point densities

	Lidar point densities					
	5 points/m^2		3 points/m^2		1 point/m^2	
	Range (m)	*RMSE (m)*	*Range (m)*	*RMSE (m)*	*Range (m)*	*RMSE (m)*
Minimum	2.0	0.173	2.0	0.095	2.8	0.035
Maximum	5.4	1.411	5.4	0.905	5.0	0.307
Mean*	3.0[a]	0.635	3.1[a]	0.355	3.6[b]	0.134
SD	0.7	0.294	0.7	0.187	0.6	0.068

*Different letters indicate significant differences at α=0.05

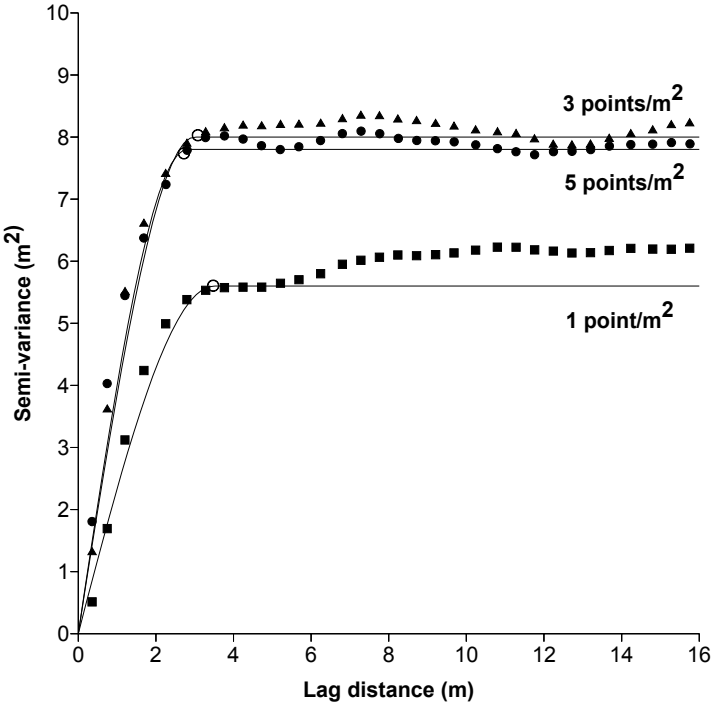

Figure 4.4 Variograms of the three point densities for a sample plot. Open circles indicate the range size on the x-axis (lag).

Table 4.6 summarises accuracy of estimations at each point density level. All statistical measures showed relative similarity in the accuracies of estimations at lidar point densities of 5 points/m^2 and 3 points/m^2. With these density levels, accuracies exceeding 50% were achieved for 75% of the plots. A density of 1 point/m^2 had significantly lower accuracy by comparison, with approximately half of

the plots exhibiting accuracies exceeding 50%. At each density, local maxima filtering based on tree spacing returned better accuracies than the semi-variogram approach, while in both approaches the accuracy decreased with decrease in density.

Table 4.6: Accuracies of SPHA estimated for the CHMs derived from three point densities using the semi-variogram range and tree spacing approaches

SPHA statistic	Lidar point densities					
	5 points/m^2		3 points/m^2		1 point/m^2	
	Variogram	*Spacing*	*Variogram*	*Spacing*	*Variogram*	*Spacing*
Minimum (%)	36	50	35	50	27	42
Maximum (%)	99	100	100	99	95	100
Mean (%)	73	82	70	80	56	74
SD (%)	17	14	18	15	16	13
Quartile 1 (%)	56	74	55	71	44	67
Quartile 2 (%)	77	85	72	83	56	75
Quartile 3 (%)	88	91	85	92	69	84

Estimations using the semi-variogram approach resulted in mean absolute errors of 295 SPHA, 332 SPHA, and 466 SPHA, for 5 points/m^2, 3 points/m^2, and 1 point/m^2, respectively (Table 4.7). Standard deviation of errors was relatively similar for all densities and ranged between 20% and 23% of the observed mean. On the other hand, RMSE showed a slight increase from the density of 5 points/m^2 (RMSE=35%) to 3 points/m^2 (RMSE=40%), compared to 51% at a density of 1 point/m^2. In comparison, mean absolute errors from local maxima filtering using the tree spacing approach were 206 SPHA, 232 SPHA, and 290 SPHA for 5 points/m^2, 3 points/m^2, and 1 point/m^2 densities, respectively. There was no large difference in standard deviation between the two approaches. In contrast, RMSE was lower at each increasing density level for the approach based on tree spacing. Root mean square error had a narrow range across densities (26% and 33%) for the tree spacing approach, compared to the semi-variogram approach (35% and 51%). The number of overestimated plots increased with increasing point density for both approaches.

There were more overestimated plots in the tree spacing approach than in the semi-variogram approach within each density level.

Table 4.7: Absolute error of estimation at the three point densities. Figures in parentheses indicate proportion to observed mean

SPHA statistic	**Lidar point densities**					
	5 points/m^2		**3 points/m^2**		**1 point/m^2**	
	Variogram	*Spacing*	*Variogram*	*Spacing*	*Variogram*	*Spacing*
Minimum (SPHA)	12	0	0	12	38	0
Maximum (SPHA)	774	682	951	773	951	763
Mean (SPHA)	295	206	332	232	466	290
SD (SPHA)	210 (20%)	172 (17%)	234 (23%)	196 (19%)	228 (22%)	177 (17%)
RMSE (SPHA)	361 (35%)	267 (26%)	405 (40%)	303 (30%)	517 (51%)	339 (33%)
Overestimated plots (n)	10	25	7	16	2	10

The semi-variogram approach resulted in mean estimates of 800 SPHA, 744 SPHA, and 566 SPHA for densities of 5 points/m^2, 3 points/m^2, and 1 point/m^2, respectively. These estimates were significantly lower than the field-observed mean of 1024 SPHA at all densities (α=0.05, p<0.001) (Figure 4.5). Improved mean estimates were found for tree spacing approach with corresponding values of 997 SPHA, 932 SPHA, and 799 SPHA, respectively. The difference between the SPHA estimate at a density of 5 points/m^2 and the observed mean was not significant for the tree spacing approach; this observation was based on the same estimates obtained using the 0.2 m spatial resolution above. There was no significant variation between 5 points/m^2 and 3 points/m^2 for each of the approaches (Figure 4.5).

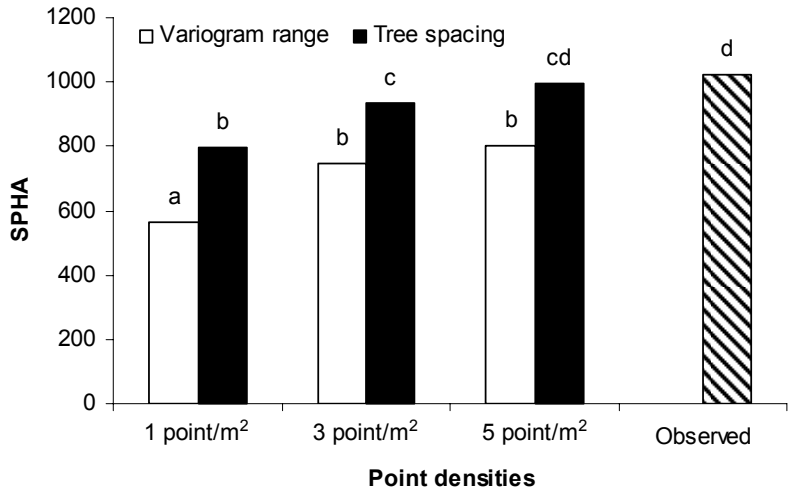

Figure 4.5 A comparison of the means between lidar estimates and field-observed values for the three lidar point densities. Different letters indicate significant differences at α=0.05.

4.4 Discussion

4.4.1 Comparison of variations in CHM spatial resolution

The use of semi-variogram range as window size input to local maxima filtering for identification of trees is an established method in high resolution aerial imagery (Lévesque and King, 1999; Wulder *et al.*, 2000). This study investigated the applicability of this approach to lidar height data. It was hypothesised that the structural information related to height and geographical position of individual tree crown elements, as conveyed by lidar data, may provide a unique opportunity for the application of semi-variogram theory to compute local maxima filtering window size for the estimation of stems per hectare. A comparative approach that utilises *a priori* knowledge of tree spacing dictated by operational protocol was also evaluated. Analysis was performed for both approaches to compare canopy height models (CHMs) derived at selected spatial resolutions using the original lidar points, as well as various simulated lidar point densities at a specified spatial resolution.

This study found that semi-variograms computed at each spatial resolution exhibited the theoretical behaviour of semi-variograms whereby the semi-variance of height between pixels increased up to the range distance and remained constant

afterwards (Figure 4.2). Comparison of spatial resolutions indicated that 0.2 m pixels returned range values (Table 4.2) closest to the physical tree spacing of the plantations. However, the specified local maxima search windows were, in general, larger than the nominal spacing between trees (2.4 m). This can be explained by the irregularity of lidar point spacing and the overlap between tree crowns. Because lidar points are irregularly spaced, the information they contain could come from any part of the horizontal and vertical forest structure. The most common problem in this regard is that tree tops are often underrepresented (Lefsky *et al.*, 2002; McCombs *et al.*, 2003), which may lead to the absence of a distinct maxima for certain trees. In the case of crown overlap, points from adjacent trees can have comparable heights and thus can appear to belong to a single tree. From an optical imagery perspective, Lévesque and King (1999) linked large range values of the semi-variogram to canopy closure in boreal forests. The top surface of the *Eucalyptus* canopy, which can be described as relatively flat rather than pointed, also contributes to less variation in lidar point heights in the vertical dimension. Moreover, inherent structural properties of a plot contribute to the semi-variogram parameter computation as opposed to results based on individual trees (Wulder *et al.*, 2000). Model goodness-of-fit was inversely related to spatial resolution (RMSE, Table 4.2). This property is also evident in Figure 4.2. The fitted model (solid line) at the 1 m spatial resolution exhibited relatively low residual error; in comparison, the sample variograms of 0.2 m and 0.5 m resolutions showed periodic deviations that were not well-modelled using the model variograms (Figure 4.2).

Estimation of SPHA using the semi-variogram approach at different spatial resolutions followed the trend of semi-variogram range variations described above. The accuracy of estimation was directly proportional to spatial resolution. A similar trend was observed in the estimates by the approach that utilised pre-determined tree spacing. Comparison between the two approaches based on accuracy (Table 4.3), residual analysis (Table 4.4), and ANOVA (Figure 4.3) showed the tree spacing approach to be superior. This was not unexpected, given the difference in local maxima filtering window sizes between the two approaches. Semi-variogram analysis returned window sizes that were larger than the pre-determined window size of 2.4 m for most plots. The use of small window size particularly in closely-

spaced trees such as the plantations of this study increases the probability of identifying more number of trees. This argument is in agreement with Lee and Lucas (2007), who reported that smaller window sizes were better for identifying stems from a lidar surface model at 1 m spatial resolution. Very small filtering windows, however, may result in an increase in SPHA overestimated plots. This phenomenon can be noted in Table 4.4 whereby local maxima filtering using window size based on tree spacing (2.4 m) had more number of overestimated plots than the semi-variogram approach, suggesting an increased likelihood of false identification (commission) errors in the former case. This corroborated findings by Wulder *et al*. (2000), who reached a similar conclusion based on data comprised of field-located individual trees.

The finding relating accuracy of SPHA estimation and spatial resolution agrees with studies undertaken elsewhere, despite the difference in species type. Hirata (2004), for example, compared 0.25 m, 0.5 m, and 1 m spatial resolution CHMs derived from lidar data and found a direct relationship between accuracy of individual tree identification and resolution. Pouliot *et al.* (2002) found a significantly higher accuracy for tree identification with 0.05 m, 0.1 m, and 0.15 m resolutions, as opposed to a 0.3 m resolution, based on results using digital imagery in a six-year old spruce plantation with a tree spacing of 1 m. Furthermore, Lévesque and King (1999) also found 0.25 m resolution imagery to be suitable for the analysis of individual tree identification, whereas images of 0.5 m and 1 m resolutions resulted in spatially aggregated forest characteristics. The relationship between accuracy and spatial resolution in this study is attributed mainly to the size of tree crowns in the plantations and the method by which the CHMs were generated. Generally speaking, the canopy size can be regarded as relatively small when one considers the associated tree spacing. Under such circumstances, availability of small pixel size (high spatial resolution) becomes critical due to the need for adequate pixel representation for each crown. An average tree canopy of 2.4 m diameter, for example, is captured by approximately 100 pixels at 0.2 m spatial resolution, compared to approximately 15 and 4 pixels at 0.5 m and 1 m spatial resolutions, respectively. It can therefore be concluded that the probability of finding local maxima for individual trees increases with increase in spatial resolution. Such a

relationship between canopy size and image resolution was identified as an important factor by Wulder *et al*. (2000). The authors regarded 1 m spatial resolution imagery as being unsuitable for identification of younger trees with a crown radius of less than 1.5 m. Pouliot *et al.* (2002) also calculated an optimal ratio related to canopy diameter and image resolution for reasonable tree identification accuracies. With regard to CHM generation in this study, the interpolation utilised a maximum of one point within a given grid cell. This approach arguably affected the information content of the data. For example, it is assumed that a CHM at 0.2 m resolution represents more detailed spatial information, while removal of points to create CHM at lower resolutions results in a loss of spatial detail. Such a loss in detail implies that height variability have been reduced by smoothing over short distances, as noted in Figure 4.2. Consequently, the spatial correlation between samples extends to a greater distance resulting in larger semi-variogram ranges.

4.4.2 Comparison of variations in lidar point densities

Semi-variogram analysis at the different point densities showed that the range values did not vary with the same magnitude as was noted in the case of varying spatial resolutions (Table 4.5). There were strong similarities between 5 points/m^2 and 3 points/m^2 while both resulted in range values significantly lower than that obtained for a density of 1 point/m^2 (Table 4.5). This observation was also confirmed by the similarity of sill values of the variograms (Figure 4.4). Statistics summarising RMSE of the model variograms showed superior goodness-of-fit for 1 point/m^2, followed by 3 points/m^2 and 5 points/m^2 (Table 4.5). The graphs (Figure 4.4) further confirmed this observation in that the sample variogram of 1 point/m^2 resulted in a superior model fit when compared to variograms of the other densities. The higher density levels exhibited relatively large degree of periodic deviations from the fitted model.

SPHA estimation from the three lidar point densities using semi-variogram approach reflected the trends observed in the ranges. Superior accuracies were obtained at density levels of 5 points/m^2 and 3 points/m^2 than at 1 point/m^2 (Table 4.6). Error analysis (Table 4.7) and ANOVA (Figure 4.5) confirmed the similarity between the higher densities. Similar trends were also observed for estimations using tree

spacing approach; results however were superior to semi-variogram approach at each density level. Comparison of results across point densities could be attributed to the extent of details that points can offer at each density level. Theoretically, there are as many as 30 and 20 points per tree (2.4 m canopy diameter) for 5 points/m^2 and 3 points/m^2 densities, respectively. This suggests that there is a strong likelihood of defining a neighbourhood comprising of local maximum point in each case. In contrast, 1 point/m^2 density amounts to approximately five points per tree and likely will result in too few points towards the creation of local neighbourhoods for the identification of a local maximum value. This is also a common occurrence when neighbouring trees are bigger (Brandtberg *et al.*, 2003). Another confounding factor is that of point returns from certain trees that do not have a local maximum and hence are included in the grouping of points belonging to adjacent trees.

These observations compared well with Hirata (2004), who simulated a number of densities ranging between 0.4 points/m^2 and 11.3 points/m^2 and found a remarkable decrease in accuracies for SPHA estimation for densities below 3-5 points/m^2, while it was virtually constant for point densities greater than 5 points/m^2. Popescu *et al.* (2002) indicated that a lidar point density of 1 point/m^2 could be sufficient to achieve an acceptable level of tree detection/delineation; however, their particular study was based on trees with significantly larger and perhaps more distinct canopies. Leckie *et al.* (2003) used an average lidar density of 8 points/m^2 over a range of three stem densities in an even-aged coniferous forest and reported accuracies of comparable magnitude to the current study. As described above, the current study presented evidence that a density of 3 points/m^2 will result in a reasonable accuracy for SPHA estimates. This result has a significant impact on the cost of a lidar survey, which is a function of lidar point density, among other things. According to the lidar data provider of the current study, for example, there is about a 30% net extra cost if a lidar survey seeks to acquire a density of 5 points/m^2 rather than 3 points/m^2 for an area of 10 000 ha.

This study has shown that SPHA was underestimated at all density levels and spatial resolutions using local maxima filtering approaches based on both window sizes equivalent to the semi-variogram range and pre-determined tree spacing. The main

source of underestimation in the majority of individual tree identification methods is the suppression of small trees by bigger trees (Popescu *et al.*, 2002; Lee and Lucas, 2007; Heurich, 2008). Using the space-scale approach of tree segmentation, Brandtberg *et al.* (2003) attributed this problem to the difficulty of obtaining sufficient lidar height returns from small trees located close to big trees. Maltamo *et al.* (2004) also pointed out that high stocking (mean=1014 SPHA) and unsampled understorey trees were contributing factors to underestimation of SPHA in a semi-natural forest. The plantations used in the current study could be considered as being well-stocked (mean=1024). Moreover, our observation of the field survey concluded that there was near-complete canopy cover. Variability in tree height according to the field data (Table 4.1) proved that there still existed vertical variation of trees, hence smaller trees potentially could be overtopped by taller trees resulting in an underestimation of SPHA.

The findings of this study also provided an interesting insight in to the selection of a local maxima filtering window size. While local maxima filtering based on the approach that utilised tree spacing was found to be relatively accurate, its application may require an in-depth knowledge regarding the stocking of the target plantation. Estimation of SPHA from plantations that have undergone silvicultural treatments, e.g., extensive thinning, that affect spacing and stocking between the time of planting and the lidar survey can have a considerably limited success of accuracy. Semi-variogram analysis, on the other hand, relies solely on the lidar data that reflect the existing structural characteristics of the plantation. The overall accuracies of estimation using the semi-variogram approach were also promising, though inferior to the tree spacing approach in this study. These accuracies were within the range reported in other studies that adopted different tree identification methods using lidar data. Leckie *et al.* (2003) applied the valley following approach (Gougeon, 1995) to delineate individual tree crowns in Douglas-fir plots and reported an overall accuracy of 67%. Maltamo *et al.* (2004) used a more complex algorithm that involved smoothing, maxima selection, and region growing segmentation from the maxima, and reported a relatively poor estimate for stem counts (RMSE>70%). Heurich (2008) adopted a watershed algorithm to detect coniferous and deciduous trees, using lidar point densities comparable to this study. The overall detection rate was

45.4%, with accuracies of 40.3% and 51.1% for coniferous and deciduous trees, respectively. It is worth noting that most of these studies focused on coniferous trees, which have a well-defined conical canopy shape. Koch *et al.* (2006), Kwak *et al.* (2007), and Heurich (2008) compared tree identification between deciduous and coniferous species and found improved accuracies in the latter group. The findings of this study can therefore be considered significant, given that *Eucalyptus* species have a relatively flattened canopy, which in turn makes it difficult to locate the centre of the canopy when compared to coniferous species (Tickle *et al.*, 2006). We have concluded that, for plantations similar to the current study, application of canopy delineation methods such as valley following and watershed segmentation is unlikely to improve on the results reported here. Firstly, these methods are more suited to tree detection in open canopies, which are not a common occurrence in plantations. Secondly, this is compounded by the shape of the upper canopy of *Eucalyptus* species, which lacks height variability sufficient for delineation based on gradients and valleys.

4.5 Conclusion

This study focussed on plot-level stems per hectare (SPHA) estimation in even-aged *Eucalyptus grandis* plantations using canopy height models (CHMs) derived from lidar data. Estimation of SPHA was based on identification of individual trees using local maxima filtering. The window size required for local maxima filtering was determined based on either the semi-variogram range or pre-determined tree spacing (*a priori* knowledge). Additionally, three CHM spatial resolutions (0.2 m, 0.5 m, and 1 m) were evaluated for each window size selection method using a lidar density of 5 points/m^2. It was found that the accuracy of estimation increased as the spatial resolution of the CHM increased. A comparison between the window size selection approaches indicated that local maxima filtering, which was based on *a priori* knowledge of tree spacing, proved superior at each spatial resolution. This was attributed to the fact that the tree spacing approach, which used a fixed window size of 2.4 m, was able to identify more context-applicable maxima than the semi-variogram range that produced window sizes varying between 2 m and 5.4 m. It was determined that a spatial resolution of 0.2 m would be appropriate for the typical tree

crown size in this study using both window size selection approaches; crown size here was a function of the silvicultural requirements for even-aged, homogeneous *Eucalyptus* plantations grown mainly for pulpwood.

The effect of lidar point density was also investigated by simulating two density levels (1 point/m^2 and 3 points/m^2) in addition to the original level (5 points/m^2), and applying these to a 0.2 m spatial resolution CHM. Results using both window size selection approaches showed superior accuracies at higher densities (5 points/m^2 and 3 points/m^2) compared to the low point density (1 point/m^2), though all densities resulted in underestimation of field-observed SPHA. The accuracy of estimations was again superior for the local maxima filtering approach that applied pre-determined tree spacing at each point density. The similarity between 5 points/m^2 and 3 points/m^2 suggested that a lidar point density of 3 points/m^2 provided a reasonable level of accuracy in the case of SPHA estimation. This will have an important implication on the cost of potential lidar surveys for assessment of forest structural attributes.

The semi-variogram range generally proved to be a useful indicator of individual tree canopy size. Accuracy of SPHA estimations based on this approach was shown to be within the range of results from several studies. This result is significant due to the fact that this approach does not require any *a priori* knowledge obtained from field surveys and that results specific to even-aged broadleaf forests/plantations were still lacking. However, it should be noted that a comparative approach, based on pre-determined tree spacing information, proved more accurate. This specific method does not constrain the use of lidar data, since it remains suitable for plantation forests which are intensively-managed and for which plant spacing are well-known. However, this approach may require careful consideration of the existing plantation condition in terms of the difference in stocking between the time of planting and the lidar data acquisition.

It might prove useful to supplement the results of this study with research aimed at characterising other important forest attributes. Future research is therefore required to investigate the significance of trees identified in this manner and at these lidar

point densities for estimating other operational forest attributes, e.g., basal area and volume. The approach, however, has the additional benefit that height quantification for identified trees is a by-product associated of the individual tree identification effort. Results such as these bode well for efforts that investigate the application of single-source lidar data for estimation of a range of forest structural and spatial attributes.

Acknowledgements

This study was conducted under a Remote Sensing Cooperative project sponsored by the Council for Scientific and Industrial Research (CSIR) and Mondi South Africa. The authors would also like to thank Wesley Roberts (CSIR) for his constructive comments on the paper. Members of the Cooperative enriched the content of the paper through continual inputs during the course of the study.

References

Ackermann, F. 1999. Airborne laser scanning—present status and future expectations. *ISPRS Journal of Photogrammetry and Remote Sensing*. 54, 64 – 67.

Atkinson, P. M. and Aplin, P. 2004. Spatial variation in land cover and choice of spatial resolution for remote sensing. *International Journal of Remote Sensing*. 25, 3687 – 3702.

Avery, T. E. and Burkhart, H. E. 2001. *Forest Measurements*. 5th edition. McGraw-Hill, New York. 456 pp.

Baltsavias, E. P. 1999a. A comparison between photogrammetry and laser scanning. *ISPRS Journal of Photogrammetry and Remote Sensing*. 54, 83 – 94.

Baltsavias, E. P. 1999b. Airborne laser scanning: basic relations and formulas. *ISPRS Journal of Photogrammetry and Remote Sensing*. 54, 199 – 214.

Beyer, H. L. 2004. Hawth's Analysis Tools for ArcGIS®. Available at: http://www.spatialecology.com/htools [Accessed 03 December 2008].

Boyd, D. S. and Danson, F. M. 2005. Satellite remote sensing of forest resources: three decades of research development. *Progress in Physical Geography*. 29, 1 – 26.

Brandtberg, T. and Walter, F. 1998. Automated delineation of individual tree crowns in high spatial resolution aerial images by multiple-scale analysis. *Machine Vision and Applications*. 11, 64 – 73.

Brandtberg, T., Warner, T. A., Landenberger, R. E., and McGraw, J. B. 2003. Detection and analysis of individual leaf-off tree crowns in small-footprint, high sampling density lidar data from the eastern deciduous forest in North America. *Remote Sensing of Environment*. 85, 290 – 303.

Chen, Q., Baldocchi, D., Gong, P., and Kelly, M. 2006. Isolating individual trees in a savanna woodland using small-footprint lidar data. *Photogrammetric Engineering and Remote Sensing*. 72, 923 – 932.

Chen, Q., Gong, P., Baldocchi, D., and Tian, Y. Q. 2007. Estimating basal area and stem volume for individual trees from lidar data. *Photogrammetric Engineering and Remote Sensing*. 73, 1355 – 1365.

Cohen, W. B., Spies, T. A., and Bradshaw, G. A. 1990. Semi-variograms of digital imagery for analysis of conifer canopy structure. *Remote Sensing of Environment*. 34, 167 – 178.

Coops, N. C., Wulder, M. A., Culvenor, D. S., and St-Onge, B. 2004. Comparison of forest attributes extracted from fine spatial resolution multispectral and lidar data. *Canadian Journal of Remote Sensing*. 30, 855 – 866.

Cressie, N. 1985. Fitting variogram models by weighted least squares. *Mathematical Geology*. 17, 563 – 586.

Curran, P. J. 1988. The semi-variogram in remote sensing: an introduction. *Remote Sensing of Environment*. 24, 493 – 507.

Curran, P. J. and Atkinson, P. M. 1998. Geostatistics and remote sensing. *Progress in Physical Geography*. 22, 61 – 78.

Franklin, S. E., Wulder, M. A., and Lavigne, M. B. 1996. Automated derivation of geographic window sizes for use in remote sensing digital image texture analysis. *Computers and Geosciences*. 22, 665 – 673.

Gougeon, F. A. 1995. A crown-following approach to the automatic delineation of individual tree crowns in high spatial resolution aerial images. *Canadian Journal of Remote Sensing*. 21, 274 – 284.

Hall, S. A., Burke, I. C., Box, D. O., Kaufmann, M. R., and Stoker, J. M. 2005. Estimating stand structure using discrete return lidar: an example from low density, fire prone ponderosa pine forests. *Forest Ecology and Management*. 208, 189 – 209.

Heurich, M. 2008. Automatic recognition and measurement of single trees based on data from airborne laser scanning over the richly structured natural forests of the Bavarian Forest National Park. *Forest Ecology and Management*. 255, 2416 – 2433.

Hirata, Y. 2004. The effects of footprint size and sampling density in airborne laser scanning to extract individual trees in mountainous terrain. *International Archives of Photogrammetry, Remote Sensing, and Spatial Information Sciences*. Vol. 36-8/W2, 102 – 107.

Holmgren, J. 2004. Prediction of tree height, basal area, and stem volume in forest stands using airborne laser scanning. *Scandinavian Journal of Forest Research*. 19, 543 – 553.

Holmgren, J., Nilsson, M., and Olsson, H. 2003. Estimation of tree height and stem volume on plots using airborne laser scanning. *Forest Science*, 49, 419 – 428.

Hyyppä, J., Hyyppä, H., Litkey, P., Yu, X., Haggrén, H., Rönnholm, P., Pyysalo, U., Pitkänen, J., and Maltamo, M. 2004. Algorithms and methods of airborne laser scanning for forest measurements. *International Archives of Phtogrammetry, Remote Sensing, and Spatial Information Sciences*. Vol. 36-8/W2, 82 – 89.

Hyyppä, J., Kelle, O., Lehikoinen, M., and Inkinen, M. 2001. A segmentation-based method to retrieve stem volume estimates from 3-D tree height models produced by laser scanners. *IEEE Transactions on Geoscience and Remote Sensing*. 39, 969 – 975.

Isaaks, E. H. and Srivastava, R. M. 1989. *Applied geostatistics*. Oxford University Press, New York. 584 pp.

Jensen, J. L. R., Humes, K. S., Vierling, L. A., and Hudak, A. T. 2008. Discrete return lidar-based prediction of leaf area index in two conifer forests. *Remote Sensing of Environment*. 112, 3947 – 3957.

Koch, B., Heyder, U., and Welnacker, H. 2006. Detection of individual tree crowns in airborne lidar data. *Photogrammetric Engineering and Remote Sensing*. 72, 357 – 363.

Kwak, D. A., Lee, W. K., Lee, J. H., Biging, G. S., and Gong, P. 2007. Detection of individual trees and estimation of tree height using lidar data. *Journal of Forest Research*. 12, 425 – 434.

Latham, P. A., Zuuring, H. R., and Coble, D. W. 1998. A method for quantifying vertical forest structure. *Forest Ecology and Management*. 104, 157 – 170.

Leckie, D., Gougeon, F., Hill, D., Quinn, R., Armstrong, L., and Shreenan, R. 2003. Combined high density lidar and multispectral imagery for individual tree crown analysis. *Canadian Journal of Remote Sensing*. 29, 633 – 649.

Lee, A. C. and Lucas, R. M. 2007. A lidar-derived canopy density model for stem and crown mapping in Australian forests. *Remote Sensing of Environment*. 111, 493 – 518.

Lefsky, M. A., Cohen, W. B., and Spies, T. A. 2001. An evaluation of alternate remote sensing products for forest inventory, monitoring, and mapping of Douglas-fir forests in western Oregon. *Canadian Journal of Forest Research*. 31, 78 – 87.

Lefsky, M. A., Cohen, W. B., Parker, G. G., and Harding, D. J. 2002. Lidar remote sensing for ecosystem studies. *Bioscience*. 52, 19 – 30.

Lévesque, J. and King, D. J. 1999. Airborne digital camera image semi-variance for evaluation of forest structural damage at an acid mine site. *Remote Sensing of Environment*. 68, 112 – 124.

Lim, K., Treitz, P., Wulder, M., St-Onge, B., and Flood, M. 2003. Lidar remote sensing of forest structure. *Progress in Physical Geography*. 27, 88 – 106.

Lovell, J. L., Jupp, D. L. B., Newnham, G. J., Coops, N. C., and Culvenor, D. S. 2005. Simulation study for finding optimal lidar acquisition parameters for forest height retrieval. *Forest Ecology and Management*. 214, 398 – 412.

Magnusson, M., Fransson, J. E. S., and Holmgren, J. 2007. Effects of estimation accuracy of forest variables using different pulse density of laser data. *Forest Science*. 53, 619 – 626.

Maltamo, M., Eerikäinen, K., Pitkänen, J., Hyyppä, J., and Vehmas, M. 2004. Estimation of timber volume and stem density based on scanning laser altimetry and expected tree size distribution functions. *Remote Sensing of Environment*. 90, 319 – 330.

Maltamo, M., Tokola, T., and Lehikoinen, M. 2003. Estimating stand characteristics by combining single tree pattern recognition of digital video imagery and a theoretical diameter distribution model. *Forest Science*. 49, 98 – 109.

McCombs, J. W., Roberts, S. D., and Evans, D. L. 2003. Influence of fusing lidar and multispectral imagery on remotely-sensed estimates of stand density and mean tree height in a managed loblolly pine plantation. *Forest Science*. 49, 457 – 466.

Morsdorf, F., Meier, E., Kötz, B., Itten, K. I., Dobbertin, M., and Allgöwer, B. 2004. Lidar-based geometric reconstruction of boreal type forest stands at single tree-level for forest and wildland fire management. *Remote Sensing of Environment*. 92, 353 – 362.

Næsset, E. 2002. Predicting forest stand characteristics with airborne scanning laser using a practical two-stage procedure and field data. *Remote Sensing of Environment*. 80, 88 – 99.

Næsset, E. 2004. Practical large scale forest stand inventory using a small-footprint airborne scanning laser. *Scandinavian Journal of Forest Research*. 19, 164 – 179.

Næsset, E. 2007. Airborne laser scanning as a method in operational forest inventory: status of accuracy assessments accomplished in Scandinavia. *Scandinavian Journal of Forest Research*. 22, 433 – 442.

Oliver, M. A. 1990. Kriging: a method of interpolation for Geographical Information Systems. *International Journal of Geographic Information Systems*. 4, 313 – 332.

Persson, Å., Holmgren, J., and Södermann, U. 2002. Detecting and measuring individual trees using an airborne laser scanner. *Photogrammetric Engineering and Remote Sensing*. 68, 925 – 932.

Pollock, R. 1998. Individual tree recognition based on a synthetic tree crown image model. *Proceedings of the International Forum on Automated Interpretation of High Spatial Resolution Digital Imagery for Forestry*. 10–12 February. Pacific Forestry Centre, Canada Forest Service, Natural Resources Canada, Victoria, BC, Canada. pp. 25 – 34.

Popescu, S. C. and Wynne, R. H. 2004. Seeing the trees in the forest: using lidar and multispectral data fusion with local filtering and variable window size for estimating tree height. *Photogrammetric Engineering and Remote Sensing*. 70, 589 – 604.

Popescu, S. C., Wynne, R. H., and Nelson, R. F. 2002. Estimating plot-level tree heights with lidar: local filtering with a canopy height based variable window size. *Computers and Electronics in Agriculture*. 37, 71 – 95.

Pouliot, D. A., King, D. J., and Pitt, D. G. 2005. Development and delineation of an automated tree detection-delineation algorithm for monitoring regenerating coniferous forests. *Canadian Journal of Forest Research*. 35, 2332 – 2345.

Pouliot, D. A., King, D. J., Bell, F. W., and Pitt, D. G. 2002. Automated tree crown detection and delineation in high resolution digital camera imagery of coniferous forest regeneration. *Remote Sensing of Environment*. 82, 322 – 334.

Reitberger, J. Schnörr, Cl., Krzystek, P., and Stilla, U. In Press. 3D segmentation of single trees exploiting full waveform lidar data. *ISPRS Journal of Photogrammetry and Remote Sensing* (2009), doi:10.1016/j.isprsjprs. 2009.04.002.

Reutebuch, S. E., Anderson, H.-E., and McGaughey, R. J. 2005. Light detection and ranging (lidar): an emerging tool for multiple resource inventory. *Journal of Forestry*. 103, 286 – 292.

Riaño, D., Valladares, F., Condes, S., and Chuvieco, E. 2004. Estimation of leaf area index and covered ground from airborne laser scanner (lidar) in two contrasting forests. *Agricultural and Forest Meteorology*. 124, 269 – 275.

Roberts, S. D., Dean, T. J., Evans, D. L., McCombs, J. W., Harrington, R. L., and Glass, P. A. 2005. Estimating individual tree leaf area in loblolly pine plantations using lidar-derived measurements of height and crown dimensions. *Forest Ecology and Management*. 213, 54 – 70.

Schreuder, H. T., Gregoire, T. G., and Wood, G. B. 1993. *Sampling methods for multisource forest inventory*. John Wiley and Sons, New York. 464 pp.

Smith, C. W., Kassier, H. W., and Cunningham, L. 2005. The effect of stand density and climatic conditions on the growth and yield of *Eucalyptus grandis*. *ICFR Bulletin 09/2005*. Institute for Commercial Forestry Research, Pietermaritzburg, South Africa. 56 pp.

St-Onge, B. and Cavayas, F. 1997. Automated forest structure mapping from high resolution imagery based on directional semi-variogram estimates. *Remote Sensing of Environment*. 61, 82 – 95.

Thomas, V., Treitz, P., McCaughey, J. H., and Morrison, I. 2006. Mapping stand-level forest biophysical variables for a mixed-wood boreal forest using lidar: an examination of scanning density. *Canadian Journal of Forest Research*. 36, 34 – 47.

Tickle, P. K., Lee, A., Lucas, R. M., Austin, J., and Witte, C. 2006. Quantifying Australian forest floristics and structure using small-footprint lidar and large scale aerial photography. *Forest Ecology and Management*. 223, 379 – 394.

Wehr, A. and Lohr, U. 1999. Airborne laser scanning—an introduction and overview. *ISPRS Journal of Photogrammetry and Remote Sensing*. 54, 68 – 82.

Woodcock, C. E., Strahler, A. H., and Jupp, D. L. B. 1988a. The use of variograms in remote sensing: I. Scene models and simulated images. *Remote Sensing of Environment*. 25, 323 – 348.

Woodcock, C. E., Strahler, A. H., and Jupp, D. L. B. 1988b. The use of variograms in remote sensing: II. Real digital images. *Remote Sensing of Environment*. 25, 349 – 379.

Wulder, M. 1998. Optical remote-sensing techniques for the assessment of forest inventory and biophysical parameters. *Progress in Physical Geography*. 22, 449 – 476.

Wulder, M., Niemann, K. O., and Goodenough, D. G. 2000. Local maximum filtering for the extraction of tree locations and basal area from high spatial resolution imagery. *Remote Sensing of Environment*. 73, 103 – 114.

Zimble, D. A., Evans, D. L., Carlson, G. C., Parker, R. C., Grado, S. C., and Gerard, P. D. 2003. Characterising vertical forest structure using small-footprint airborne lidar. *Remote Sensing of Environment*. 87, 171 – 182.

CHAPTER FIVE

ESTIMATING PLOT-LEVEL TREE HEIGHT AND VOLUME USING LIDAR HEIGHT DATA

Based on

Tesfamichael, S. G., van Aardt, J. A. N., and Ahmed, F. B. In Review. Estimating plot-level tree height and volume of *Eucalyptus grandis* plantations using small-footprint, discrete return lidar as singular data source. *ISPRS Journal of Photogrammetry and Remote Sensing*.

Abstract

Remote sensing has been identified as a viable means of acquiring forestry information that complements current labour-intensive inventories and minimises overall cost. The introduction of lidar remote sensing to forest inventory has shown potential, especially given the ability of the technology to capture three dimensional (3-D) information about vegetated areas. This study explored the utility of small-footprint, discrete return lidar data in deriving important forest structural attributes with the primary objective of estimating plot-level mean tree height, dominant height, and volume of *Eucalyptus grandis* plantations. The secondary objectives of the study were related to investigating the effect of lidar point densities (1 point/m^2, 3 points/m^2, and 5 points/m^2) and height and stems per hectare (SPHA) variability on volume estimates using sensitivity analysis. Tree tops were located by applying local maxima filtering to canopy height surfaces created at each density level, followed by buffering using circular polygons. Maximum and mean height values of the original lidar points falling within each tree polygon were used to generate lidar mean and dominant heights. Lidar mean value was superior to the maximum lidar value approach in estimating mean plot height (R^2~0.95, RMSE~7%), while the maximum height approach resulted in superior estimates for dominant plot height (R^2~0.95, RMSE~5%). These observations were similar across all lidar point density levels. Plot-level volume was calculated using approaches based on lidar-derived height attributes and stems per hectare, as well as stand age. Volume estimates did not vary considerably due to variations in lidar point density (R^2=0.83-0.93). All estimates, however, exhibited negative biases and RMSE ranging in the order of 32-51%. Sensitivity analysis, performed by varying input variables based on RMSE, showed that SPHA explained most of the variability in volume. Increasing the values of independent variables by magnitudes equivalent to their respective RMSE values improved volume estimates. These results bode well for the application of lidar-based approaches to structural assessment in commercial plantations, even though further research is required on improving SPHA estimation.

5.1 Introduction

Forest structural assessment is an important component in timber resources management (von Gadow and Bredenkamp, 1992). Traditional assessment methods employ very expensive and time consuming manual inventories that involve field visits by personnel. These surveys often cover a portion of forest population and are designed according to specific sampling strategies (Schreuder *et al.*, 1993; Avery and Burkhart, 2001). The required accuracy, spatial extent, cost, and time, among others, are in turn critical considerations when selecting an appropriate sample size. The introduction of remote sensing technologies in forestry has proven crucial in addressing these challenges (Wulder, 1998; Boyd and Danson, 2005). However, conventional imaging remote sensing technology has been widely used in selected areas of forest structural assessment including crown cover, leaf area (index), and stand density assessments – features characterised mainly in the horizontal dimension (Lefsky *et al*., 2002). Information related to the vertical dimension of forest components are thus not typically derived from imagery.

This problem is being researched by a new generation of remote sensing systems, namely lidar sensors. Lidar is an active system and emits pulses of its own electromagnetic energy in the near-infrared region of the light spectrum (Baltsavias, 1999). Current technologies of the system are capable of generating pulses at very high frequencies reaching up to 200 kHz (Hyyppä *et al*., 2008). Accurate measurement of reflected laser pulses in the vertical and horizontal dimensions is effected by recording the geographical position and orientation of the platform with GPS (global positioning system) and IMU (inertial management unit) embedded in the system (Wehr and Lohr, 1999). The elapsed time between emittance and reflectance is used to calculate the distance between the lidar sensor and the reflecting object and is translated into elevation above mean sea level (Wehr and Lohr, 1999). Lidar pulses are able to penetrate relatively dense vegetation canopies because they are emitted at very short time intervals, resulting in dense point spacing. This characteristic enables such sensors to capture a large volume of information about the underlying ground surface (Ackermann, 1999) and has attracted a rapidly growing interest in the forestry community over the past few

decades (Lefsky *et al.*, 2002; Lim *et al.*, 2003; Reutebuch *et al.*, 2005; Hyyppä *et al*., 2008). Research has shown that accuracies of forest structural prediction using lidar is superior to other remote sensing methods (Lefsky *et al.*, 2001; McCombs *et al.*, 2003; Coops *et al*., 2004). Accuracies of lidar-based predictions are also reported to be equivalent or superior to field inventories (e.g., Hyyppä *et al*., 2001; Coops *et al*., 2004; Holmgren, 2004; Næsset, 2004; Maltamo *et al*., 2006).

Given the 3-D nature of lidar data it is possible to quantify various structural attributes such as tree height, basal area, leaf area index, canopy cover, volume, and biomass. Most studies have followed area-based analysis to estimate these attributes where multiple trees are treated as a unit. This is basically the most appropriate approach for lidar systems that have large-footprint laser returns (e.g., Means *et al*., 1999; Lefsky *et al*., 1999; Drake *et al*., 2002). Numerous studies involving small-footprint discrete laser returns have also adopted a similar approach in terms of spatial scale (Lefsky *et al.*, 2001; Næsset, 2002; Holmgren, 2004; Næsset, 2004; Hall *et al*., 2005; Thomas *et al*., 2006; van Aardt *et al*., 2006; Næsset, 2007). Typically, these studies predicted structural attributes using lidar distributional (e.g., maximum, mean, coefficient of variation, and percentiles of canopy height, as well as canopy density distributions) metrics extracted either from point data or interpolated canopy surface. This method can be used for large area inventories, as is applied routinely in Scandinavia (a summary is given in Næsset, 2007). Other advantages include easy integration with traditional forest inventory methods due mainly to similarity in support scale (Hyyppä *et al*., 2008) and the insensitivity to lidar point density (Reutebuch *et al*., 2005; Hyyppä *et al*., 2008). A notable drawback of the method is the requirement for robust models to serve as prediction tools (Hyyppä *et al*., 2008). The cost of developing such models is directly related to the spatial coverage of the forest under consideration due to the necessity for sufficient sample size to represent the variability present in the population. Furthermore, area-based expressions of forest structures often lack information on individual trees and thus do not contribute to management approaches that require assessment of individual trees (Bortolot and Wynne, 2005). In comparison, individual tree-based analysis are preferable due to the detail of information extracted, the low amount of field

reference data required, and the scalability of results to larger spatial areas (Hyyppä *et al*., 2008).

It is therefore logical that increased interest is being shown in the research community to design methods that are capable of extracting lidar information from individual trees (Hyyppä *et al*., 2001; Persson *et al*., 2002; Popescu *et al*., 2002; Brandtberg *et al*., 2003; Morsdorf *et al*., 2004; Bortolot and Wynne, 2005; Roberts *et al*., 2005; Chen *et al*., 2007). Popescu *et al*. (2003) used a variable window size and local maxima filtering to locate and segment crowns of individual trees in stands of deciduous, coniferous, and mixed species. Stepwise regression was used to estimate field-measured crown diameter from lidar-derived height, diameter of crown segments, and the number of trees, with the best models being similar for both deciduous and coniferous trees (R^2=0.62-0.63). The best models for estimating plot-level tree volume and biomass also included crown diameter as independent variable. The corresponding R^2-values for coniferous trees were 0.83 and 0.78, while poorer results were obtained for deciduous species. Homgren *et al*. (2003) derived tree height and stem volume from lidar data using different approaches for forests dominated by Norway spruce, Scots pine, and birch. Tree height was derived at the plot- and single tree-levels (local maxima filtering) with results showing strong similarities between the two methods (R^2=0.89-0.91, RMSE=10-11%). Height assessment was followed by computation of volume. The first method utilised height derived using the area-based approach and canopy area, which was assumed to inherit the generally good correlation between total crown area and basal area. The second method used the number of stems and height derived from lidar data as inputs. The first method (area-based approach) returned superior results (R^2=0.90, RMSE=22%) to the second approach (R^2=0.82, RMSE=26%). Maltamo *et al*. (2004) derived stem counts and volume from lidar-derived height and DBH for similar species studied by Holmgren *et al*. (2003). The accuracies in RMSE were reported to be 25% and 75% for volume and tree count, respectively. The use of a Weibull distribution to account for small trees decreased the corresponding values to 16% and 49%. Heurich (2008) estimated tree-level attributes from laser-derived height and crown radius for coniferous and deciduous trees. Watershed segmentation was used to identify trees before applying regression analysis to estimate tree height

(R^2=0.97-0.98, RMSE=4-6%), crown radius (R^2=0.45-0.56, RMSE=11-19%) diameter at breast height (R^2=0.79-0.92, RMSE=17-23%), and volume (R^2=0.87-0.95, RMSE=49-70%).

The studies cited here showed that modelling efforts range from plot- to tree-level analysis. For example, Maltamo *et al*. (2004) relied on DBH models that are calibrated using field inventory data, while Holmgren *et al*. (2003) used regressed field volume with lidar-derived attributes. Chen *et al*. (2006) argued that combining area-based and individual tree-based analysis constitutes an acceptable compromise. However, more research is needed to further minimise the reliance on models that require continual training or calibration. Additionally, an increased emphasis should be placed on translating current research outputs into operational applications. This in particular has an important significance for commercial forest industries which essentially perform pre-harvest structural assessments for monetary valuation purposes. In a rare example, Peuhkurinen *et al*. (2007) demonstrated such an assessment using lidar data and field-developed models in forest stands dominated by Norway spruce. The study compared information derived from lidar canopy height with other methods, including systematic plot sampling and inventory by compartments. An actual harvest inventory was used as reference data. Comparisons of the methods based on diameter distributions, volumes, number of trees, and bucking simulations showed superior results for the lidar-based approach.

This study extends the efforts of the above studies to retrieve important forest structural attributes in tropical plantation environments using lidar data only. As such, we purposely avoided inputs from ground data that require field-based measurements. The specific objectives of this study were to

1. Determine the utility of discrete return, small-footprint lidar data for derivation of accurate plot-level mean and dominant tree height,
2. Assess the usefulness of lidar-derived tree height and stems per hectare (SPHA) for estimation of plot-level volume,
3. Explore the effect of simulated lidar point densities on the estimation of tree height and volume, and

4. Assess the effect of variability in tree height and SPHA on the estimation of plot-level volume.

Potential trees were first identified using local maxima filtering in order to achieve these objectives. Although not stated as an objective in this study, the local maxima filtering compared two methods of window size determination, namely the semi-variogram range and tree spacing of the plantations, as recorded at the time of planting. As a result, the effects of these methods on attribute estimation also will be presented. This was followed by computing height of individual trees using a suitable estimator. Stand density and estimated height were then used to calculate plot-level volume.

5.2 Methods

5.2.1 Field data

Field data were collected during spring (October) of 2006. The age of the trees at the time of the survey ranged from four to nine years. Spacing between and within rows of the stands were approximately 3 and 2.4 m, respectively. A total of 63 plots were sampled in 19 selected stands. Wherever possible, a minimum distance of 50 m was maintained between adjacent plots, thereby capturing as much variability within the compartment as possible. Management of the forest plantations in the area uses circular plots of 10 m radius; however, a 15 m radius was specified for this study in order to include more trees and thereby strengthen the statistical reliability of the results. The geographical coordinates of an open location outside of a stand and closest to a plot was recorded using a differential global positioning system (DGPS) within a sub-meter accuracy level. The centre tree the plot was then referenced to the GPS-located spot using bearing and distance measurements. Plot area was then adjusted for slope, since this has an implication on the conversion of tree count to stems per hectare (SPHA) and volume (von Gadow and Bredenkamp, 1992).

Only trees with a diameter at breast height (DBH) greater than 5 cm were considered for enumeration within each plot. This is commensurate to inventory protocol of the industry managing the plantations and has also been followed by other studies (e.g.

Holmgren, 2004; Maltamo *et al.*, 2004). Trees that appeared to be damaged, dead, or dying were excluded from the counting process for two main reasons. Firstly, the commercial industry rarely includes such trees in an accounting scheme and secondly, the number of lidar returns from trees devoid of canopies was deemed less significant. Tree counts in each plot were then converted to SPHA based on the area of the respective plot. Tree height was measured on a sub-sample of trees selected across the range of DBH values. Relationships between DBH and corresponding height were established at plot-level using regression analysis with R^2 exceeding 80% for the majority of plots. Heights of all trees within a plot were estimated using the resulting regression equations. Subsequently, two area-based definitions of height were derived, namely mean height and dominant height. Mean height was calculated as the arithmetic mean of all trees. Dominant height can be defined as the mean height of a selected number of trees per hectare (García, 1998). The selection of these trees could be based on DBH or height. Dominant height was derived as the mean of the top 20% tallest trees, as per the forest mensuration protocol of the forestry company that manages the study area.

Tree height and DBH are the two most important attributes explaining the variability in tree volume (Avery and Burkhart, 2001). Thus, when these attributes are known for individual trees, volume can be calculated for each tree. The volume function based on Schumacher and Hall (1933) is used in this study (Equation 5.1).

$$\ln V_t = b_0 + b_1 \times \ln(DBH) + b_2 \times \ln HT \quad \text{..... (5.1)}$$

where V_t is volume of the mean tree, *DBH* and *HT* are lidar-derived diameter at breast height and mean tree height, respectively, and b_0 - b_2 are species specific coefficients (Coetzee, 1992). Plot-level volume was derived by adding volume of individual trees. The aggregate volume was then converted to a hectare scale based on the area of a plot. Summaries of the field inventory and analysis data are presented in Table 5.1.

Table 5.1: Summary of field survey data

Attribute	Mean ± SD	Minimum	Maximum
Mean Height (m)	21.5 ± 4.2	15.2	31.6
Dominant height (m)	25.2 ± 5.8	14.5	40.8
Stand density (trees/ha)	1024 ± 211	529	1504
DBH (cm)	16.9 ± 3.1	12.2	24.8
Volume (m^3/ha)	278.5 ± 136.7	95.1	597.9

5.2.2 Lidar data

A lidar survey of the study area was carried out by Airborne Laser Solutions (ALS, www.alsafrica.com) on November 8, 2006, using the Optech ALTM 3033 sensor. The system uses discrete return near-infrared laser pulses (wavelength 1064 nm) with a pulse rate of 33 kHz and was configured to record first and last returns per pulse. The footprint size of a pulse on the ground was approximately 0.2 m at an average flying height of 550 m above the ground and a beam divergence of 0.2 mrad. The overlap between successive flight lines was set to 25%, which resulted in a nominal point density of five points per square meter (points/m^2). The vertical and horizontal accuracies of the height returns were 0.15 m and 0.28 m, respectively. The data provider classified the points as ground and non-ground using Terrasolid's TerraScan® software. Briefly, the process involved an initial automated classification using the software, which attained accuracies between 60-80% depending on terrain variation. This was followed by a manual editing process aided by 0.15 m resolution orthophoto images. Accuracy of the final digital terrain model (DTM) was assessed using ground control points. Based on this, a mean error for the DTM was reported as +0.031 m (range: -0.017 to +0.078 m). The data were referenced to a local coordinate system (WGS 84 with Gauss Conform projection at longitude of 31°E).

5.2.3 Estimation of height

The identification of potential trees using local maxima filtering preceded estimation of plot-level tree height. A parallel study was dedicated to the analysis of local maxima filtering and the estimation of stems per hectare (SPHA, Chapter 4). A brief summary is presented here. Lidar point densities of one and three points per square meter (points/m^2) were simulated from the original density (5 points/m^2), in order to

assess the effect of point density on estimations of SPHA, height, and volume. A digital elevation model (DEM) was created at each density level by interpolating values from lidar ground points at 1 m spatial resolution for each stand using ordinary kriging in Surfer 8.0 (Golden Software, Inc., Golden, CO, USA). Actual canopy return heights subsequently were derived by subtracting DEM values from non-ground lidar returns. Such normalised points were essentially appropriate for height estimation using the distributional approach in a previous study (Tesfamichael *et al*., Accepted). These points were then used to create a canopy height model (CHM) at 0.2 m spatial resolution, as this resolution was found to be superior to 0.5 m and 1 m resolutions for the estimation of SPHA for each point density. A CHM subset was then created for each plot.

Identification of individual trees was preceded by applying a plot-level local maximum filtering to the CHM, where the filter size was determined using two methods, namely semi-variogram range and tree spacing. In the first method, the range value was used as the average canopy diameter of a tree for a plot and consequently the filter size in the local maxima filtering. In the second method, a fixed filter size, equal to within-row tree spacing at the time of planting, was used for local maxima filtering. The number of maxima on each plot was converted to a stems per hectare (SPHA) estimate for that plot. Overall accuracies of estimations using the semi-variogram range were 56%, 70%, and 73% for 1 point/m^2, 3 points/m^2, and 5 points/m^2, respectively. Corresponding accuracies for estimations using the tree spacing approach were 74%, 80%, and 82%. A summary of the results is given in Table 5.2. All lidar-derived SPHA underestimated field-enumerated SPHA significantly, with the exception of the approach that utilised tree spacing at the density of 5 points/m^2. The magnitude of underestimation tended to vary directly with SPHA.

Table 5.2: Comparison of observed and estimated SPHA using local maxima filtering

Lidar density (points/m^2)	LM filtering window	
	Variogram range*	Tree spacing*
1	566^a	799^b
3	744^b	932^c
5	800^b	997^{cd}
Field	1024^d	

*Different letters indicate significant differences at α=0.05

In order to estimate plot-level mean and dominant heights, circular polygons, which simulate canopies of individual trees, were first delineated. This delineation was based on window sizes specified by the semi-variogram range and tree spacing approaches. It has been reported that gridding introduces error in estimates of canopy surfaces due to the interpolation procedure and the choice of grid size (Smith *et al*., 2004), which led to our use of points rather than rasterised information. Non-ground points thus were assigned to each of the polygons, after which mean and maximum heights were extracted from each polygon as estimates of individual tree heights. Average values of these heights were calculated and compared with field-measured mean height for each plot. Dominant height of each plot was calculated using the same approach employed to the field data, that is, the average height of the tallest 20% tree-level point heights. Derivation of mean and dominant height was replicated for each set of trees identified at the three lidar point densities (1 point/m^2, 3 points/m^2, and 5 points/m^2).

5.2.4 Estimation of volume

Volume typically can be calculated for each tree, followed by aggregation to a plot- or stand-level, given the availability of necessary information at individual tree-level. Tree height and DBH are the most common independent variables needed for the estimation of tree volume (Avery and Burkhart, 2001). The intention of this study was to derive both these attributes from the lidar data. Although height can be retrieved in a relatively straightforward manner, DBH cannot be measured from airborne lidar scanning directly. Relationships between height and DBH could be used to estimate the latter; however, establishing such a relationship breaches the assumption of

variable independence. An alternative approach to DBH derivation is to make use of information on stand stocking, which relates to basal area (von Gadow and Bredenkamp, 1992). In an even-aged plantation, mean basal area can be computed from SPHA, dominant height, and the age of trees. SPHA and dominant height were estimated using the procedures described above while age is documented for each plantation. We assumed that the derivation of basal area, and thus resultant DBH, remained independent from the *mean height* independent variable in the volume estimation (dependent variable). This assumption is based on the facts that (i) basal area and subsequent DBH are derived from *dominant (maximum) heights* and (ii) basal area estimation furthermore relies on two additional non-height-specific variables (SPHA and age). The basal area function chosen in this study is given in Equation 5.2 (Pienaar and Kotze, 2000). The model was developed based on an age range of 2-10 years, and has an R^2 of 0.97 and a mean square error of 0.0066 m^2/ha.

$$BA = \exp\left[\beta_0 + \frac{\beta_1}{Age} + \beta_2 \cdot \ln(SPHA) + \beta_3 \cdot \ln(HD) + \beta_4 \cdot \frac{\ln(SPHA)}{Age} + \beta_5 \cdot \frac{\ln(HD)}{Age}\right] \quad \text{....(5.2)}$$

where *BA* is basal area in m^2/ha, *age* is the age of trees, *HD* is dominant height per plot, and β_0 - β_5 are site specific coefficients. The resulting BA was then used to derive quadratic mean DBH (QDBH) using Equation 5.3. QDBH and mean height, which was derived from the mean lidar returns, were then used as inputs to Equation 5.1 to calculate volume of the mean tree. Multiplying volume of the mean tree by SPHA of a plot yielded volume per hectare for that plot. Similar to height estimations, volume estimation was replicated for the three lidar point densities.

$$QDBH = \sqrt{\frac{BA/SPHA}{\pi/40000}} \quad \text{...(5.3)}$$

5.2.5 Sensitivity analysis

Sensitivity analysis was performed to examine the effects of the variability in lidar-derived mean height, dominant height, and SPHA on volume estimates at the tree- and plot-level. This process can be expressed as a measure of variable importance and is often quantified using variance-based methods. One of the characteristics of an ideal sensitivity analysis is consideration of the range or variance of the inputs (Saltelli *et al*., 2004). This study, however, intended to explore the trend in the comparative influence of variations of input variables. Each of the inputs was therefore varied based on the input variable RMSE values. The variability included low, intermediate, and high values, computed as mean estimate minus RMSE, mean estimate, and mean estimate plus RMSE, respectively (Figure 5.1). Intermediate refers to the case where no adjustment based on RMSE was made. A total of 27 combinations of three variables each were synthesised for each of the density levels. Please note that the letters or numbers under each variable were chosen arbitrarily to avoid lengthy use of terms in the presentation of results for the different combinations. For example, a combination *yb3* (shown on the figure) symbolises intermediate SPHA, intermediate mean height, and high dominant height.

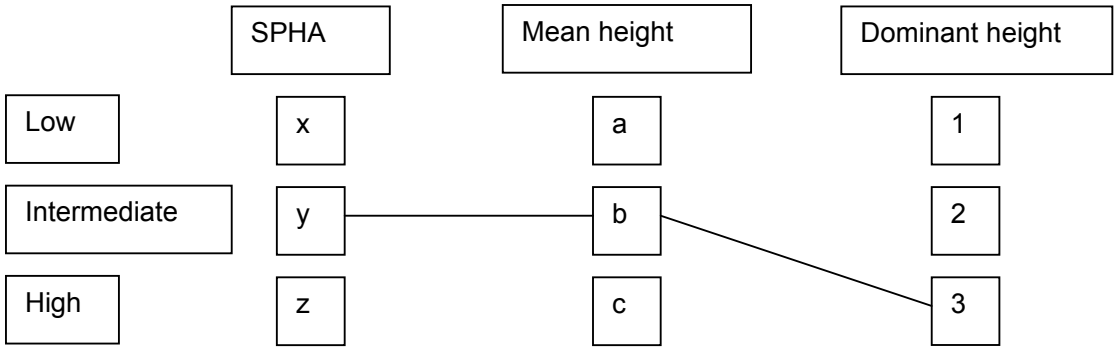

Figure 5.1 Schematic diagram showing the levels of variability in each input.

5.2.6 Accuracy assessment

Lidar estimates and field observations were compared among density levels and between local maxima filtering approaches. Comparisons also included estimates of height derived from mean and maximum lidar metrics. Analysis of variance (ANOVA)

was used to determine if the estimated means differed significantly from the observed mean and among each other. Residual analysis was used to quantify the difference between observed and estimated plot-level means using RMSE (Equation 5.4). Root mean square error was expressed as a percentage of the observed mean. A linear relationship between estimated and observed values was established for each of the attributes (mean height, dominant height, and volume). The relationship was evaluated both graphically and based on the coefficient of determination. Results of sensitivity analysis were examined by comparing the estimates at the different combinations of variability with the observed mean. Analysis of variance was used to assess whether or not there was a significant difference between observed and estimated mean volume for each combination.

$$\text{RMSE} = \sqrt{\frac{\sum (\text{Estimated} - \text{Observed})^2}{n}} \quad \text{.....(5.4)}$$

where *n* is the number of samples.

5.3 Results

5.3.1 Height

Table 5.3 summarises results of ANOVA, regression analysis, and errors of estimation for mean tree height. The difference between observed and estimated mean height using mean lidar height values was not significant. In contrast, estimates using maximum lidar height values varied significantly from field observations. The difference between estimates of the two metrics was also significant. The local maxima filtering technique and lidar point density did not affect height estimation for a given metric. Error analysis showed higher RMSE values for the maximum lidar than for the mean lidar estimation approach. This observation held true for all lidar point densities and local maxima filtering approaches. The relationship between observed and estimated mean heights, based on mean lidar points, consistently exhibited R^2-values exceeding 0.90 for both local maxima filtering approaches. Such accuracies were achieved at all density levels. Similar R^2-

values were obtained when maximum lidar points within delineated trees were used. Figure 5.2 provides various graphical representations of the results. The graph relating observed and estimated mean height shows that nearly all plots were overestimated by maximum lidar height values (Figure 5.2A). In general, the overestimation by both lidar height values increased with height. Errors of estimation were also plotted and exhibited a direct relationship with mean height (Figure 5.2B). This behaviour was in particular more noticeable for maximum lidar height values. These characteristics were deemed similar across lidar point densities (Figure 5.2C) and for both local maxima filtering approaches (Figure 5.2D).

Table 5.3[1]: Comparison of observed and estimated plot-level mean height

Lidar density (points/m^2)	**LM filtering**	**Metric**	**Mean (m)***	**RMSE (%)**	**R^2**
		Field	21.5[a]		
1, 3, 5	Variogram range / Tree spacing	Lidar_mean	21.5–21.8[a]	7	0.93–0.94
1, 3, 5	Variogram range / Tree spacing	Lidar_max	23.5–24.2[b]	13 – 15	0.93

[1]Lidar estimates range for densities and local maxima filtering techniques
*Different letters indicate significant differences at α=0.05

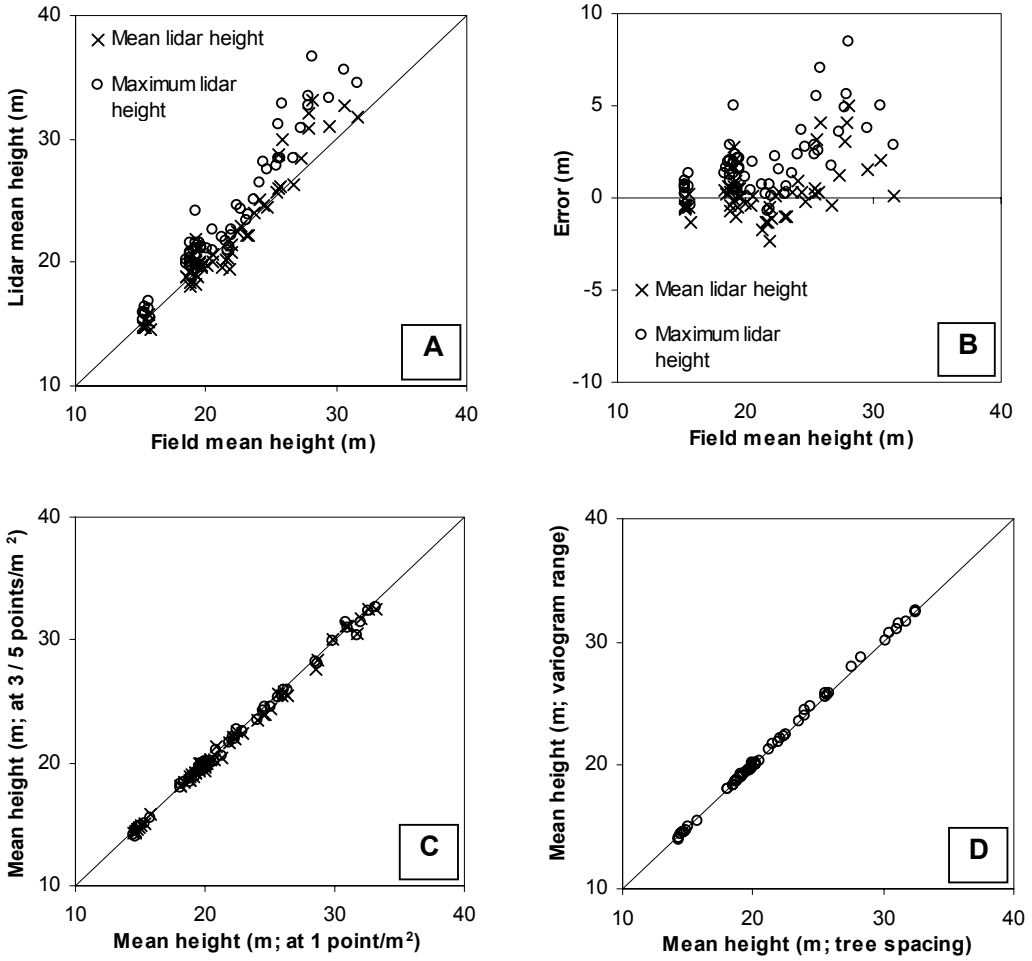

Figure 5.2 Mean tree height estimation: (A) estimated vs. observed at 1 point/m^2; (B) estimation error at 1 point/m^2; (C) comparison of estimates at the three lidar point densities; (D) comparison of estimates between local maxima filtering approaches.

Table 5.4 summarises the comparison between observed and estimated dominant height at all density levels and local maxima filtering approaches. Estimated and observed dominant height did not vary significantly. There were also no significant differences between estimates based on lidar metrics at all density levels and for both local maxima filtering approaches. However, the difference between the mean and maximum estimates and the observed values appears to be considerable with approximately 1-2 m for mean and ~0.5 m or less for maximum lidar height values. Root mean square error was also relatively similar across all estimates. Coefficients of determination for the linear relationship between estimated and observed dominant height at all density levels and local maxima filtering approaches were

similar for both lidar metrics (R^2~0.95). Figure 5.3 shows the relationship between estimated and observed dominant height as well as the error analysis; the graphs indicate that maximum lidar height input values yielded higher estimates than mean values (Figures 5.3A and B). The lidar point density (Figure 5.3C) and local maxima filtering approaches (Figure 5.3D) did not have any effect, as can be seen from the similar estimates in the respective graphs.

Table 5.4[1]: Comparison of observed and estimated dominant height

Lidar density (points/m^2)	**LM filtering**	**Metric**	**Mean (m)***	**RMSE (%)**	**R^2**
		Field	25.3[a]		
1, 3, 5	Variogram range / Tree spacing	Lidar_mean	23.5–24.4[a]	7 – 9	0.95
1, 3, 5	Variogram range / Tree spacing	Lidar_max	25.3–25.9[a]	5 – 6	0.94–0.95

[1]Lidar estimates range for densities and local maxima filtering techniques
*Different letters indicate significant differences at α=0.05

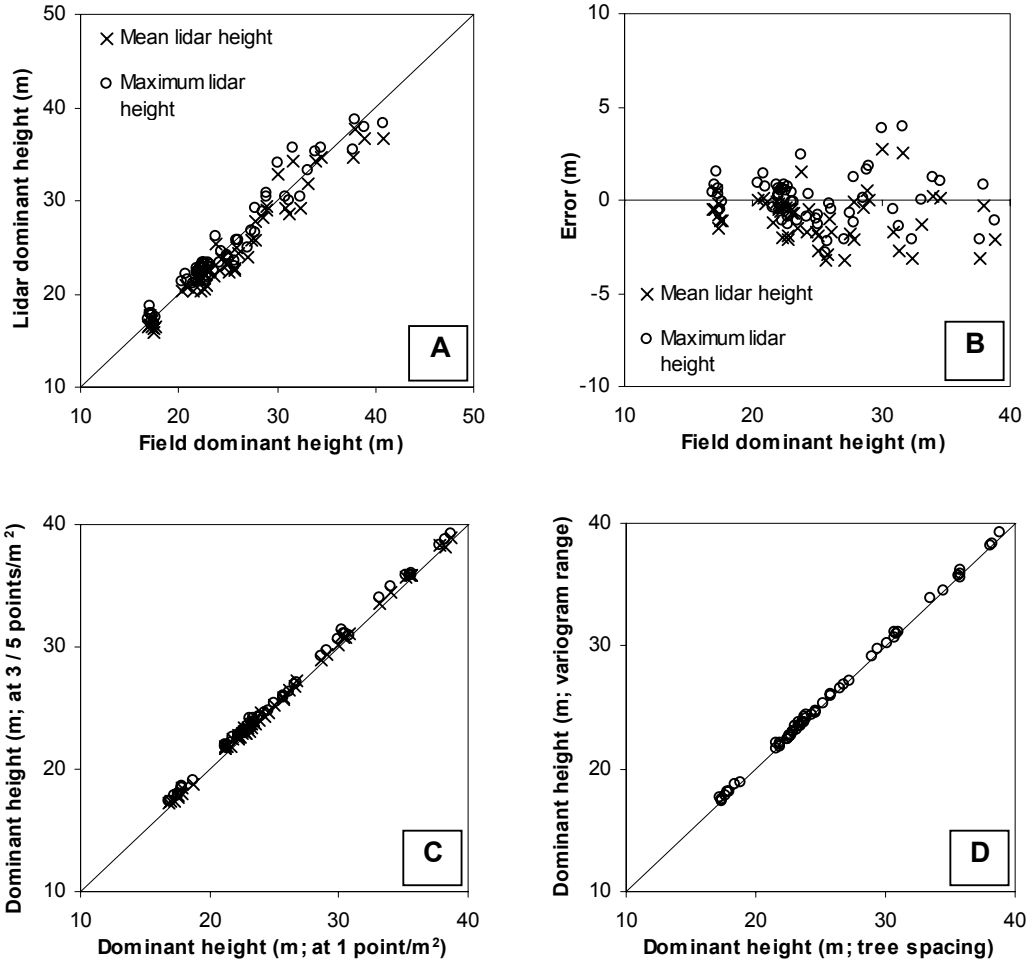

Figure 5.3 Dominant height estimation: (A) estimated vs. observed at 1 point/m^2; (B) estimation error at 1 point/m^2; (C) comparison of estimates at the three lidar point densities; (D) comparison of estimates between local maxima filtering approaches.

5.3.2 Volume

Although the objective was to estimate volume at the plot-level, volume of the mean basal area tree had to be computed first. It is therefore useful to explore the derivatives of lidar that will serve as independent variable inputs to the tree volume estimation. These inputs are mean height and QDBH of the tree with mean basal area. Calculation of mean basal area, in turn, requires dominant height, in addition to SPHA and age. Results presented above showed that dominant height computed from maximum lidar height values was marginally better than when mean lidar values were used. Hence maximum lidar height values were chosen for computing

QDBH. Mean lidar height values, on the other hand, were superior for estimating plot-level mean height. These estimates were, therefore, used in the equation to calculate mean tree volume (Equation 5.1).

A summary of the results of mean tree volume estimation is presented in Table 5.5. The mean values of volume estimates ranged between 0.21-0.28 m^3 compared to 0.26 m^3 of field-observation. No significant differences were noted between either observed and estimated means or among estimated means. Error analysis resulted in similar RMSE values for all estimates involving lidar point densities for both local maxima filtering approaches. Linear model fitness between observed and estimated volume resulted in R^2-values ranging between 0.74-0.81 across all lidar point densities for both local maxima filtering approaches. Graphical representation of observed-estimated relationships shows increased overestimation in the case of the semi-variogram, as opposed to the tree spacing local maxima filtering approach (Figure 5.4A). This is confirmed by the graph showing the error distribution (Figure 5.4B). Figures 5.4A and B also show that only a limited number of samples were considerably underestimated at higher tree volume values. Comparison of estimation among densities (Figure 5.4C) exhibited slightly higher values for 1 point/m^2 than for 3 points/m^2 and 5 points/m^2 for most of the samples.

Table 5.5: Comparison of observed and estimated mean tree volume

Lidar density (points/m^2)	**LM filtering window**	**Mean (m^3)***	**RMSE (%)**	**R^2**
	Field	0.26[a]		
1, 3, 5	Variogram range	0.25-0.28[a]	30–35	0.74–0.81
1, 3, 5	Tree spacing	0.21-0.23[a]	34–38	0.80–0.81

*Different letters indicate significant differences at α=0.05

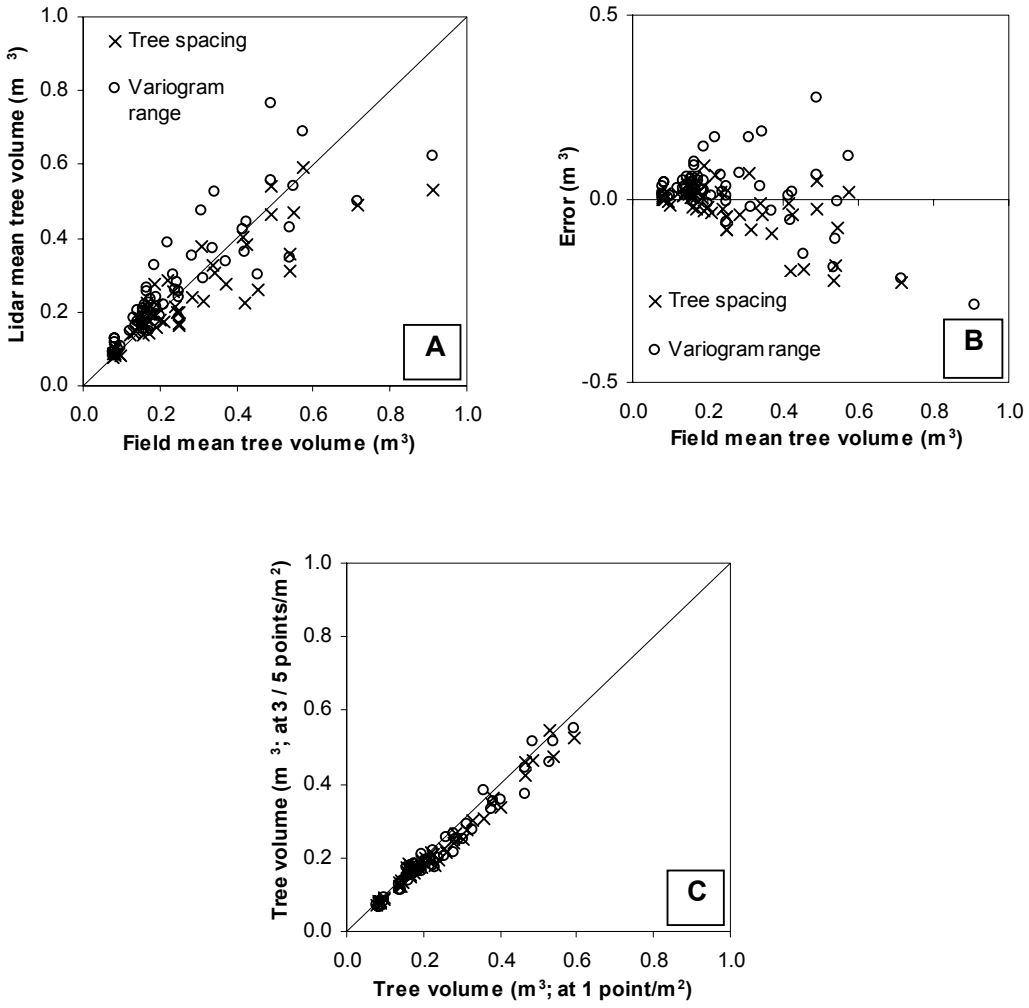

Figure 5.4 Mean tree volume estimation: (A) estimated vs. observed at 1 point/m^2; (B) estimation error at 1 point/m^2; (C) comparison of estimates at the three lidar point densities.

Plot-level volume estimates were significantly lower than field-observed values at all point density levels and for trees identified using the two respective local maxima filtering methods (Table 5.6). Differences among estimates were, however, not significant, except for estimates between the semi-variogram range at 1 point/m^2 and the tree spacing approach at 5 points/m^2. There also appeared to be relatively strong similarities among estimates within each local maxima filtering approach. Superior accuracies were obtained for trees identified using local maxima filtering based on tree spacing, as opposed to the semi-variogram range approach. It can also be seen

that mean volume estimates increased with lidar point density within each local maxima filtering approach. Error of estimation (RMSE) and fit statistics (R^2) hinted at improved estimation potential when the tree spacing approach, rather than semi-variogram range, was used for local maxima filtering.

The coefficients of determination for linear relationships between estimated and observed volume ranged between 0.83-0.93 for all lidar point density levels using both local maxima filtering techniques (Table 5.6). Figure 5.5 illustrates underestimations of field volume at all density levels and local maxima filtering approaches. A comparative evaluation of the graphs indicates less underestimation when tree spacing rather than semi-variogram range was used in the tree identification procedure (Figure 5.5A). The graph depicting error distributions indicates the level of underestimation for both local maxima filtering approaches (Figure 5.5B). It can also be seen from Figures 5.5A and B that error of estimation increased as volume increased. Comparison of the effects of lidar point density on the estimation of volume indicates higher values for nearly all samples in the case of 3 points/m^2 and 5 points/m^2, as opposed to 1 point/m^2 (Figure 5.5C).

Table 5.6: Comparison of observed and estimated plot-level volume

Density (points/m^2)	LM filtering window	Mean (m^3/ha)*	RMSE (%)	R^2
1	Field	274.7^{a}		
	Variogram range	152.4^{b}	51	0.87
	Tree spacing	182.2^{bcd}	40	0.91
3	Variogram range	175.5^{bcd}	43	0.83
	Tree spacing	196.9^{cd}	34	0.90
5	Variogram range	180.2^{bcd}	42	0.84
	Tree spacing	202.3^{cd}	32	0.93

*Different letters indicate significant differences at α=0.05

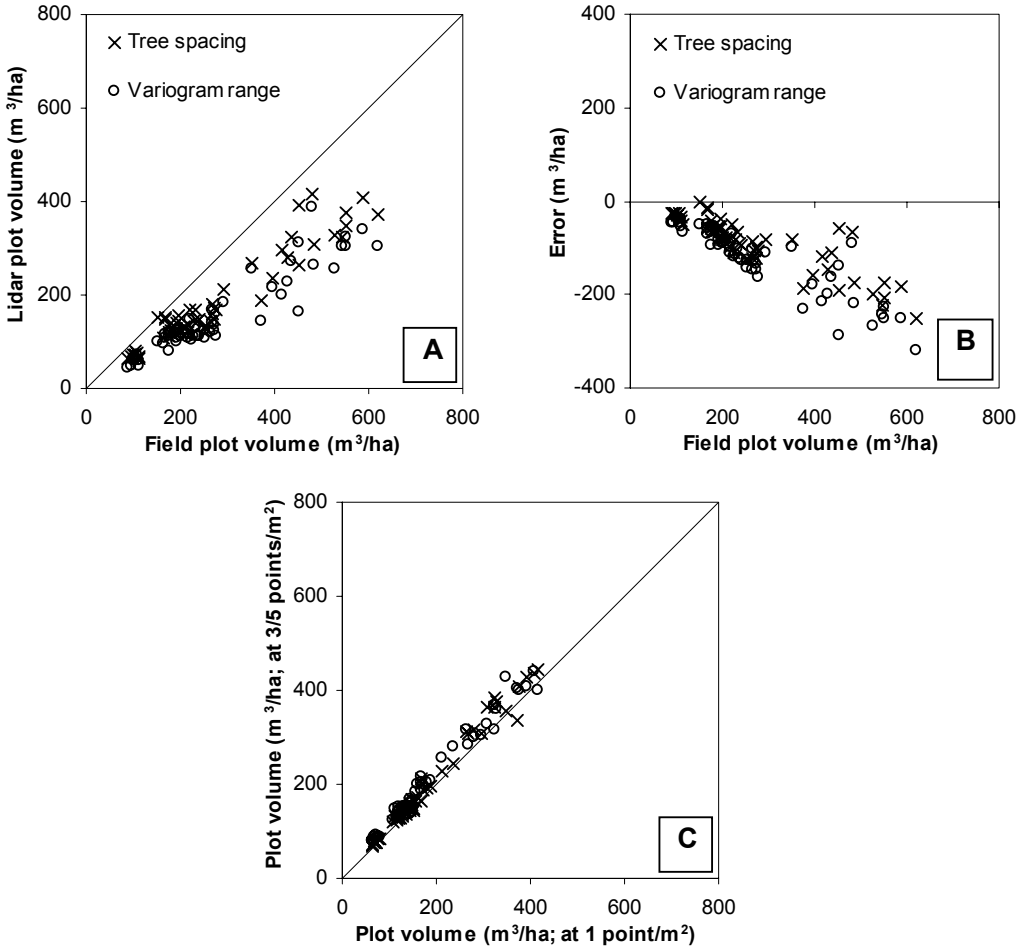

Figure 5.5 Plot-level volume estimation: (A) estimated vs. observed at 1 point/m^2; (B) estimation error at 1 point/m^2; (C) comparison of estimates at the three lidar point densities.

5.3.3 Sensitivity analysis

As mentioned in the methodology section, sensitivity analysis was performed at each lidar point density. The semi-variogram approach for estimating SPHA led to plots with volume estimates less than or equal to RMSE at each density level. Subtraction of RMSE from volume estimates in these plots resulted in values smaller than zero. The volume estimation approach that followed tree spacing for SPHA modelling, on the other hand, resulted in estimates greater than RMSE for all plots. These estimates were therefore used in the sensitivity analysis. We furthermore focused on results at the plot-level, as per the objective of the study.

Field volume was underestimated by all combinations of the attributes, as shown by the negative errors in Figure 5.6. The underestimation was significant in most cases, except for all densities at a combination of ‘zc3’ (all attributes at high values; see Figure 5.1 for clarification) and for densities of 3 points/m^2 and 5 points/m^2 at ‘zb3’ and ‘zc2’ combinations. Volume estimation error decreased as an attribute was increased to a higher level. There was also an inverse relationship between estimation error and lidar point density. The higher point densities (3 points/m^2 and 5 points/m^2) exhibited closer similarity than the lower densities (1 point/m^2 and 3 points/m^2).

It can be interpreted from Figure 5.6 that there is an interaction effect among lidar point density, SPHA, mean height, and dominant height on volume estimation. The overall effect of each attribute was therefore summarised by averaging the differences in volume estimates between high and low, intermediate and low, and intermediate and high value of that attribute. Figure 5.7 presents the results of this analysis for the three lidar point densities. Varying SPHA resulted in the largest mean difference in plot-level tree volume, while mean height exhibited marginally more influence than dominant height. It should be noted that dominant height is related to DBH, as the former was used as one of the independent variables to derive the latter. The mean difference in plot volume among estimates increased slightly in response to variability in mean height and dominant height as lidar point density increased. The effect of lidar density on SPHA was comparatively higher and resulted in decreasing mean difference in the estimates of volume with an increase in lidar point density.

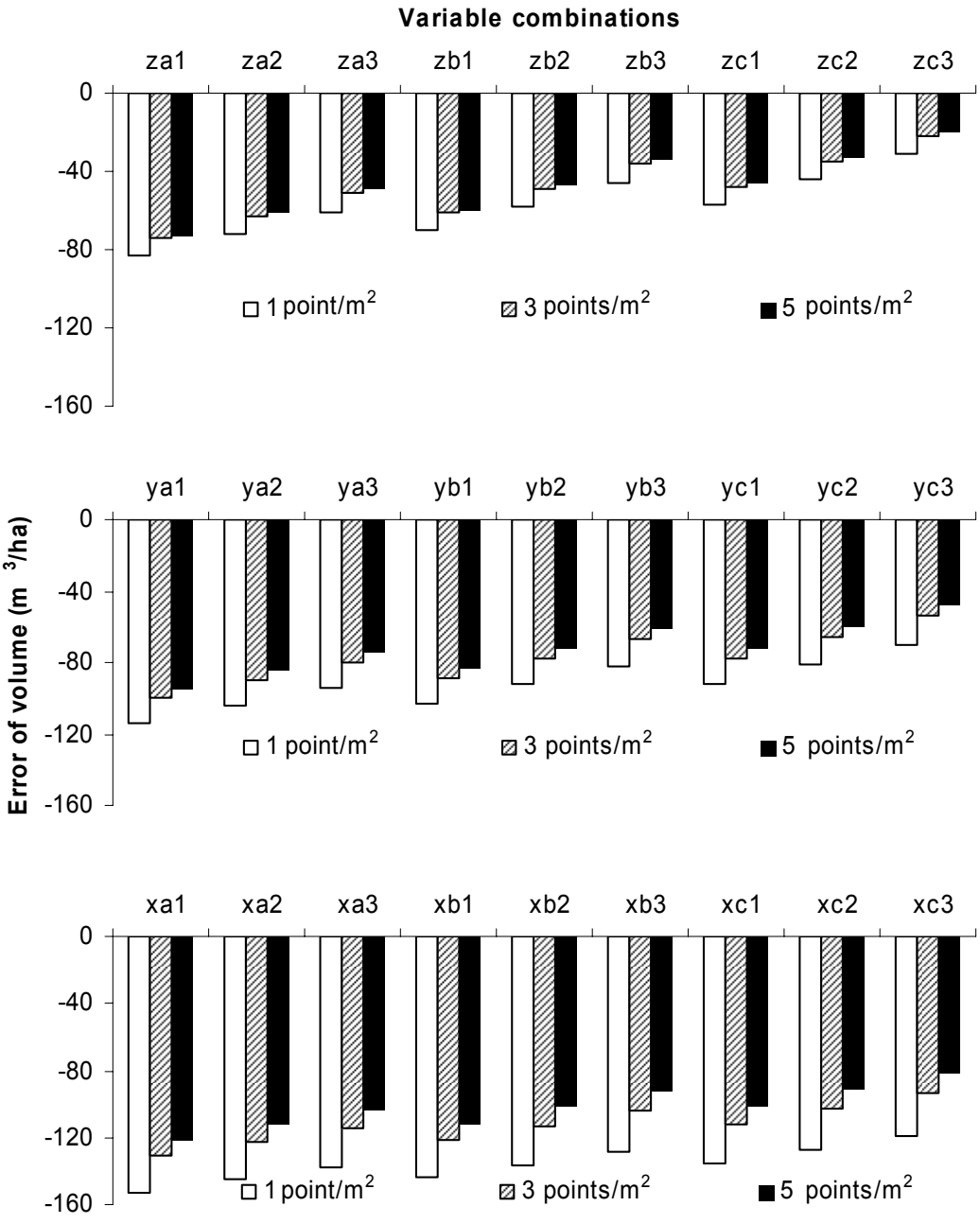

Figure 5.6 Differences between lidar-estimated and field-observed plot-level volume at different combinations of input variable levels. The symbols x, y, and z represent low, intermediate, and high SPHA, respectively. Corresponding representations for mean height and dominant height are a, b, and c and 1, 2, and 3, respectively.

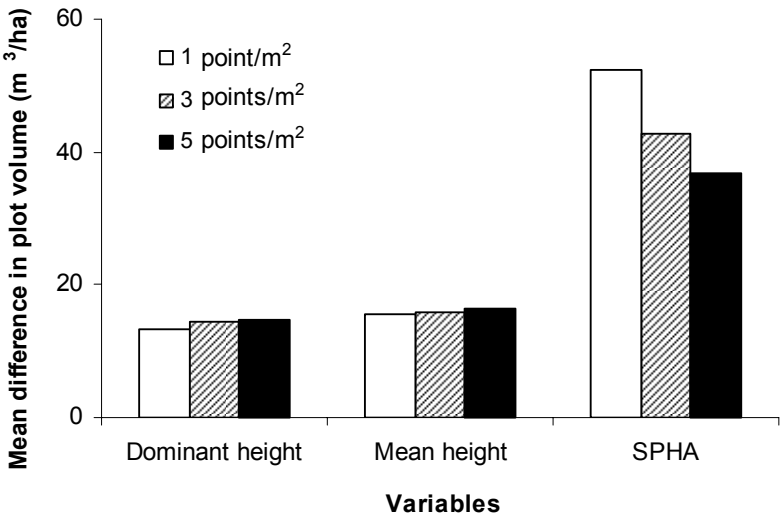

Figure 5.7 Overall difference in estimated tree volume due to changes in each attribute for three lidar densities.

5.4 Discussion

The aim of this study was to estimate tree height and volume, and ultimately plot-level volume, using discrete return lidar data. Tree height was derived for individual trees, identified using two local maxima filtering approaches. Mean and maximum height values of the lidar points were extracted for each tree and averaged per plot before comparing with observed mean heights. Dominant height was also calculated from the identified trees. Tree-level volume was calculated using a standard function that utilises mean height and DBH. This estimate was scaled to plot-level based on SPHA estimates. Estimations of these attributes were also compared at lidar point densities of 1 point/m^2, 3 points/m^2, and 5 points/m^2. The intention of this study was to investigate the potential of deriving all the attributes needed in timber inventory by using lidar data only. The study also examined the effects of variability within height and SPHA on the estimation of volume.

5.4.1 Height

The relationship between field-observed and lidar-derived mean height using either mean or maximum lidar height values was regarded as strong (R^2=0.93-0.94) (Table 5.3). Analysis of variance and error comparisons between the two estimates in relation to field observations indicated that mean lidar height values were superior to maximum values, which overestimated field height significantly (Table 5.3). A relatively poor accuracy for the maximum lidar height estimates may contradict the assumption that the maximum point within each tree should approximate the top height of a tree measured on the ground. This view holds, particularly, when comparisons are made based on individual trees (e.g., Clark *et al*., 2004). The observation in this study was attributed to various reasons. Since fewer trees were identified than exist on the ground, it is probable that small trees were omitted due mainly to a lidar shadow effect by taller trees. The absence of such small trees from a plot is likely to inflate the mean height calculated only from the lidar-identified trees. Another possible explanation relates to the field measurement. This was a closed-canopy environment and crowns of the trees were often interleaved, which led to errors in identification of tree tops. Falkowski *et al*. (2008) also noted this issue as a potential reason for overestimation of mean tree height in their study. Furthermore, the tops of *Eucalyptus* trees are not distinctively pointed, as is evident in coniferous species, resulting in difficulty when finding the tree apex from the ground (Tickle *et al*., 2006). It is thus likely that the field measurements generally underestimated actual tree height, exacerbated by the marginally inflated mean tree height in the case of lidar estimates due to the exclusion of smaller trees. The fact that overestimation was greater for taller trees using both metrics, also hinted at the difficulty of measuring such trees in the field. As a result, it is logical to assume that the negative bias of field measurement increased with height. These arguments also explain why lidar mean height did not underestimate field mean height, as was observed in other studies that followed individual tree height estimation (e.g., McCombs *et al*., 2003; Morsdorf *et al*., 2004; Suárez *et al*., 2005; Heurich, 2008).

Similar to mean height, the goodness-of-fit of the relationship between observed and estimated dominant height was strong for both mean and maximum lidar height metrics (R^2=0.94-0.95, Table 5.4). Although there was no significant variation

between observed and estimated values, a difference in mean values of 1-2 m using mean lidar height values compared to a maximum of 0.5 m using maximum lidar height values (Table 5.4) could be considered large in commercial forest management contexts. A variation of such magnitude could have an impact on characterising site quality of a plantation area. In addition, dominant height is also an essential input to the computation of basal area, since it generally relates to the stocking of a plantation.

Both mean height and dominant height did not vary across lidar point densities, as was previously shown in a concurrent study (Tesfamichael *et al*., Accepted). This phenomenon is worth noting, given that the current study extracted the height of individual trees as identified from lidar data. The number of trees extracted using local maxima identification differed significantly between lower (1 point/m^2) and higher lidar point density levels (3 points/m^2 or 5 points/m^2), as well as between the tree spacing based and semi-variogram based local maxima filtering methods (Table 5.2). It is likely that the variability in point height is comparable across the study area, provided that identified trees in most cases represented the tallest trees. In addition, the relatively high canopy closure of the plantations favours point returns from the very top surface of canopy. A generally rounded or flattened canopy top of *Eucalyptus* trees further adds to this effect, since the variability in height for such canopy geometries is relatively low (Nelson, 1997).

5.4.2 Volume

Studies that attempted to estimate stem volume from lidar data only are rare (e.g., Holmgren *et al*., 2003; Maltamo *et al*., 2004). However, even these studies have employed models developed from field data to derive certain tree attributes. In contrast, this study relied on lidar data and tree age, which is recorded at the time of planting. The noted studies furthermore focused on coniferous trees, while it is generally accepted that species type may have a considerable effect on tree counting accuracies (Koch *et al.*, 2006; Heurich, 2008). Our results corroborated these findings. The relationship between observed and estimated volume of the mean tree was relatively strong for both approaches of local maxima filtering (R^2=0.74-0.81, Table 5.5). Although the errors of estimations (RMSE) were deemed

large, the graphical illustrations did not show considerable systematic error (Figure 5.4), supporting the non-significant difference between the observed and estimated tree volume (Table 5.5). Moreover, there were distinct similarities among estimates at the three lidar point densities.

Model fit between observed and estimated volume at the plot-level was satisfactory (R^2=0.83-0.93, Table 5.6). Unlike mean tree volume, however, plot-level volumes were significantly underestimated in the cases of all point densities and local maxima filtering techniques. The high RMSE values were therefore the reflection of systematic rather than random error of lidar estimates. These results were not surprising since the mean tree volume was multiplied by stems per hectare, which was significantly underestimated at all, but one, lidar densities (Table 5.2). Comparison among estimates indicated close similarities among all densities (ANOVA). Similarities were also observed between estimates of local maxima filtering methods. These observations are valuable, given the significant variations in SPHA due to varying lidar point densities, as well as local maxima filtering techniques at a given point density level. It was mentioned above that the local maxima identification procedures identified most of the tall (dominant) trees. It has been shown that these trees often constitute a large proportion of volume within a plot (Hyyppä *et al*., 2001; Maltamo *et al*., 2004; Heurich, 2008). However, it is important to note the linear increase in underestimation with an increase in volume. This is attributable to higher underestimation of SPHA in denser plots. We concluded that the accuracy of volume estimation at the tree- and plot-level can be regarded as relatively accurate in light of the different methods followed in deriving the field and lidar volume. The field method computed the volume of each tree from known height and DBH, while the average tree volume was calculated using the lidar data. This may also hint at the ability of lidar data to accurately estimate plot-level mean DBH, an attribute that has traditionally been difficult to assess from remotely-sensed data.

5.4.3 Sensitivity analysis

Sensitivity analysis was deemed useful to generalise the importance of each of the independent variables that were derived for the eventual estimation of plot-level volume. All combinations of changes in input variables resulted in underestimation of the field plot-level volume (Figure 5.6). Comparison among the attributes indicated that SPHA explained most of the variability in plot-level volume, followed by mean height and dominant height, respectively (Figure 5.7). Such a relationship was not unexpected, since plot volume was the product of linear multiplication of tree volume and SPHA.

Results of the analysis with respect to the effect of lidar point densities indicated a fair degree of comparability, although a greater effect was observed for SPHA than mean height and dominant height. This was particularly evident in the correspondence of attribute combinations that returned estimates which were significantly/non-significantly different from the field mean for each attribute. It was mentioned above that trees (SPHA) identified using the local maxima filtering technique explained most of the variability in volume. This might lead to the assertion that the adjustment of SPHA by a few number of trees was sufficient to result in comparable levels of volume, even at low point density. For instance, when all attributes were adjusted by adding their respective RMSE, error of volume estimation ranged between 8.9% and 9.3%, depending on lidar point density. This is an encouraging outcome, in that it is known that SPHA is generally underestimated, with the subsequent upward adjustment also contributing to improved plot-level volume estimates. The lack of a significant effect due to lidar point density indicated that densities of approximately 1 point/m^2 could be used for volume estimation. While such accuracy results are very encouraging, one of the drawbacks of this approach would be the reliance on RMSE adjustments, which requires reference data from a ground survey. The utility of alternative adjustment factors, such as standard deviation of estimates, should be explored to avoid ground surveys and thereby keep such an approach lidar-centric.

5.5 Conclusions

This study outlined a methodology for quantifying timber resources in *Eucalyptus grandis* plantations using discrete return lidar height data as stand-alone data source. It has already been proven in a previous study (Tesfamichael *et al*., Accepted) that two height attributes (mean and dominant height) can be accurately estimated using local maxima filtering techniques. Combining estimates of height and stems per hectare, along with documented information on age of plantations, resulted in accurate estimates of mean tree volume. Furthermore, tree volume estimates were similar in all cases of local maxima filtering approaches and lidar point densities, although significant variations were observed in stems per hectare (SPHA) estimates. Plot-level volume estimates, however, were significantly lower than observed values from field-enumerations. There were no significant differences among estimates across lidar point densities and local maxima filtering approaches.

Sensitivity analysis was performed to gauge the importance of individual attributes to volume estimation. A small window of variation was applied to each of the attributes, based on RMSE values of the estimates. The analysis indicated that SPHA explained most of the variability in plot-level volume. Mean height and dominant height were ranked second and third, respectively, in terms of explaining the variability in plot-level volume estimation. It was found that increasing SPHA by the amount equivalent to the RMSE returned significantly improved volume estimates at the plot-level. This is encouraging, since SPHA is often underestimated and an adjustment of this value, based on a logical application of SPHA RMSE, is thus within reason. The improvement was observed at the three lidar point densities and confirmed the finding that lidar point density did not affect volume estimates significantly. We concluded that operational surveys based on lidar data only have significant potential, given the fact that height attributes and volume can be accurately estimated even at low point densities.

We suggest that future research place more emphasis on improving SPHA estimation, given its importance reported in this study. One approach could involve the development of advanced tree counting procedures that are suitable for

Eucalyptus plantation forests, which are typically characterised by overlapping crowns and near-rounded/flat canopy tops. The adjustment of SPHA based on RMSE, as shown in this study, showed great promise as an alternative approach. Rigorous studies are therefore needed to investigate the characteristics of these errors in order to minimise any uncertainties. Finally, it is essential to also evaluate other error statistics as a comparison, even though these might require field observations.

Acknowledgements

This study was conducted under a Remote Sensing Cooperative project sponsored by the Council for Scientific and Industrial Research (CSIR) and Mondi South Africa. The authors would like to thank Wesley Naidoo and Thamsanqa Mzinyane for their support throughout the field data collection. The authors are also grateful to Wesley Roberts (CSIR) for his constructive comments on the manuscript. Members of the Cooperative enriched the content of the paper through continual inputs during the course of the study.

References

Ackermann, F. 1999. Airborne laser scanning—present status and future expectations. *ISPRS Journal of Photogrammetry and Remote Sensing*. 54, 64 – 67.

Avery, T. E. and Burkhart, H. E. 2001. *Forest Measurements*. 5th edition. McGraw-Hill, New York. 456 pp.

Baltsavias, E. P. 1999. A comparison between photogrammetry and laser scanning. *ISPRS Journal of Photogrammetry and Remote Sensing*. 54, 83 – 94.

Bortolot, Z. J. and Wynne, R. H. 2005. Estimating forest biomass using small-footprint lidar data: an individual tree-based approach that incorporates training data. *ISPRS Journal of Photogrammetry and Remote Sensing*. 59, 342 – 360.

Boyd, D. S. and Danson, F. M. 2005. Satellite remote sensing of forest resources: three decades of research development. *Progress in Physical Geography*. 29, 1 – 26.

Brandtberg, T., Warner, T. A., Landenberger, R. E., and McGraw, J. B. 2003. Detection and analysis of individual leaf-off tree crowns in small-footprint, high sampling density lidar data from the eastern deciduous forest in North America. *Remote Sensing of Environment*. 85, 290 – 303.

Chen, Q., Baldocchi, D., Gong, P., and Kelly, M. 2006. Isolating individual trees in a savanna woodland using small-footprint lidar data. *Photogrammetric Engineering and Remote Sensing*. 72, 923 – 932.

Chen, Q., Gong, P., Baldocchi, D., and Tian, Y. Q. 2007. Estimating basal area and stem volume for individual trees from lidar data. *Photogrammetric Engineering and Remote Sensing*. 73, 1355 – 1365.

Clark, M. L., Clark, D. B., and Roberts, D. A. 2004. Small-footprint lidar estimation of sub-canopy elevation and tree height in a tropical rain forest landscape. *Remote Sensing of Environment*. 91, 68 – 89.

Coetzee, J. 1992. A revised tree volume table for short rotation *Eucalyptus grandis* timber crops. *ICFR Bulletin 09/1992*. Institute for Commercial Forestry Research, Pietermaritzburg, South Africa. 5 pp.

Coops, N. C., Wulder, M. A., Culvenor, D. S., and St-Onge, B. 2004. Comparison of forest attributes extracted from fine spatial resolution multispectral and lidar data. *Canadian Journal of Remote Sensing*. 30, 855 – 866.

Drake, J. B., Dubayah, R. O., Clark, D. B., Knox, R. G., Blair, J. B., Hofton, M. A., Chazdon, R. L., Weishampel, J. F., and Prince, S. D. 2002. Estimation of tropical forest structural characteristics using large-footprint lidar. *Remote Sensing of Environment*. 79, 305 – 319.

Falkowski, M. J., Smith, A. M. S., Gessler, P. E., Hudak, A. T., Vierling, L. A., and Evans, J. S. 2008. The influence of conifer forest canopy cover on the accuracy of two individual tree measurement algorithms using lidar data. *Canadian Journal of Remote Sensing*. 34, 338 – 350.

García, O. 1998. Estimating top height with variable plot sizes. *Canadian Journal of Forest Research*. 28, 1509 – 1517.

Hall, S. A., Burke, I. C., Box, D. O., Kaufmann, M. R., and Stoker, J. M. 2005. Estimating stand structure using discrete return lidar: an example from low density, fire prone ponderosa pine forests. *Forest Ecology and Management*. 208, 189 – 209.

Heurich, M. 2008. Automatic recognition and measurement of single trees based on data from airborne laser scanning over the richly structured natural forests of the Bavarian Forest National Park. *Forest Ecology and Management*. 255, 2416 – 2433.

Holmgren, J. 2004. Prediction of tree height, basal area, and stem volume in forest stands using airborne laser scanning. *Scandinavian Journal of Forest Research*. 19, 543 – 553.

Holmgren, J., Nilsson, M., and Olsson, H. 2003. Estimation of tree height and stem volume on plots using airborne laser scanning. *Forest Science*. 49, 419 – 428.

Hyyppä, J., Hyyppä, H., Leckie, D., Gougeon, F., Yu, X., and Maltamo, M. 2008. Review of methods of small-footprint airborne laser scanning for extracting forest inventory data in boreal forests. *International Journal of Remote Sensing*. 29, 1339 – 1366.

Hyyppä, J., Kelle, O., Lehikoinen, M., and Inkinen, M. 2001. A segmentation-based method to retrieve stem volume estimates from 3-D tree height models produced by laser scanners. *IEEE Transactions on Geoscience and Remote Sensing*. 39, 969 – 975.

Koch, B., Heyder, U., and Welnacker, H. 2006. Detection of individual tree crowns in airborne lidar data. *Photogrammetric Engineering and Remote Sensing*. 72, 357 – 363.

Lefsky, M. A., Cohen, W. B., Acker, S. A., Parker, G. G., Spies, T. A., and Harding, D. 1999. Lidar remote sensing of the canopy structure and biophysical properties of Douglas-fir western Hemlock forests. *Remote Sensing of Environment*. 70, 339 – 361.

Lefsky, M. A., Cohen, W. B., and Spies, T. A. 2001. An evaluation of alternate remote sensing products for forest inventory, monitoring, and mapping of Douglas-fir forests in western Oregon. *Canadian Journal of Forest Research*. 31, 78 – 87.

Lefsky, M. A., Cohen, W. B., Parker, G. G., and Harding, D. J. 2002. Lidar remote sensing for ecosystem studies. *Bioscience*. 52, 19 – 30.

Lim, K., Treitz, P., Wulder, M., St-Onge, B., and Flood, M. 2003. Lidar remote sensing of forest structure. *Progress in Physical Geography*. 27, 88 – 106.

Maltamo, M., Eerikäinen, K., Pitkänen, J., Hyyppä, J., and Vehmas, M. 2004. Estimation of timber volume and stem density based on scanning laser altimetry and expected tree size distribution functions. *Remote Sensing of Environment*. 90, 319 – 330.

Maltamo, M., Hyyppä, J., and Malinen, J. 2006. A comparative study of the use of laser scanner data and field measurements in the prediction of crown height in boreal forests. *Scandinavian Journal of Forest Research*. 21, 231 – 238.

McCombs, J. W., Roberts, S. D., and Evans, D. L. 2003. Influence of fusing lidar and multispectral imagery on remotely-sensed estimates of stand density and mean tree height in a managed loblolly pine plantation. *Forest Science*. 49, 457 – 466.

Means, J. E., Acker, S. A., Harding, D. J., Blair, J. B., Lefsky, M. A., Cohen, W. B., Harmon, M. E., and McKee, W. A. 1999. Use of large-footprint scanning airborne lidar to estimate forest stand characteristics in the western cascades of Oregon. *Remote Sensing of Environment*. 67, 298 – 308.

Morsdorf, F., Meier, E., Kötz, B., Itten, K. I., Dobbertin, M., and Allgöwer, B. 2004. Lidar-based geometric reconstruction of boreal type forest stands at single tree-level for forest and wildland fire management. *Remote Sensing of Environment*. 92, 353 – 362.

Næsset, E. 2002. Predicting forest stand characteristics with airborne scanning laser using a practical two-stage procedure and field data. *Remote Sensing of Environment*. 80, 88 – 99.

Næsset, E. 2004. Practical large scale forest stand inventory using a small-footprint airborne scanning laser. *Scandinavian Journal of Forest Research*. 19, 164 – 179.

Næsset, E. 2007. Airborne laser scanning as a method in operational forest inventory: status of accuracy assessments accomplished in Scandinavia. *Scandinavian Journal of Forest Research*. 22, 433 – 442.

Nelson, R. 1997. Modelling forest canopy heights: the effects of canopy shape. *Remote Sensing of Environment*. 60, 327 – 334.

Persson, Å., Holmgren, J., and Södermann, U. 2002. Detecting and measuring individual trees using an airborne laser scanner. *Photogrammetric Engineering and Remote Sensing*. 68, 925 – 932.

Peuhkurinen, J., Maltamo, M., Malinen, J., Pitkänen, J., and Packalén, P. 2007. Preharvest measurement of marked stands using airborne laser scanning. *Forest Science*. 53, 653 – 661.

Pienaar, B. and Kotze, H. 2000. *Growth and yield functions*. Unpublished Mensuration and Modelling Consortium (MMRC) report. MMRC, Pietermaritzburg. 70 pp.

Popescu, S. C., Wynne, R. H., and Nelson, R. F. 2002. Estimating plot-level tree heights with lidar: local filtering with a canopy height based variable window size. *Computers and Electronics in Agriculture*. 37, 71 – 95.

Popescu, S. C., Wynne, R. H., and Nelson, R. F. 2003. Measuring individual tree crown diameter with lidar and assessing its influence on estimating forest volume and biomass. *Canadian Journal of Remote Sensing*. 29, 564 – 577.

Reutebuch, S. E., Anderson, H.-E., and McGaughey, R. J. 2005. Light detection and ranging (lidar): an emerging tool for multiple resource inventory. *Journal of Forestry*. 103, 286 – 292.

Roberts, S. D., Dean, T. J., Evans, D. L., McCombs, J. W., Harrington, R. L., and Glass, P. A. 2005. Estimating individual tree leaf area in loblolly pine plantations using lidar-derived measurements of height and crown dimensions. *Forest Ecology and Management*. 213, 54 – 70.

Saltelli, A., Tarantola, S., Campolongo, F., and Ratto, M. 2004. *Sensitivity analysis in practice: a guide to assessing scientific models*. John Wiley and Sons, England. 232 pp.

Schreuder, H. T., Gregoire, T. G., and Wood, G. B. 1993. *Sampling methods for multisource forest inventory*. John Wiley and Sons, New York. 464 pp.

Schumacher, F. X. and Hall, F. D. S. 1933. Logarithmic expression of timber-tree volume. *Journal of Agricultural Research*. 47, 719 – 734.

Smith, S. L., Holland, D. A., and Longley, P. A. 2004. The importance of understanding error in lidar digital elevation models. *International Archives of Photogrammetry, Remote Sensing, and Spatial Information Sciences*. Vol. 35-4/W5, 996 – 1001.

Suárez, J. C., Ontiveros, C., Smith, S., and Snape, S. 2005. Use of airborne lidar and aerial photography in the estimation of individual tree heights in forestry. *Computers and Geosciences*. 31, 253 – 262.

Tesfamichael, S. G., Ahmed, F. B., and van Aardt, J. A. N. Accepted. Investigating the impact of discrete return lidar point density on estimations of mean and dominant plot-level tree height in *Eucalyptus grandis* plantations. *International Journal of Remote Sensing*.

Thomas, V., Treitz, P., McCaughey, J. H., and Morrison, I. 2006. Mapping stand-level forest biophysical variables for a mixedwood boreal forest using lidar: an examination of scanning density. *Canadian Journal of Forest Research*. 36, 34 – 47.

Tickle, P. K., Lee, A., Lucas, R. M., Austin, J., and Witte, C. 2006. Quantifying Australian forest floristics and structure using small-footprint lidar and large scale aerial photography. *Forest Ecology and Management*. 223, 379 – 394.

van Aardt, J. A. N., Wynne, R. H., and Oderwald, R. G. 2006. Forest volume and biomass estimation using small-footprint lidar-distributional parameters on a per-segment basis. *Forest Science*. 52, 636 – 649.

von Gadow, K. and Bredenkamp, B. 1992. *Forest management*. Academica, Pretoria. 164 pp.

Wehr, A. and Lohr, U. 1999. Airborne laser scanning—an introduction and overview. *ISPRS Journal of Photogrammetry and Remote Sensing*. 54, 68 – 82.

Wulder, M. 1998. Optical remote-sensing techniques for the assessment of forest inventory and biophysical parameters. *Progress in Physical Geography*. 22, 449 – 476.

CHAPTER SIX

SUMMARY AND CONCLUSIONS

6.1 Introduction

This thesis has as its main objective the derivation of forest structural attributes of even-aged *Eucalyptus grandis* plantations using small-footprint discrete return lidar data. Several studies have been carried out over the past few decades in this regard with results typically showing great promise for future applications of lidar data. The target of most of these studies was limited to species of importance to the northern hemisphere environment (e.g., conifers). Moreover, despite reported accuracies comparable to the traditional field inventories, translation of the technology into operational inventory programs is still lacking with few exceptional examples, such as the experiences from the Scandinavian region (Næsset, 2007). One of the most important factors that limit the integration of the system as a stand-alone or complementary tool in routine forest inventories is the relatively high cost of acquisition (Næsset, 2009). The cost of lidar data is influenced by lidar point density, among other factors. It therefore becomes intuitive that acquisitions be optimised with accuracy of outputs maintained at acceptable levels.

In light of the aforementioned problems, the studies in this thesis focused on even-aged *Eucalyptus grandis* plantations which received little attention in previous studies. This species is an important timber source in the forestry industry by yielding end products of economic significance. There thus exists a need to support management of the species using lidar data, particularly in the assessment of structural components. The effect of simulated lidar point densities on the accuracy of estimating structural attributes was also investigated. A brief summary of the findings is presented below, followed by conclusions and recommendations.

6.2 Summary

Tree height estimation included mean tree height and dominant height of geographically located plots. Estimation was based on a distributional approach, followed by regression analysis to relate metrics derived from non-ground lidar point data to field data (Chapter 3). Twenty-eight statistical metrics were extracted from the lidar data, following a widely practiced method in the literature. In order to assess the effect of lidar point density, seven densities were simulated at 0.25 points/m^2, 1 point/m^2, 2 points/m^2, 3 points/m^2, 4 points/m^2, 5 points/m^2, and 6 points/m^2. Stepwise regression analysis was used to select the best lidar metric(s) for the estimation of both mean and dominant tree height. The relationships relating mean tree height and lidar metrics returned high accuracies across all densities (R^2=0.94, RMSE=5% of field-observed mean). A similar magnitude of accuracies was observed for dominant tree height estimation at all point densities (R^2=0.95, RMSE=5% of field-observed mean). Similarities of estimations among density levels were also confirmed using analysis of variance and error statistics. Accuracies reported here confirmed the usefulness of lidar data for the estimation of height. Such accuracies are also in agreement with the standard required by plantation forest inventory using field measurements. It was also found that lidar did not underestimate height values – a problem commonly mentioned in different studies (Næsset, 1997; Magnussen and Boudewyn, 1998; Næsset, 2002; Clark *et al*., 2004; Holmgren, 2004). The non-significant differences of estimations among lidar point densities implied that a relatively low point density could be used for height estimation purposes. Similar findings were reported by Holmgren (2004) and Thomas *et al*. (2006). This has a significant effect on reducing the cost of lidar surveys.

Forest structural attribute estimation based on lidar point distributions and regression analysis, as employed in the study described in Chapter 3, has limitations despite the high level of accuracies. First, developing a regression model requires field inventory data. Second, spatial information of individual trees is often not addressed. Locating individual trees can be used to overcome these limitations. A common method of tree identification from lidar data is using local maxima filtering from a

canopy height model (CHM) created by interpolating the lidar points (Chapter 4). The window size in relation to crown area determines the number of trees located. An average window size for a plot was determined using the semi-variogram range computed from a CHM of the plots. A comparative approach of determining window size utilised pre-determined within-row tree spacing. Three spatial resolutions (0.2 m, 0.5 m, and 1 m) of the CHM were compared to determine the appropriate resolution for the specific plantations. The numbers of trees counted using the above procedures were converted to SPHA. Accuracy assessment was based on the ratio of lidar-derived to field-observed SPHA, as well as RMSE relative to field-observed mean; the reported mean accuracies were 73% (RMSE=35%), 56% (RMSE=50%), and 41% (RMSE=65%) for 0.2 m, 0.5 m, and 1 m resolutions, respectively, when the semi-variogram approach was applied. The corresponding accuracies for estimates based on tree spacing were 82% (RMSE=26%), 82% (RMSE=27%), and 68% (RMSE=42%), respectively. Following these results three lidar point densities (1 point/m^2, 3 points/m^2, and 5 points/m^2) were compared using a 0.2 m spatial resolution CHM for both tree spacing and semi-variogram based window size determination methods. Accuracies of estimations based on the semi-variogram approach were 56% (RMSE=51%), 70% (RMSE=40%), and 73% (RMSE=35%) for 1 point/m^2, 3 points/m^2, and 5 points/m^2, respectively. Corresponding figures for the approach that utilised tree spacing were 74% (RMSE=33%), 80% (RMSE=30%), and 82% (RMSE=26%). All estimations using both window size determination methods were biased negatively.

The accuracy of SPHA estimations in comparison to other studies was found to be satisfactory. The increase in accuracy of SPHA estimation with an increase in spatial resolution reflects the relationship between canopy size and resolution. Studies based on high spatial resolution remotely-sensed imagery have shown that a sufficient number of pixels is required to identify the crown of a single tree (Wulder *et al*., 2000; Pouliot *et al*., 2002). A resolution of 0.2 m was found to be an appropriate size for an average canopy diameter (based on pre-determined within-row tree spacing) of the trees in the study area. Comparison of lidar point densities revealed superior accuracies for 3 points/m^2 and 5 points/m^2, as opposed to 1 point/m^2. There were also strong similarities between the higher densities. Thus, a lidar density of

approximately 3 points/m^2 can be used for *Eucalyptus* species grown under such management conditions and canopy characteristics. Although inferior to the tree spacing approach, estimation based on the semi-variogram range proved promising, since it relied entirely on the lidar data.

While SPHA in itself is an important component of forest inventory, it is useful to extend its usage to deriving other structural attributes. Plot-level mean height, dominant height, and volume of trees were derived from trees that were located using local maxima filtering techniques (Chapter 5). The study reported in Chapter 5 also sought to investigate the effect lidar point density has on the estimates by adopting the results of SPHA estimations at the three densities (1 point/m^2, 3 points/m^2, and 5 points/m^2). A circular polygon, simulating crown area of a tree, was created around each local maximum using the semi-variogram range or tree spacing value as the diameter. Coincident non-ground lidar points were then spatially joined to the 'tree' polygons. Points with the mean and maximum values within each polygon were extracted for comparison in the estimation of plot-level mean and dominant height. Mean height was separately computed as the arithmetic mean of the mean and maximum values for each plot. Dominant height was separately calculated as the mean of the top 20% tallest mean and maximum height values for a given plot. Both mean and maximum values exhibited acceptable correlation with field-observed mean height; however, the former was preferred due to the results showing a non-significant difference from field observations. Lidar point density and the method of local maxima filtering did not influence accuracies of mean height derivation (R^2=0.93-0.94, RMSE=7% of field mean). Dominant height was marginally better when derived from maximum rather than mean lidar points. Local maxima filtering techniques and lidar point density did not have any significant effect on the results (R^2=0.94-0.95, RMSE=5-6% of field mean).

Mean height and dominant height derived from located potential trees compared favourably with those obtained using regression analysis (Chapter 3). Therefore, one would theoretically not need to undertake field measurements for establishing statistical models, except for model validation. Similarity of derived height results was also noted among all estimates, despite differences in the number of located

‘trees’ across local maxima filtering techniques and lidar point densities. This was attributed to the probability that mainly tall trees are located in all local maxima filtering procedures. The canopy closure and canopy geometry of the trees also favour point returns from the upper canopy layer, thereby resulting in low height variability.

It has been shown that SPHA and height attributes, estimated based on local maxima filtering, can be used to derive volume of trees at the plot-level. Calculation of volume followed an approach which can be summarised in three orderly steps: deriving DBH of the mean tree, estimating volume of the mean tree, and estimating volume of all trees within a plot. These procedures were repeated for the three lidar point densities and two local maxima filtering techniques used above for SPHA estimations. Basal area per plot was first derived using a function developed by the forestry industry for even-aged plantations. The function requires SPHA and dominant height, both of which can be derived from lidar data, and age of trees documented at the time of planting. Plot-level basal area can be converted to quadratic mean DBH (QDBH) using SPHA and hectare area as conversion factors. QDBH is an approximation of the DBH of the tree with mean basal area and in combination with mean height can be used as an independent variable in a standard volume estimation equation. The volume calculated in such a manner is assumed to represent the volume of the mean tree. Multiplication of the mean tree volume by SPHA of a plot yielded the cumulative volume of trees within that plot. Although there was significant underestimation of volume at all lidar point densities and for all local maxima filtering approaches, the relationship between lidar-estimated and field-observed volume was relatively high (R^2=0.83-0.93). Differences among estimates at all local maxima filtering techniques and lidar point densities were in general non-significant. Sensitivity analysis was performed to investigate the degree of influence of mean height, dominant height, and SPHA on volume estimation. Each attribute was varied at three levels based on RMSE of the attribute, while all possible combinations of the attributes were explored. Increasing attributes by adding their respective RMSE improved the resultant volume estimates, although all estimates were negatively biased. Comparison among attributes indicated that SPHA had the

highest influence on plot-level volume estimation. Hence, more emphasis should be placed on gauging SPHA.

Accuracies of volume estimation were comparable to other studies carried out in different forest environments. The overall result was therefore considered satisfactory, especially given the fact that the approach employed here utilised lidar data as stand-alone data source. The results also showed that volume estimates did not significantly vary due to lidar point density and local maxima filtering technique, despite variances in SPHA estimates. Findings of the sensitivity analysis furthermore confirmed the similarities of estimates across lidar point densities. This was attributed to the size of the trees located by local maxima filtering, which often identifies dominant trees. Such trees represent the majority of the volume within a plot (Hyyppä *et al*., 2001; Maltamo *et al*., 2004; Heurich, 2008).

6.3 Conclusions

The studies reported in each chapter of this thesis explored the utility of lidar data for retrieving forest structural attributes in an even-aged *Eucalyptus grandis* forest environment. The results of the studies should be viewed in terms of their contribution to research in general, as well as potential applications to timber resource inventories.

Mean and dominant height

Although height estimations using regression analysis were highly accurate, the requirement for field surveys as a reference tool does not bode well for a strategy that strives for cost reduction. Hence the need to develop a stand-alone lidar approach. Heights estimated for potential trees located from a lidar CHM using local maxima filtering provided results that are highly accurate and comparable to several reported studies. The accuracies also satisfy the requirement set by the commercial forestry industry. The lack of any significant impact that lidar point density has on estimation accuracy implies that lidar data can be acquired at a relatively low density and hence at a lower acquisition costs.

SPHA

Studies have shown that counting trees from remotely-sensed data is, in general, a difficult task, especially for operational purposes. Estimation of SPHA here has achieved accuracies that were deemed comparable to other studies. The use of semi-variogram range for determining mean window size in local maxima filtering yielded promising results, especially given that *a priori* assumptions and knowledge of field data are not required. An alternative approach, which applied pre-determined tree spacing as window size, resulted in superior accuracy for SPHA estimation. This approach has strong relevance to intensively-managed forests with known planting densities; however, the difference in stand density between the times of planting and lidar data acquisition must be taken into consideration. Comparison of estimates at the density levels showed that 3 points/m^2 can be used to obtain results similar to those obtainable from 5 points/m^2.

Volume

Tree height attributes and SPHA were used in combination with known stand age for computing plot-level tree volume. Field volume was underestimated for all scenarios of local maxima filtering techniques and lidar point densities due to underestimation of SPHA. Comparison among estimates across the simulated lidar point densities revealed a lack of significant differences, hence a relatively low lidar point density could be used in estimating volume. Of all the independent variables, SPHA played the most significant role in the estimation of plot-level volume. More focus should therefore be given to address SPHA underestimation.

6.4 Recommendations

Numerous studies have proven the applicability of lidar data to forest structural assessment. The focus of these studies was mostly limited to species of significance to the northern hemisphere environment, such as boreal forests. It has been reported that lidar provides accurate estimation of tree height, given the spatial resolution and the type of data (range or height) such systems collect. Estimation of SPHA and volume has had limited success in terms of accuracy. In addition, most of these attributes have been estimated with a combination of lidar and field data.

Inclusion of field data in the analysis inflates the cost of estimation and therefore has to be minimised.

The studies reported in this thesis attempted to estimate forest structural attributes of importance to timber management from lidar data only. The target of the studies was commercially grown *Eucalyptus* species. The findings of the study present useful insights related to the implementation of lidar data for operational inventory purposes.

- It is important that lidar data be used for multiple structural attributes, given the cost of data acquisition. It has been established that the inherent characteristics of lidar data and the information content they provide enable direct measurement of multiple attributes.
- The results showed promise for estimating plot-level height attributes, SPHA, and volume. Such capabilities offer the forestry industry an important indicator as to the use of lidar in operational forest structural inventories.
- The accuracy of tree height derived from lidar data meets the high-accuracy requirement of the forestry industry. There was, however, a systematic error in volume estimation which was negatively biased, mainly due to the underestimation of SPHA.

Future research should therefore focus on improving SPHA estimation, as opposed to height attributes, which were estimated at high levels of accuracy. The results of point density analysis indicated the invariance of height attributes and volume estimates across densities, even though there was a marginal effect on SPHA estimation. Therefore, studies that strive to improve SPHA estimation should also consider lidar point density. It is desirable to have an acceptable estimation at low lidar point densities in order to minimise the cost of data acquisition. This study has taken a step forward in terms of justifying light detection and ranging (lidar) as stand-alone plantation forest inventory tool – what now remains is to hone estimation of variables that influence volume outcomes, especially SPHA, and to do so while keeping operational implications in mind.

References

Clark, M. L., Clark, D. B., and Roberts, D. A. 2004. Small-footprint lidar estimation of sub-canopy elevation and tree height in a tropical rain forest landscape. *Remote Sensing of Environment*. 91, 68 – 89.

Heurich, M. 2008. Automatic recognition and measurement of single trees based on data from airborne laser scanning over the richly structured natural forests of the Bavarian Forest National Park. *Forest Ecology and Management*. 255, 2416 – 2433.

Holmgren, J. 2004. Prediction of tree height, basal area, and stem volume in forest stands using airborne laser scanning. *Scandinavian Journal of Forest Research*. 19, 543 – 553.

Hyyppä, J., Kelle, O., Lehikoinen, M., and Inkinen, M. 2001. A segmentation-based method to retrieve stem volume estimates from 3-D tree height models produced by laser scanners. *IEEE Transactions on Geoscience and Remote Sensing*. 39, 969 – 975.

Magnussen, S. and Boudewyn, P. 1998. Derivations of stand heights from airborne laser scanner data with canopy-based quantile estimators. *Canadian Journal of Forest Research*. 28, 1016 – 1031.

Maltamo, M., Eerikäinen, K., Pitkänen, J., Hyyppä, J., and Vehmas, M. 2004. Estimation of timber volume and stem density based on scanning laser altimetry and expected tree size distribution functions. *Remote Sensing of Environment*. 90, 319 – 330.

Næsset, E. 1997. Determination of mean tree height of forest stands using airborne laser scanner data. *ISPRS Journal of Photogrammetry and Remote Sensing*. 52, 49 – 56.

Næsset, E. 2002. Predicting forest stand characteristics with airborne scanning laser using a practical two-stage procedure and field data. *Remote Sensing of Environment*. 80, 88 – 99.

Næsset, E. 2007. Airborne laser scanning as a method in operational forest inventory: status of accuracy assessments accomplished in Scandinavia. *Scandinavian Journal of Forest Research*. 22, 433 – 442.

Næsset, E. 2009. Effects of different sensors, flying altitudes, and pulse repetition frequencies on forest canopy metrics and biophysical stand properties derived from small-footprint airborne laser data. *Remote Sensing of Environment*. 113, 148 – 159.

Pouliot, D. A., King, D. J., Bell, F. W., and Pitt, D. G. 2002. Automated tree crown detection and delineation in high resolution digital camera imagery of coniferous forest regeneration. *Remote Sensing of Environment*. 82, 322 – 334.

Thomas, V., Treitz, P., McCaughey, J. H., and Morrison, I. 2006. Mapping stand-level forest biophysical variables for a mixedwood boreal forest using lidar: an examination of scanning density. *Canadian Journal of Forest Research*. 36, 34 – 47.

Wulder, M., Niemann, K. O., and Goodenough, D. G. 2000. Local maximum filtering for the extraction of tree locations and basal area from high spatial resolution imagery. *Remote Sensing of Environment*. 73, 103 – 114.